DOKUZ EYLÜL UNIVERSITY

GRADUTE SCHOOL OF NATURAL AND APPLIED SCIENCES

PROPOSAL OF SEAFRONT BUILDINGS FOR IMPROVING URBAN VENTILATION AND PEDESTRIAN WIND COMFORT ON IZMIR COASTLINE

by

Hakan BAŞ

June, 2022

İZMİR

PROPOSAL OF SEAFRONT BUILDINGS FOR IMPROVING URBAN VENTILATION AND PEDESTRIAN WIND COMFORT ON IZMIR COASTLINE

A Thesis Submitted to the

Graduate School of Natural and Applied Sciences of Dokuz Eylül University

In Partial Fulfilment of the Requirements for the Degree of Doctor of

Philosophy in Architecture, Architectural Design Program

by

Hakan BAŞ

June, 2022

İZMİR

Ph.D. THESIS EXAMINATION RESULT FORM

We have read the thesis entitled **"PROPOSAL OF SEAFRONT BUILDINGS FOR IMPROVING URBAN VENTILATION AND PEDESTRIAN WIND COMFORT ON IZMIR COASTLINE"** completed by **HAKAN BAŞ** under the supervision of **PROF. DR. İLKNUR TÜRKSEVEN DOĞRUSOY** and we certify that in our opinion it is fully adequate, in scope and in quality, as a thesis for the degree of Doctor of Philosophy.

....

Prof. Dr. İlknur TÜRKSEVEN DOĞRUSOY

Supervisor

....

Prof. Dr. Sibel ECEMİŞ KILIÇ   **Assoc. Prof. Dr. Ayça TOKUÇ**

Thesis Committee Member   **Thesis Committee Member**

....

Prof. Dr. Sigrid REITER   **Assoc. Prof. Dr. Zeynep Durmuş ARSAN**

Examining Committee Member   **Examining Committee Member**

———————————————————

Prof. Dr. Okan FISTIKOĞLU

Müdür

Fen Bilimleri Enstitüsü

ACKNOWLEDGMENT

I would like to thank my thesis monitoring committee members for their discussions and comments by carefully following the development process of the thesis, Prof. Dr. Sibel ECEMİŞ KILIÇ and Assoc. Prof. Dr. Ayça TOKUÇ. I also specially thank them for agreeing to be on my thesis committee.

I would like to thank my thesis examiners, Prof. Dr. Sigrid REITER and Assoc. Prof. Dr. Zeynep DURMUŞ ARSAN, for their insightful comments on my thesis.

Last but not least, I am greatly indebted to my family, especially my mother and my father, who have supported me in my academic pursuits all these years.

<div align="right">Hakan BAŞ</div>

PROPOSAL OF SEAFRONT BUILDINGS FOR IMPROVING URBAN VENTILATION AND PEDESTRIAN WIND COMFORT ON IZMIR COASTLINE

ABSTRACT

Urban areas face severe environmental problems such as global warming, urban heat islands (UHI), and air pollution; however, coastal cities in the Mediterranean region have cool sea breezes that can reduce the effects of these environmental problems. However, in many coastal cities, impermeable urban seafront buildings prevent cool sea breezes from penetrating the city, causing the accumulation of hot and polluted air in urban areas while also posing a risk of pedestrian wind discomfort. This study aims to design wind-adaptive urban seafront buildings to improve urban ventilation and pedestrian wind comfort in İzmir, a high-density Mediterranean city where UHI, air pollution, and the risk of pedestrian wind discomfort coexist. For this purpose, a complementary field and design study was carried out using the parametric design and computational fluid dynamics (CFD) method. Alternative seafront buildings consisting of two-rows and shifted configurations were designed using two proposed urban geometric indicators. Among the configurations, the denser and more compact seafront building configuration prevents the risk of wind discomfort and achieves the highest ventilation efficiency (82%). The results show that a compromise between pedestrian wind comfort and ventilation efficiency requirements can be achieved in the seafront urban area without neglecting urban density/compactness. This study provides theoretical and practical outcomes and promotes the consideration of wind in the urban spatial planning process. The pedestrian-level wind climate in the coastal part of Izmir can be improved by applying the findings. The resulting implications can apply to similar coastal urban environments and help urban policymakers and designers.

Keywords: Urban seafront buildings, urban ventilation, pedestrian wind comfort, shifted building configuration, computational fluid dynamics (CFD).

İZMİR KIYI ŞERİDİ'NDE KENTSEL HAVALANDIRMA VE YAYA RÜZGÂR KONFORUNU İYİLEŞTİRMEYE YÖNELİK YAPILAŞMA ÖNERİSİ

ÖZET

Kentsel alanlar küresel ısınma, kentsel ısı adası (KIA), hava kirliliği gibi önemli çevresel sorunlarla karşı karşıyadır ve Akdeniz bölgesindeki kıyı kentleri bu sorunların etkilerini azaltabilecek serin deniz meltemlerine sahiptir. Fakat birçok kıyı kentinde, rüzgâra karşı geçirimsiz kentsel kıyı yapıları, serin deniz meltemlerinin kente işlemesini engelleyerek kentsel alanlarda sıcak ve kirli havanın birikmesine neden olurken diğer yandan yaya rüzgâr konforsuzluğu riski oluşturmaktadır. Bu çalışma, KIA, hava kirliliği ve yaya rüzgâr konforsuzluğu riskinin bir arada bulunduğu yüksek yoğunluklu bir Akdeniz kenti olan İzmir'de kentsel havalandırma ve yaya rüzgâr konforunu sağlayabilecek, rüzgârla uyumlu kentsel kıyı yapılarının tasarımını amaçlamaktadır. Bu amaçla, parametrik tasarım ve hesaplamalı akışkanlar dinamiği (HAD) yöntemi kullanılarak tamamlayıcı bir saha ve tasarım çalışması yapılmıştır ve önerilen iki kentsel geometrik gösterge kullanılarak iki sıralı ve şaşırtmalı konfigürasyonlardan oluşan alternatif kıyı yapıları tasarlanmıştır. Tasarlanan yapı konfigürasyonları arasında, daha yoğun ve daha kompakt kıyı şeridi yapı konfigürasyonu, yaya rüzgâr konforsuzluğu riskini önler ve en yüksek havalandırma verimliliğini (%82) sağlar. Bulgular, kıyı kesimindeki kentsel alanlarda, kentsel yoğunluk/kompaktlık ihmal edilmeden yaya rüzgâr konforu ve havalandırma verimliliği gereksinimleri arasında bir uzlaşmanın sağlanabileceğini göstermektedir. Bu çalışma hem teorik hem de pratik sonuçlar sağlamakta ve kentsel mekânsal planlama sürecinde rüzgârın dikkate alınmasını teşvik etmektedir. İzmir kentinin kıyı kesimlerinde yaya seviyesindeki rüzgâr iklimi, bulguların uygulanmasıyla iyileştirilebilir. Bulgular, benzer kıyı kentsel çevreleri için de geçerlidir ve kentsel politika yapıcılara ve tasarımcılara yardımcı olmaktadır.

Anahtar kelimeler: Kentsel kıyı yapıları, kentsel havalandırma, yaya rüzgâr konforu, şaşırtmalı yapı konfigürasyonu, hesaplamalı akışkanlar dinamiği (HAD).

CONTENTS

CHAPTER 3 – EXPERIMENTAL FIELD STUDY: WIND FLOW ASSESSMENT of URBAN BUILDING CONFIGURATIONS **63**

LIST OF FIGURES

Page

xviii

xix

LIST OF TABLES

LIST OF SYMBOLS

C_d :Drag coefficient

C_S :Roughness constant (0-1)

C_μ :Model constant (=0.09)

E   :Empirical wall constant (9.793)

k   :Turbulence kinetic energy (m^2/s^2)

k_S :Equivalent sand-grain roughness height (m)

κ :von Karman constant (0.40-0.42)

ρ :Density of air (kg/m^3)

P_k :Production of turbulent kinetic energy

V, U   :Mean wind speed (m/s)

V_{ref}, U_{ref} :Reference wind speed (m/s)

VR_w :Wind velocity ratio

u^* :ABL friction velocity (m/s)

y^+ :Non-dimensional distance from the wall (-)

y_P :Centre point (P) of the first cell

(z_0) :Aerodynamics roughness length (m)

z   :Height (m)

z_{ref} :Reference height (m)

τ_w :Wall shear stress

x, y, z   :Cartesian coordinates

H, W, L   :Building height, width, length (m)

S_{x1} :Passage width between upwind buildings (m)

S_{x2} :Passage width between downwind buildings (m)

S_y :Passage width between upwind and downwind buildings (m)

m/s   :Meter per second

°C   :Santigrat

α   :Power law exponent

ε   :Turbulence dissipation rate (m^2/s^3)

ω   :Specific turbulence dissipation rate (m^2/s^3)

σ_u :Root Mean Square (RMS) streamwise velocity fluctuation

         amplitude(m/s)

μ   :Dynamic viscosity of air (kg/m/s)

ABBREVIATIONS

UHI   : Urban heat island effect

GA   : Genetic algorithm

GDfD   : Grammars derived from design

GfD   : Grammars for designing

CFD   : Computational fluid dynamics

STAR   : STAR-CCM+

Re   : Reynolds number

ABL   : Atmospheric boundary layer

LCZ   : Local climate zone

BSF   : Building surface fraction

TSMS   : Turkish State Meteorological Service

NEN   : Netherlands Normalisation Institute

AIJ   : Architectural Institute of Japan

FV   : Finite-volume method

RANS   : Reynolds-averaged Navier Stokes

LES   : Large eddy simulation

RSM   : Reynolds Stress Model

PCA   : Passage centre axis

SCA   : Seating centre axis
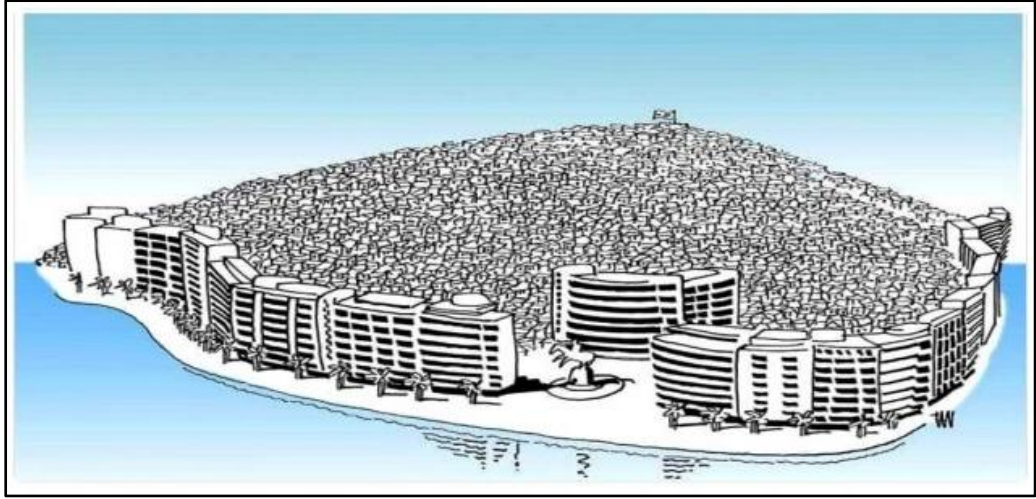
A cartoon representing the city of İzmir and its coastline (Yeni Vizyon, 2016)

CHAPTER 1

INTRODUCTION

In this chapter of the thesis, the research problems, scope, objectives, questions, method(s) and thesis structure are presented.

1.1 Problem Statement and Motivation

In today's urban environments, the outdoor climatic comfort, bio-climatic design of urban open spaces, and health of the inhabitants using urban open spaces are often neglected due to the automobile-oriented and speculative urbanization policies, as well as the intensification of cities. As a result, urban areas face severe environmental problems such as the urban heat islands (UHI) effect, air pollution, and pedestrian wind discomfort risk. However, in recent years, due to the driving effects of global temperature increase and sustainable urbanization policies, there have been emerging trends and tendencies in urbanism towards considering climate parameters in urban design processes, increasing the comfort and liveability of urban open spaces.

The comfort of urban open spaces is at the focus of urban environmental design and urban physics fields. However, it is difficult to provide comfort in urban open spaces as they are exposed to many climatic factors such as sun, rain, and wind. Among the climatic factors, the wind is more difficult to control due to its dynamic nature. For this reason, it easily creates disturbing effects on pedestrians. Especially coastal cities are critical places for pedestrian wind comfort. They are exposed to open wind conditions, mostly sea breezes, so they suffer from the risk of pedestrian wind discomfort (Johansson & Yahia, 2020; Szűcs, 2013).

Strong wind conditions in urban open spaces pose a risk of pedestrian wind discomfort and necessitate sheltered urban open spaces for inhabitants. Moreover, the increase in the size of the buildings also increases the risk of pedestrian wind discomfort. In particular, the increase in the height and the coverage ratio of the

buildings cause strong mechanical effects of the wind on the human body and threaten the comfort and safety of pedestrians (Penwarden, 1973; Stathopoulos and Blocken, 2016; Wise, 1971). Due to increased building sizes, wind discomfort in urban areas is often more severe than in rural areas.

Despite the adverse effects of the wind, there are desirable effects on urban areas. Wind plays a critical role in reducing the intensity of the urban heat islands (UHI) effect (He, Ding & Prasad, 2020; Jamei et al., 2020; Memon and Leung, 2010). The fact that the air temperature is higher in dense urban areas than in rural areas around the city is defined as the effect of urban heat islands (Georgakis and Santamouris 2008). In particular, refreshing sea breezes play a key role in reducing the stagnated heat in urban areas (Lim and Ooka, 2021) and improving thermal comfort in warmer climates. The sea breeze is unique and of high quality compared to other winds in many ways. Since its origin is the sea, the sea breeze carries the clean and fresh air mass from the sea to urban environments.

The wind substantially affects the air quality of the urban open spaces (Chen, Rong, & Zhang, 2021). It helps to reduce outdoor air pollution by removing toxic emissions from the urban environment. In particular, it is the driving force for the transport and distribution of airborne pollutants from vehicles. Murty (1975) noted that speed and wind direction were effective in reducing sulfur dioxide concentrations in Metropolitan Toronto. Samson (1988) points out that higher wind speed dilutes pollutants, and the dispersion rates of pollutants depend on the strength of the wind. Moreover, many studies point out that the pollutant concentration increases either in calm weather conditions or at very low wind speeds (Lawrence 1970). During the development of the COVID-19 pandemic, a higher number of COVID-19 cases were reported in cities with a low average wind flow velocity (Coccia, M. 2020). Therefore, a certain amount of wind speed must be maintained for better air quality in urban environments. A wind speed of at least 1.0 m/s is recommended as a standard for urban air pollution diffusion (Q., Xu, & Z., Xu, 2020).

Insufficient ventilation makes the urban environment a place where hot and polluted air is collected. For this reason, the wind climate in urban open spaces

should be comfortable for pedestrian activities and reduce the effects of UHI and air pollution. This can be achieved through multi-purpose planning policies that require criteria related to ventilation of urban open spaces along with pedestrian wind comfort. However, urban policymakers require pedestrian wind comfort assessments around new buildings but do not require urban ventilation criteria to counteract the impact of UHI and air pollution. New studies that consider wind comfort and ventilation holistically are needed. This is also needed in coastal cities in the Mediterranean region of Türkiye. Although there are many discussions about the inappropriate form of seafront buildings causing wind discomfort risk and blocking refreshing sea breeze, there is no study in the academic literature considering wind comfort and ventilation together. This shortcoming constitutes the motivation of this research. In this context, this research focuses on the wind adaptation of urban seafront buildings to reduce the risk of wind discomfort, UHI, and air pollution in the Alsancak city center of the coastal city of Izmir, Türkiye.

1.2 Scope of the Research

This research was limited to providing the objectives of urban ventilation and pedestrian wind comfort on the coastline of the compact and dense city of Izmir in the Mediterranean climate region. In this context, the target problems are pedestrian wind comfort and also urban ventilation, which links to UHI and pollution dilution. The target urban area is seafront buildings located along the seashore. Finally, the target urban typology is the medium-height, compact and dense urban blocks as today's sustainable urbanization trend highlight the compact city model (Holden, 2004).

Urban spatial planning studies are performed at the macroscopic city level, the mesoscopic block level, and the microscopic building level (Yang et al., 2020). This study is at the mesoscopic block level and focuses on the seafront buildings on the Alsancak coastline. The main reason for this is that the seafront buildings are critical places where the sea breeze first interacts with the urban fabric and the risk of wind discomfort occurs. Second, although there are numerous studies in the literature focused on inner-city ventilation (Oke, 1988; Rajagopalan et al., 2014), there is no study focused on the design of the seafront buildings for ventilation and pedestrian

wind comfort. Third, the target urban area, Alsancak is the recreation center of the city and includes many pedestrian activities therefore requires improvements in terms of pedestrian wind comfort. Fourth, the seafront buildings in the Alsancak coastline need more rehabilitation as they are denser and less permeable than the inner urban areas. Unlike inner urban areas that usually only need ventilation due to the high density, this area needs both ventilation and pedestrian wind comfort requirements.

1.3 Objectives of the Research

The Introduction emphasized that urban ventilation and pedestrian wind comfort should be provided together in the Mediterranean coastal cities within the context of a multi-objective wind planning strategy. Therefore, the wind flow should be continuous for urban ventilation, and it should not cause the risk of pedestrian wind discomfort. In other words, wind flow should be in the streets without accelerating. In this context, seafront buildings should be in a form that will allow the wind to enter the city while preventing the acceleration of the wind flow at the wind entrance passages. This argument shapes the objective of the study. Such a design could reduce the intensity of UHI and air pollution and the pedestrian wind discomfort risk for the residents using urban open spaces for long-term seating in Izmir all year round. In this context, this study aims to create an alternative design of wind-adaptive urban seafront buildings to improve urban ventilation and reduce the risk of pedestrian wind discomfort on the Alsancak coastline. However, the objective is not to derive site-specific wind solutions acting only in the city of Izmir. On the contrary, it aims to develop solutions in a generalizable and transferable format to other cities.

1.4 Research Questions

After determining the general scope and objectives of the research, problem-oriented research questions can be examined. In the introduction, the scope of the research is restricted considering three parameters:

- The target problems: inadequate urban ventilation and pedestrian wind discomfort risk

- The target urban area: seafront buildings that are exposed to the sea breeze along the seashore
- The target urban block typology: mid-rise, compact, and dense urban blocks.

  Therefore, the overarching research question in this study is as follows:

- *How can urban seafront buildings optimally be designed to provide both urban ventilation and pedestrian wind comfort in mid-rise, high-density, and compact Mediterranean cities?*

This research question includes four specific sub-questions:

- *How do building form, building size, building configuration, street width, and urban geometric indicators affect wind behaviour?*
- *What is the role of urban building configuration in providing urban ventilation and pedestrian wind comfort?*
- *What are the key and predominant urban geometric indicators in providing urban ventilation and pedestrian wind comfort?*
- *How should urban open spaces between buildings along the seashore be positioned, and how size should they be for urban ventilation and pedestrian wind comfort?*

The sub-questions are interrelated based on the main topics, urban ventilation and pedestrian wind comfort in urban environments, and aim to help find the solution to the overarching research question.

1.5 Method(s) of the Research

This research is handled holistically addressing the urban environmental problems based on urban design and urban physics aspects. For this reason, this research develops a methodology that integrates the parametric design method with the experimental method to tackle the urban environmental problems with the design of urban seafront buildings. The CFD simulations provide the performance evaluation of the proposed seafront building configurations. The process between parametric design and simulations is based on the iterative approach. It continues until the best

possible urban seafront building configuration which is morphologically suitable for the given site conditions and provides the best performance for urban ventilation and pedestrian wind comfort.

Parametric Design Method
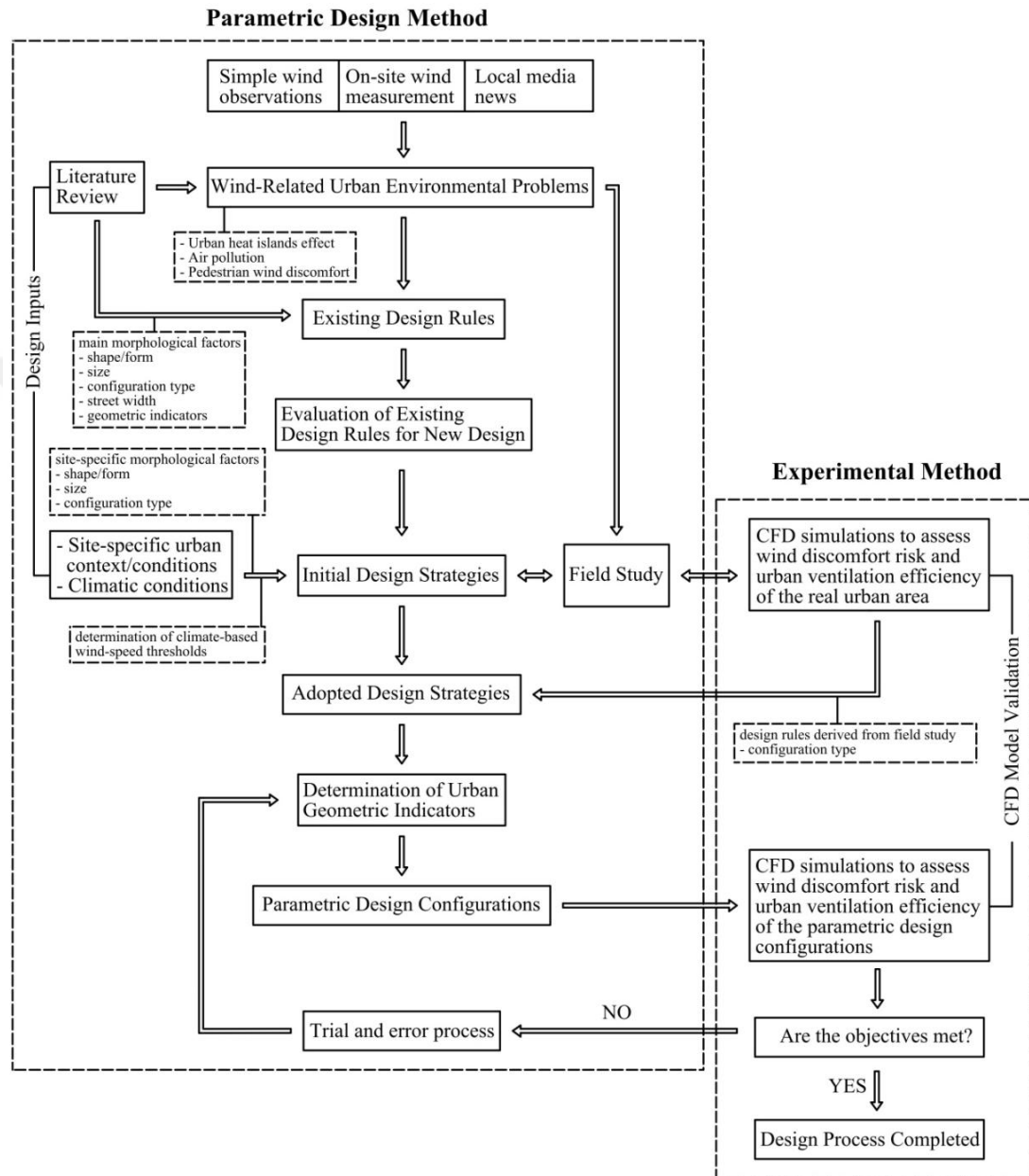
Figure 1.1 Framework and workflow of experimental design optimization method

The parametric design method initially begins addressing the background of the problems with earlier on-site wind measurement studies and simple wind observations and is supported by an extensive literature review evaluating the wind-related urban environmental issues and current design knowledge for wind

adaptation of buildings. Then, urban geometric indicators and climate-based wind speed thresholds are determined by considering site-specific climatic conditions and urban context. Finally, seafront building configurations in parametric order are created and tested with CFD simulations. The process between the parametric design and the experimental method is supported by the traditional trial and error process. The entire process continues until the best possible urban seafront building configuration that provides acceptable results for urban ventilation, and pedestrian wind comfort is found. Each of these steps will be described in the following chapters. Figure 1.1 shows the experimental design optimization method of urban seafront buildings.

1.5.1 Design Method

The design part of the experimental design optimization method is fundamentally based on the *shape grammar method* (Mandić et al., 2015). The *shape grammar* is a method of creating unlimited designs by linking the random design to grammar and rules. This method has a generative and analytical design process that begins with the definition of an initial shape and produces a set of transformation rules to reach unlimited design proposals. The *shape grammar* method is widely used to understand and analyze the texture of an urban area. First, Stiny and Gips (1972) proposed the shape grammars in the design process to produce the language of design. Then, Knight (1981) proposed an analytical approach for developing new designs using shape grammar following this work.

Along with the new design, the shape grammar method is also used to analyse historical urban areas to produce new urban solutions. This approach was named grammars derived from design (GDfD) by Mandic and Tepavčević (2015). GDfD evaluates the rules and shapes in a particular area and then selects the appropriate ones to create new designs. Figure 1.2 shows the GDfD process and its application. Compared to the flexible urban design method, GDfD is more limited due to its application to the strong local character. GDfD was used by Duarte, Rocha & Soares (2007) for the development of the Zaouiat Lakhdar neighbourhood in Marrakech and by Paio et al. (2011) to generate urban solutions by analysing informal settlements. Also, it was used by Paio and Turkienicz (2011) to examine the historical urban

design of Portugal. GDfD provides less flexibility than other methods such as the grammars for designing (GfD) and computer-generated architecture (CGA) method. However, GDfD is often preferred in places with strong local character. Figure 1.3 shows the flexibility and interaction level of GDfD.

The experimental design optimization method is based on the shape grammar and, more specifically, the context-dependent and less flexible design grammar (GDfD) method. This method was specifically chosen as the selected study area has many site-specific conditions and restrictive planning rules such as predetermined building height limit, plot, and street sizes. These issues will be explained in detail in Chapter 3 Field Study. In addition, the proposed method will systematically investigate the performance of the urban seafront building configurations in terms of urban ventilation and pedestrian wind comfort.
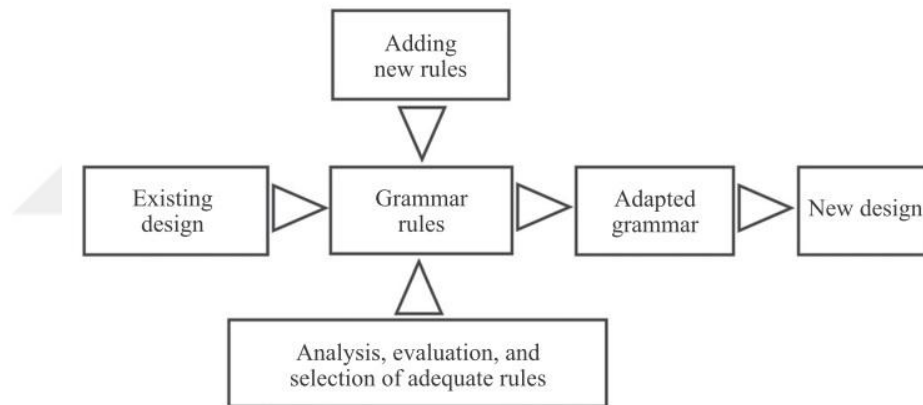
Figure 1.2 Grammars derived from designs (GDfD) method (Mandić et al., 2015)
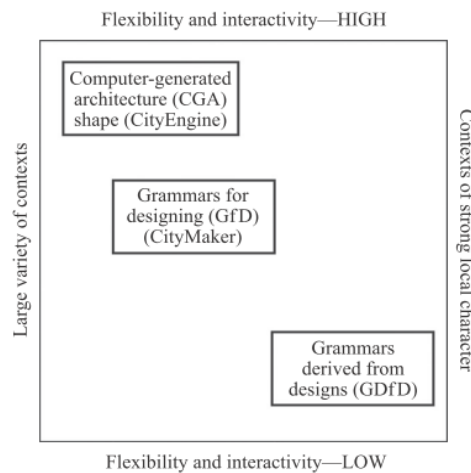
Figure 1.3 Comparison of the shape grammar methods (Mandić et al., 2015)

The experimental design optimization method is used to find the most appropriate solution to the design problem. One of the design optimization methods is the stochastic method, which is based on repetition in each iteration calculation and the search for a better solution in the next iteration. Genetic Algorithms (GAs) are one of the stochastic optimization methods. GAs tries to find the best solution to the problem by simulating the most appropriate natural selection and survival in nature (Holland, 1975). Holland developed the first GAs in 1960. The primary objective of GAs is to examine natural adaptations and understand how these events can be simulated on computers. O'Reilly et al. (1998) investigated the application of genetic algorithms as form generators to provide the designer with the first ideas they could be inspired by and know which direction to go when designing.

Genetic Algorithms (GA) are based on the concept of genotype and phenotype developed to explain genetic variations in evolutionary biology (Johanssen, 1911). GAs represents the initial rules of the urban pattern (genotype) that will help to generate more complex scenarios (phenotype). Figure 1.4 illustrates the code transmission from genotype to phenotype within the concept of evolutionary biology.
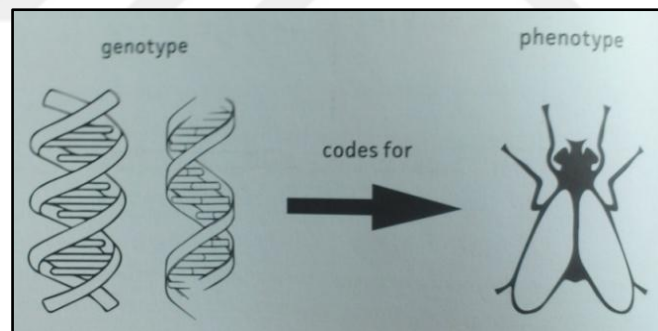
Figure 1.4 Code transmission from genotype to phenotype within the concept of evolutionary biology, Krautheim, Pasel, Pfeiffer, & Granberg, (2014)

The experimental design optimization method aims to create genetic algorithms and design rules to adapt the urban form to the wind, and more specifically, to provide pedestrian wind comfort without neglecting the urban ventilation by producing the best genetic algorithm. Using the GAs and design rules generated at the end of this research, the architects and planners can create their own phenotypic urban spaces in different contexts and situations.

1.5.2 Experimental Method

Wind flow studies around buildings cover several topics such as outdoor airflow, natural ventilation, heat transfer, thermal comfort, and pedestrian wind comfort. Because each study has its nature, it is critical to select the appropriate method based on the study's characteristics. There are three methods for performing urban wind flow studies in the literature:

- Mathematical method
- Wind tunnel method
- Computational Fluid Dynamics (CFD) method

There is no single universally accepted method as all have both advantages and disadvantages, and there is an ongoing debate about the performance of CFD and the wind tunnel method. The wind tunnel is considered more reliable than CFD as it provides actual experimental conditions. However, this method is time-consuming and costly compared to CFD. CFD allows rapid testing of more design variations using computer power and enables visualization of the whole flow field better than a wind tunnel. Wind tunnel uses a scale model, but CFD can be tested in a full-scale model (Blocken and Carmeliet, 2006). However, CFD requires a high degree of expertise in mathematical modelling, numerical methods, and fluid dynamics, unlike other building simulation tools. In addition, CFD calculations often require a lot of computer power and are often criticized because turbulence models are based on some assumptions and simplifications. (American Society of Civil Engineers Task Committee on Urban Aerodynamics, 2011).

Despite many programs offering a user-friendly interface and automatic meshing option, CFD is still very complex for designers as it requires a high degree of expertise in fluid mechanics and numerical methods. Also, the applicability of CFD to the design process is still difficult due to the time restriction if fully resolved results are necessary for the turbulent atmospheric boundary layer (ABL).

In this research, the computational fluid dynamics (CFD) method was specifically chosen to assist the experimental design study. It is more suitable for parametric

design studies (Van Hooff and Blocken, 2010) and allows for rapid testing of parametric design variations and visualization of the entire flow field. However, since it is claimed that CFD is still disadvantageous in terms of the reliability of the results and user error can cause uncertainty, and numerical errors in the results, the scientific validity of CFD is ensured by comparing CFD with wind tunnel tests.

1.6 Structure of the Research

The research consists of five different but interconnected chapters, as shown in Figure 1.5. The proposed structure begins with an introductory section that outlines the thesis. It then continues with a literature review that critically analyzes the previous studies. Finally, as the main part of the thesis, complementary field and design chapters based on CFD simulations are presented and concluded with the chapter results. Each chapter, in its context, attempts to answer a single research question posed earlier. Although each chapter has relatively independent structures, the cross relations to be established between these chapters ensure the integrity of the research. The contents of the chapters are briefly introduced below.

In general, the research requires broad knowledge that will include both urban design and urban physics fields. In the first chapter, the structure of the thesis is presented. Problems, arguments, objectives, scope, research questions, and methodology are explained in detail. Urban environmental issues related to wind are discussed in the context of the climatic adaptation and comfort of urban open spaces and, in the broader context, sustainable urbanization. The research questions and research objectives define the scope and research framework. The second chapter is based on the literature review, which aims to provide three aims:

- to discuss extensive knowledge in the field of urban design, and building and urban aerodynamics
- to reflect current theoretical and practical knowledge with a critical perspective
- to decode the unknown but needed design knowledge.

1. Introduction

- Problem statements & motivation
- Scope of the research
- Objectives
- Research questions
- Methods
- Structure of the research

⇩

2. Literature Review

- *How do building form, size, configuration and urban geometric indicators affect wind flow?*

    Urban Design
    - Sustainable urbanization & compact city paradigm
    - Wind phenomenon & quality of the wind
    - Wind-adaptation in vernacular urban settlements
    - Wind & comfort of urban open spaces

    Urban Physics
    - Aerodynamic science & building/urban aerodynamics

⇩

3. Experimental Field Study: Wind Flow Assessment of Building Configurations

- *What is the role of urban building configuration type in providing urban ventilation and pedestrian wind comfort?*

- Properties of the study area & urban morphological analysis
- CFD validation & comparison of the CFD tools (STAR CCM+ and SIMSCALE)
- CFD simulations to assess ventilation and wind discomfort risk in the real urban area
- Assessing the effect of urban building configuration type on wind flow

⇩

Transfer of findings from experimental field study to experimental design study

⇩

4. Experimental Design Study: Aerodynamic Design of Urban Seafront Buildings

- *How can urban seafront buildingsoptimally be designed to provide both urban ventilation and pedestrian wind comfort for mid-rise, dense, and compact Mediterranean cities?*
- *What are the key urban geometric indicators to provide urban ventilation and pedestrian wind comfort?*
- *How should urban open spaces between buildings along the seashore be positioned and how size should they be for urban ventilation and pedestrian wind comfort?*

- Analysis of site-specific context and climatic considerations
- Geometric definition of urban geometric indicators (design variables)
- Design of parametric urban seafront building configurations
- CFD simulations
- Analysis of the mean wind velocity in terms of ventilation efficiency and wind discomfort risk
- Synthesis & Discussion

⇩

5. Conclusion

- Summary of the research
- Findings
- Concluding remarks
- Perspectives and Future research

Figure 1.5 Structure of the research

This research includes the areas from building and urban aerodynamics, urban climatology, and computational wind engineering, and therefore requires a comprehensive, cross-cutting, and multidisciplinary study approach. In this conceptual framework, the research extensively reviews the literature on the two primary scientific areas: urban design and urban physics. In this chapter, the author aims to increase the permeability and interaction of extensive knowledge between urban design and urban physics.

The literature review addresses five topics in total. Although each chapter comprises relatively independent issues, they evaluate the different aspects of the main problems and the research questions in their context. This disjunction provides the reader with detailed background information. The five essential topics addressed in the literature review are the following:

- sustainable urbanization & compact city paradigm
- the wind phenomenon & the quality of wind
- wind-adaptation in vernacular urban settlements
- wind & comfort of urban open spaces
- aerodynamic science & building/urban aerodynamics

The literature review begins with an introductory chapter discussing today's dense and compact sustainable urbanization trend as the research aims to address the urban wind problems in dense and compact Mediterranean cities. The compact city paradigm which is the emerging trend in the context of sustainable urbanization is widely discussed, and also the classification of local urban zones by climate (LCZs) that refers to the compactness of urban form is presented.

In the second section of the literature review, wind and urban form are evaluated together and then, the chapter continues by discussing the wind phenomena and the quality of the wind depending on the wind source. In this way, it is aimed to discuss more clearly in the next section the reasons for applying distinct wind strategies in different climates depending on the quality of the wind.

In the third section of the literature review, the vernacular urban cases are presented where the wind is considered one of the prominent climatic factors in creating urban settlements. The vernacular urban cases are classified according to the basic climatic types and wind adaptation strategies. This section highlights how the basic wind design strategies in vernacular settlements in different climates differ according to site-specific, diversified climatic conditions. The vernacular urban cases included in the research do not only aim to answer the research question but also provide a comparison of the diversified wind adaptation strategies of buildings in different climates.

In the fourth section of the literature review, the comfort of urban open spaces and the impact of urban form on pedestrian wind comfort and ventilation of urban open spaces were addressed.

In the fifth section of the literature review, the foundations of aerodynamic science and its relation with building and urban form are discussed in detail. This part is important because examining and understanding the fundamental mechanisms of aerodynamic science in depth is essential for evaluating urban wind flow studies. Therefore, in this part, the author essentially aims to reveal fundamental mechanisms of wind flow characteristics. Urban wind studies that test the effects of various urban geometric indicators through a comprehensive literature review are also presented in this section.

In the third chapter of the research, a field study based on a morphological analysis of the actual urban fabric in the Alsancak neighbourhood, İzmir, was conducted to understand the relation between urban morphology and aerodynamic processes. This part aims explicitly to understand the role of urban building configuration on urban ventilation and pedestrian wind comfort with the CFD method. The field study aims to gain new insights from the existing urban area and shape the design study in the next chapter. In this chapter, the validation process of the CFD method for turbulent atmospheric boundary layer (ABL) is also described step-by-step. This part provides detailed explanations of CFD validation, including all calculations, to help architects and urban planners to follow the same protocol in urban wind flow studies and increase the CFD solution accuracy. A flowchart

outlining the CFD validation process is presented for the use of architects and urban planners in urban wind flow analysis. This flowchart is derived from Best Practice Guidelines and the author's experience obtained during the research process. Also, in this chapter of the research, the predictive accuracy of two popular CFD codes, STAR-CCM+ (STAR) and SIMSCALE, are compared to find the most suitable CFD code for the current research.

The fourth part of the research presents an experimental design study that complements the fieldwork. There are many reasons for this. In the actual urban area, some details and morphological features make the urban fabric non-orthogonal. The buildings are in different sizes and configurations. Moreover, the findings from the field study are limited to a specific location as they take into account site-specific knowledge such as surrounding buildings and prevailing winds. This makes it difficult to generalize and transfer the results obtained from the field study to other studies. Internal validity of field studies is generally lower than design studies due to many factors that make the generated information site-specific. The relationships between morphological parameters and flow patterns can be studied more comprehensively by simplifying urban configurations and testing them in generic form (Merlier, 2015).

As different from the field study, the experimental design study systematically investigates the research questions to obtain empirical results. In particular, design studies based on simple generic building blocks abstracted from real urban fabric have higher internal validity. In addition, the findings obtained from the design study can be transferred to similar situations and environments because, in the configurations, the buildings and streets are sharp-edged, straight, and orthogonal. But it is more hypothetical and far from the real problem. Therefore, a field and a design study are structured in a complementary relationship so that the internal and external validity of the research is high.

Starting the field study with the analysis of actual urban buildings of different building sizes and configurations on wind flow, the author felt the need to construct the design study in a format where only the building configuration was tested. Thus, it has created a working plane that increases the internal validity of the research and

is free from the influence of confounding factors such as different building sizes and non-orthogonal urban fabric.

The experimental design study should be clearly emphasized that the design study is not intended to assign a *macro form* to the seafront urban buildings but rather to construct a *functional system* based on the selected GAs for urban ventilation and pedestrian wind comfort. Moreover, the aim here is to provide the comfort of urban open spaces between seafront buildings rather than the design of urban seafront buildings. To achieve this, the aerodynamic flow tests of the proposed urban seafront buildings were carried out by means of computational fluid dynamics. The results of CFD modelling were revealed, and the best possible urban seafront buildings were found. But, the design study aims not only to find the best possible urban seafront building configuration for urban ventilation and pedestrian wind comfort but also to reveal critical design variables (urban geometric indicators) in the design of urban seafront buildings. The design study initially focuses on the design of seafront buildings, but in the specific context, it addresses the factors of building configuration and urban geometric indicators.

In the light of the findings, an alternative urban seafront building configuration in dense and compact form is proposed at the end of the chapter. Finally, the generated empirical knowledge is synthesized and presented in the form to be used in the early design (sketch) process. This stage is critical because complex empirical knowledge of airflows is required to eliminate the outdoor wind-related problems. However, the knowledge needs to be easily understood and easily transferred to the architects or urban planners so that they can easily apply the knowledge to practical situations. For this reason, a comparative classification of simplified generic urban forms in terms of ventilation and pedestrian wind discomfort risk is presented together at this stage. This comparison chart summarises the information obtained and explained in depth in the literature, fieldwork, and design chapters and compares the wind behaviour of the proposed urban seafront building configurations with the well-known building configurations.

In the fifth chapter, the main findings and conclusions are presented, and perspectives and suggestions for future work are made. Moreover, the degree of

applicability of the study to the field and its scientific contribution to the area with limitations were discussed.

CHAPTER 2

LITERATURE REVIEW

This section of the literature review discusses the compact urban planning approach in the context of sustainable urbanization. Then, following the discussion of the wind phenomena and the quality of the wind, the vernacular urban cases adapted to the wind are presented. Finally, the impact of urban form on pedestrian wind comfort and ventilation of urban open spaces is discussed.

2.1. Urban Form and Sustainable Urbanization

The last years of the twentieth century were the years when the sustainability debates were on local, regional, and global agendas. Studies to find the ideal urbanization continues in the 21st century, including the concept of sustainability. The concept of sustainable development has emerged at the international level with the first report of the UN, Our Common Future (WCED, 1987) pointing out that humanity faces the destruction of natural resources, increased pollution, and poverty. In discussing how to reach a sustainable world and the future, cities are defined as 'building blocks'. More specifically, the city form is at the centre of the debate on sustainable urbanization. EPA (2001) reported that the urban form directly affects the habitat, ecosystems, endangered species, fragmentation of land and the replacement of natural land cover directly on impermeable surfaces. Cervero (1998) stated that the city form also affects travel behaviour, air quality, cultivated, planted and early extinction of wetlands, soil pollution, global climate, and noise.

Today, there is a general negative point of view to the urban sprawling planning initiative, and the sprawling city ('urban sprawl') is not considered a sustainable planning approach. The sprawling city refers to the urban planning approach where urban functions, including residential, industrial, and commercial services, are placed away. In this planning initiative, the settlements are sparser and open-type, and there is no restriction on land use. The problems of transportation, access and disappearance of rural areas, high infrastructure and service expenses, and social problems constitute the negative aspects of this planning initiative.

Holden (2004) places the urban form on centralization-decentralization and concentration-sprawl tendencies. Figure 2.1 shows the formation of four different models for sustainable urban form. According to this approach, the compact city represents a centralized and concentrated urban planning approach, while the sprawling city represents a centralized and sprawling urban planning approach.
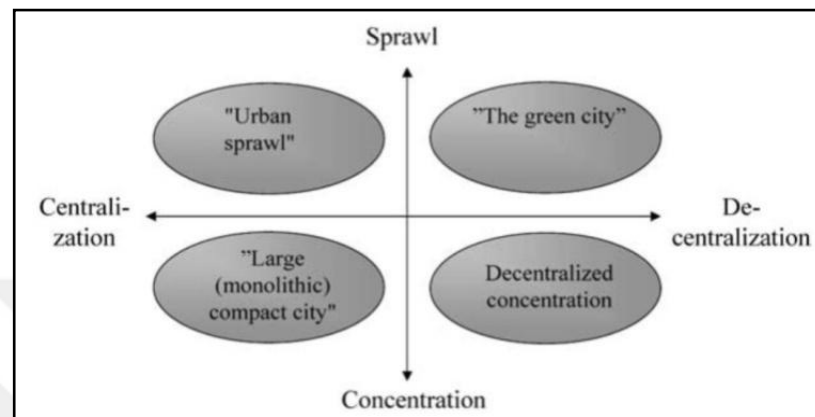
Figure 2.1 Four models for sustainable urban forms (Holden 2004)

The compact city planning initiative spread after 1980 with the *new urbanization movement* in the US. It was first proposed by Dantzing and Saaty (1973) as an alternative to the conventional modern city based on an automobile-oriented planning approach to improve the quality of life in the city. The compact city is based on the planning approach that the problems of the modern city can be prevented by a more intense, dense, and tightly textured urban form. It mainly focuses on concentration rather than sprawl. Although the concentration of residential areas in the city center is shown to be the leading cause of environmental problems, it is thought that this concentration increases resource efficiency and provides environmental advantages by providing the common use of land, infrastructure, water, energy, road, and public transportation systems.

The compact city is based on the anti-sprawl planning approach. It aims to counter the negative social, economic, and environmental impacts of the sprawled city. The Commission of the European Communities (1990) in the Green Paper on Urban Environment Report and the UK Department of the Environment (1993) in the Sustainable Development Strategy Report stated that the compact urban model has more environmental benefits compared to the most decentralized urban form of the

United States, England and Australia. According to Lin and Yang (2006), the paradigm of the compact city consists of three main elements: density, the mix of uses, and intensification, as shown in Figure 2.2.
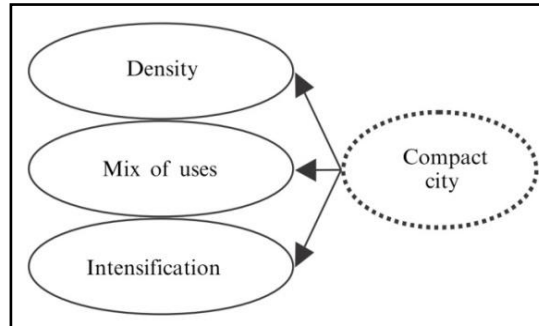
Figure 2.2 Three basic components of compact city form (Lin and Yang, 2006)

Today's ideal urbanization points to the concept of sustainable urbanization and proposes dense and compact city form as the ideal sustainable urban form (Holden, 2004). On the other hand, the city form has a significant impact on urban ventilation and pedestrian wind comfort, and a compactly organized city significantly reduces wind speed (Hu et al., 2018). In this section, sustainable urbanization and compact city form are discussed in detail in this context. Since the compact urban form is proposed in the context of sustainable urbanization and has an impact on urban ventilation and pedestrian wind comfort, this study particularly aims to provide wind adaptation of seafront buildings for pedestrian wind comfort and urban ventilation within a compact urban organisation.

2.1.1 Local Climate Zones (LCZs)

The density and compactness of urban form are variable in urban and rural sites. For this reason, along with the Holden's classification of urban form from the point of urban planning, Stewart and Oke (2012) presented the local climate zones (LCZ) from the point of urban physics to quantitatively describe and classify the density and compactness level of urban and rural sites. The "local climate zone" (LCZ) classification system physically describes a city. This classification is widely used for urban temperature and heat island studies. Figure 2.3 shows the local climatic zones with complete descriptions of built and land cover types.
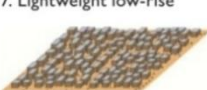
Built types	Definition	Land cover types	Definition
1. Compact high-rise	Dense mix of tall buildings to tens of stories. Few or no trees. Land cover mostly paved. Concrete, steel, stone, and glass construction materials.	A. Dense trees	Heavily wooded landscape of deciduous and/or evergreen trees. Land cover mostly pervious (low plants). Zone function is natural forest, tree cultivation, or urban park.
2. Compact midrise	Dense mix of midrise buildings (3–9 stories). Few or no trees. Land cover mostly paved. Stone, brick, tile, and concrete construction materials.	B. Scattered trees	Lightly wooded landscape of deciduous and/or evergreen trees. Land cover mostly pervious (low plants). Zone function is natural forest, tree cultivation, or urban park.
3. Compact low-rise	Dense mix of low-rise buildings (1–3 stories). Few or no trees. Land cover mostly paved. Stone, brick, tile, and concrete construction materials.	C. Bush, scrub	Open arrangement of bushes, shrubs, and short, woody trees. Land cover mostly pervious (bare soil or sand). Zone function is natural scrubland or agriculture.
4. Open high-rise	Open arrangement of tall buildings to tens of stories. Abundance of pervious land cover (low plants, scattered trees). Concrete, steel, stone, and glass construction materials.	D. Low plants	Featureless landscape of grass or herbaceous plants/crops. Few or no trees. Zone function is natural grassland, agriculture, or urban park.
5. Open midrise	Open arrangement of midrise buildings (3–9 stories). Abundance of pervious land cover (low plants, scattered trees). Concrete, steel, stone, and glass construction materials.	E. Bare rock or paved	Featureless landscape of rock or paved cover. Few or no trees or plants. Zone function is natural desert (rock) or urban transportation.
6. Open low-rise	Open arrangement of low-rise buildings (1–3 stories). Abundance of pervious land cover (low plants, scattered trees). Wood, brick, stone, tile, and concrete construction materials.	F. Bare soil or sand	Featureless landscape of soil or sand cover. Few or no trees or plants. Zone function is natural desert or agriculture.
7. Lightweight low-rise	Dense mix of single-story buildings. Few or no trees. Land cover mostly hard-packed. Lightweight construction materials (e.g., wood, thatch, corrugated metal).	G. Water	Large, open water bodies such as seas and lakes, or small bodies such as rivers, reservoirs, and lagoons.
8. Large low-rise	Open arrangement of large low-rise buildings (1–3 stories). Few or no trees. Land cover mostly paved. Steel, concrete, metal, and stone construction materials.	**VARIABLE LAND COVER PROPERTIES** Variable or ephemeral land cover properties that change significantly with synoptic weather patterns, agricultural practices, and/or seasonal cycles.	
9. Sparsely built	Sparse arrangement of small or medium-sized buildings in a natural setting. Abundance of pervious land cover (low plants, scattered trees).	b. bare trees	Leafless deciduous trees (e.g., winter). Increased sky view factor. Reduced albedo.
		s. snow cover	Snow cover >10 cm in depth. Low admittance. High albedo.
10. Heavy industry	Low-rise and midrise industrial structures (towers, tanks, stacks). Few or no trees. Land cover mostly paved or hard-packed. Metal, steel, and concrete construction materials.	d. dry ground	Parched soil. Low admittance. Large Bowen ratio. Increased albedo.
		w. wet ground	Waterlogged soil. High admittance. Small Bowen ratio. Reduced albedo.

Figure 2.3 Local Climate zones, built and land cover types with complete definitions (Stewart 2011)

In the "local climate zone" (LCZ) classification system, two fundamental indicators are used to physically describe the urban geometry: aspect ratio (mean height-to-width ratio of street canyons-H/W) and the building surface fraction (ratio of building plan area to total plan area-%). The LCZs are detailed in Table 2.1,

including the values of all geometric indicators. In the fourth chapter of this research, the author used Oke's classification system to describe the density and compactness level of the designed urban seafront building configurations.

Table 2.1 Values of geometric indicators for local climate zones, Stewart and Oke, (2012)

Local climate zone (LCZ)	Sky view factor[a]	Aspect ratio[b]	Building surface fraction[c]	Impervious surface fraction[d]	Pervious surface fraction[e]	Height of roughness elements[f]	Terrain roughness class[g]
LCZ 1 _Compact high-rise_	0.2–0.4	> 2	40–60	40–60	< 10	> 25	8
LCZ 2 _Compact midrise_	0.3–0.6	0.75–2	40–70	30–50	< 20	10–25	6–7
LCZ 3 _Compact low-rise_	0.2–0.6	0.75–1.5	40–70	20–50	< 30	3–10	6
LCZ 4 _Open high-rise_	0.5–0.7	0.75–1.25	20–40	30–40	30–40	>25	7–8
LCZ 5 _Open midrise_	0.5–0.8	0.3–0.75	20–40	30–50	20–40	10–25	5–6
LCZ 6 _Open low-rise_	0.6–0.9	0.3–0.75	20–40	20–50	30–60	3–10	5–6
LCZ 7 _Lightweight low-rise_	0.2–0.5	1–2	60–90	< 20	<30	2–4	4–5
LCZ 8 _Large low-rise_	>0.7	0.1–0.3	30–50	40–50	<20	3–10	5
LCZ 9 _Sparsely built_	> 0.8	0.1–0.25	10–20	< 20	60–80	3–10	5–6
LCZ 10 _Heavy industry_	0.6–0.9	0.2–0.5	20–30	20–40	40–50	5–15	5–6
LCZ A _Dense trees_	<0.4	>1	<10	<10	>90	3–30	8
LCZ B _Scattered trees_	0.5–0.8	0.25–0.75	<10	<10	>90	3–15	5–6
LCZ C _Bush, scrub_	0.7–0.9	0.25–1.0	<10	<10	>90	<2	4–5
LCZ D _Low plants_	>0.9	<0.1	<10	<10	>90	<1	3–4
LCZ E _Bare rock or paved_	>0.9	<0.1	<10	>90	<10	<0.25	1–2
LCZ F _Bare soil or sand_	>0.9	<0.1	<10	<10	>90	< 0.25	1–2
LCZ G _Water_	>0.9	<0.1	<10	<10	>90	–	1

[a] Ratio of the amount of sky hemisphere visible from ground level to that of an unobstructed hemisphere

[b] Mean height-to-width ratio of street canyons (LCZs 1–7), building spacing (LCZs 8–10), and tree spacing (LCZs A–G)

[c] Ratio of building plan area to total plan area (%)

[d] Ratio of impervious plan area (paved, rock) to total plan area (%)

[e] Ratio of pervious plan area (bare soil, vegetation, water) to total plan area (%)

[f] Geometric average of building heights (LCZs 1–10) and tree/plant heights (LCZs A–F) (m)

[g] Davenport et al.'s (2000) classification of effective terrain roughness (z_0) for city and country landscapes. See Table 5 for class descriptions

2.1.2 Wind and Urban Form

The urban form has the potential to significantly alter wind flow in urban environments. Depending on the quality of the wind, the urban form can be arranged to block, deflect or divert the wind flow. Therefore, this section primarily focuses on analysing the quality of the wind in developing design strategies for wind adaptation of the buildings.

2.1.2.1 The Wind Phenomenon and the Quality of Wind

The wind is the movement of the atmospheric gases driven by differences in atmospheric pressure (Krautheim et al., 2014). The difference in atmospheric pressure results from the uneven distribution of solar radiation on Earth. Therefore, the development of winds on Earth is mainly related to the distribution and the location of land, water sources, and green areas. The diurnal and seasonal surface temperature differences between these areas cause differences in atmospheric pressure and the occurrence of the winds.

When a piece of land is warmer than a water source, the wind blows from the water source towards the land and carries the air molecules. Depending on the wind source, the wind can be hot or cool, fast or slow, dry or humid, clean or dusty, and regular or irregular (Gut and Ackerknecht, 1993). Accordingly, the wind source gives information about the quality of the wind depending on where it originally came from.

Figure 2.4 A sandstorm that brings hot desert air to an urban settlement (World Meteorological Organization, 2022)

The quality of the wind differs in various climates: it might be of low quality to be avoided or of high quality to be used in urban environments. For example, in hot-arid climates, the hot desert wind is undesirable since it carries dry, dusty, and hot air that is undesirable for human health and comfort. Therefore, many vernacular urban settlements avoid exposure to the hot desert wind to protect urban open spaces. Figure 2.4 shows a sand storm that brings hot desert air to an urban settlement. Since the source of the sand storm is the desert, it carries hot and dusty air masses and causes undesirable air conditions in urban settlements. However, in tropical climates, the sea breeze is desirable. Because its origin is the sea, the sea breeze carries the clean and cool air mass from the sea to urban environments. Its formation is regular because it depends on the temperature difference between the sea and the land. In addition, since the sun's energy to heat land and water masses increases in summer, it is faster in summer and weaker in winter. These features are desirable to reduce excessive city temperature in summer, avoid the wind chill effect in winter, and ventilate the city with fresh air.

2.1.3 Wind-Adaptation in Vernacular Urban Settlements

This section of the literature review examines vernacular urban settlements built using traditional *trial and error* methods without architects and urban planners. This section requires an in-depth analysis of climatic factors in vernacular settlements because, in such settlements, urban form is mainly influenced by climatic factors as much as geography and culture. Moreover, each climate has its own unique climatic conditions, and therefore it creates unique urban design solutions over the years by trial and error method. However, climatic factors are not taken into account by today's urban producers to maximize economic benefits and who think speculative. In this context, the reassessment and in-depth analysis of local climate knowledge obtained from vernacular urban settlements can be helpful to re-adapt climatic factors to the sustainable development process of cities and reshape today's sustainable urban settlements.

Vernacular design develops with the tradition of observation and practice accumulated in a specific region. This is "design without a designer method" traditionally passed down from one generation to another (Golany, 1996). In

24

addition, micro-climatic factors such as sun and wind have been taken into account to create the urban form in vernacular urban settlements (Evans, 1980; Olgyay, 1963; Tablada, 2006). However, this chapter only focuses on the influence of the wind factor.

Although both show hot climate characteristics, the adaptation of the urban form to the wind may be different in hot-arid and tropical climates. Therefore, it is necessary to analyze climate types separately. This section examines four different climatic zones, hot and arid, tropical, temperate and Arctic climatic regions.

2.1.3.1 Wind-Adaptation in Hot-arid Climate

In hot and arid climates, winds are quite strong due to high daily temperature variations. Usually, in this climate, the Northwind carries cold fresh air and provides a feeling of thermal relief, while winds from the hot desert carry warm air and often cause thermal stress and sand turbulence.

Free flow of wind in urban open areas is undesirable as wind is often dusty and fast in hot and arid climates. Therefore, avoiding such winds is critical to improving the urban microclimate and the quality of life of urban residents. Desired microclimate conditions can be achieved with dense urban forms consisting of inward-looking buildings and narrow streets. Specifically, the irregular urban form of narrow, zigzag streets and central courtyards impedes the free flow of wind. However, the urban form is not precisely dense and compact, as adequate ventilation is required to mitigate hot climatic conditions. The urban form, therefore, allows limited wind flow for ventilation.

Figure 2.5 shows the various urban block typologies commonly seen in hot and arid climates. A dense and concentrated urban configuration consisting of several streets removes undesirable winds from the streets and reduces the penetration of hot and dusty wind into the urban fabric. Such an urban form corresponds to a semi-porous urban configuration with less windy streets and more protected open public spaces.

In the urban configuration, a centrally located courtyard has a pivotal role in this climate. It is desirable as long as the aspect ratio of the courtyard (H: building height/W: building width) is high to protect the outdoor areas from the wind. The high aspect ratio also shields open spaces from the sun.
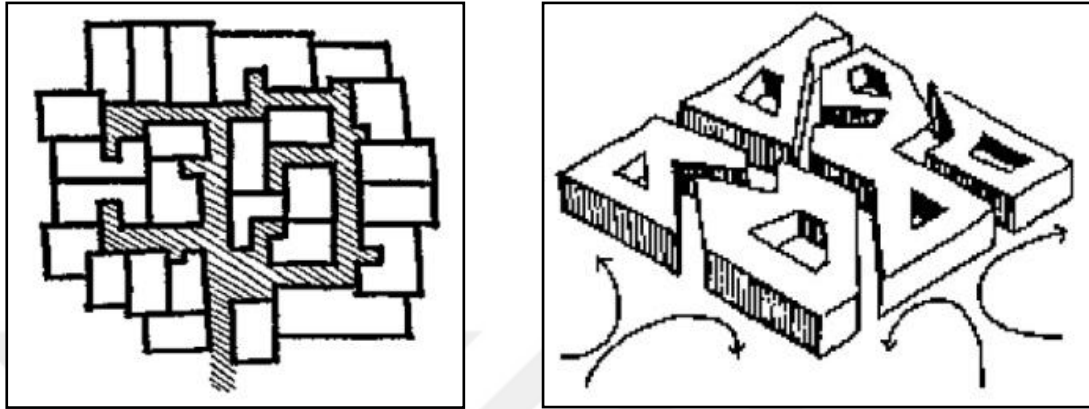
Figure 2.5 Urban form typologies in hot-arid climate (Gut and Ackerknecht, 1993)

The shifted urban block configuration is often used to block the hot and dusty desert wind in the hot and arid climate. Figure 2.6 shows the combined use of shifted and grid-aligned urban block configurations. The shifted part blocks the hot wind into the urban fabric, while the grid-aligned part of the configuration allows the desired wind in urban open spaces. The urban form can respond to different wind regimes and characteristics with this configuration.
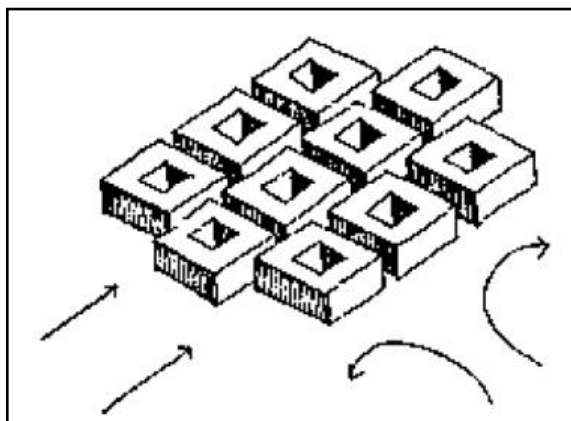
Figure 2.6 Combined use of shifted and grid-aligned urban block configurations (Gut and Ackerknecht, 1993)

Figure 2.7 shows the town of Kahan, which was founded in ancient Egypt around 2,000 BC. There are two prevailing wind directions in the town: pleasant north winds

and hot desert west winds. The north wind is desirable and is directed to the urban fabric. Therefore, the official's housing is located on the north side to benefit from the pleasant north wind. However, the workers' housing is located on the west part of the site to protect the official's housing from hot desert west winds.
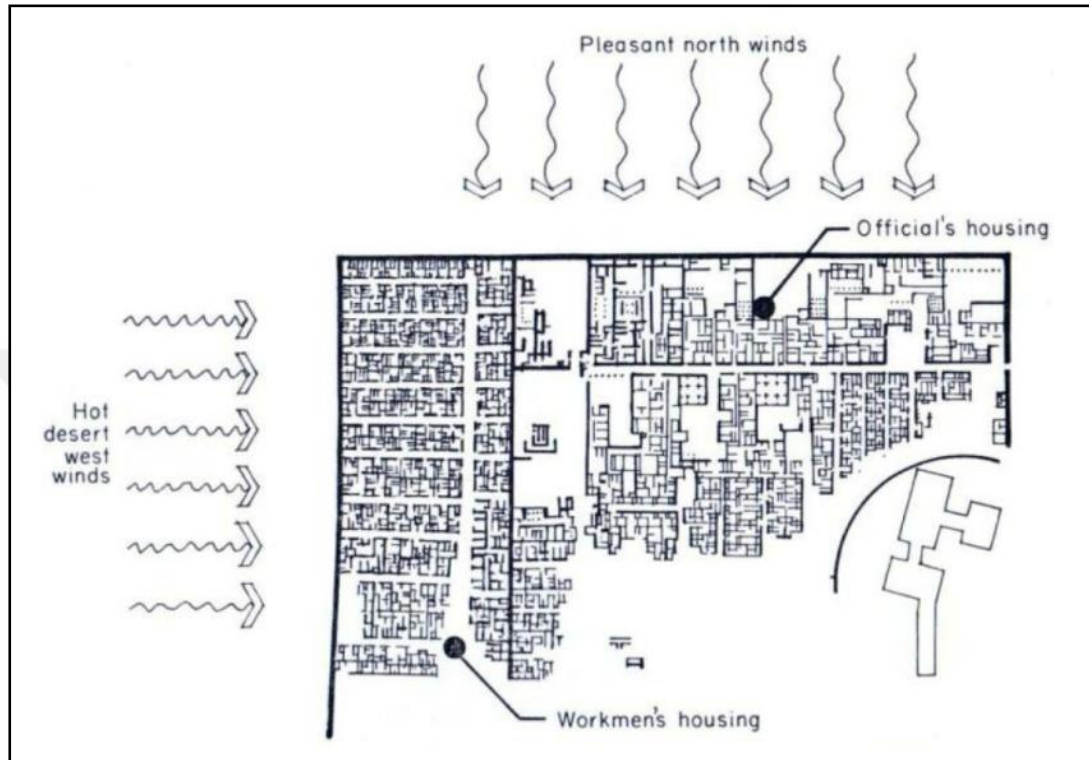
Figure 2.7 Wind-adapted housing arrangement in Kahan, Egypt, around 2000 B.C. (Aynsley, Melbourne, & Vickery, 1977)

2.1.3.2 Wind-Adaptation in Tropical Climate

In tropical climates, winds are light, gentle, and short-term (Gut and Ackerknecht, 1993) due to the small diurnal temperature variations. However, summer breezes blowing from the sea are desirable and have a significant cooling effect, as they accelerate cooling through transpiration and reduce the sensible temperature.

In tropical climates, cross ventilation is one of the strategies to mitigate high temperature and humidity. Elongated urban settlements (Figure 2.8) arranged in a line promote cross ventilation. An open and dispersed urban configuration maximizes wind exposure for ventilation and provides cooling. In this climate, an urban fabric providing more permeability and minimum resistance to summer winds is more advantageous than dense urban configurations that prevent wind flow and

cause large stagnant wind flow areas behind the structures. Figure 2.9 shows a typical urban configuration in a tropical climate. The settlement is windswept and has a low density. Large open spaces between buildings provide a free flow of wind.
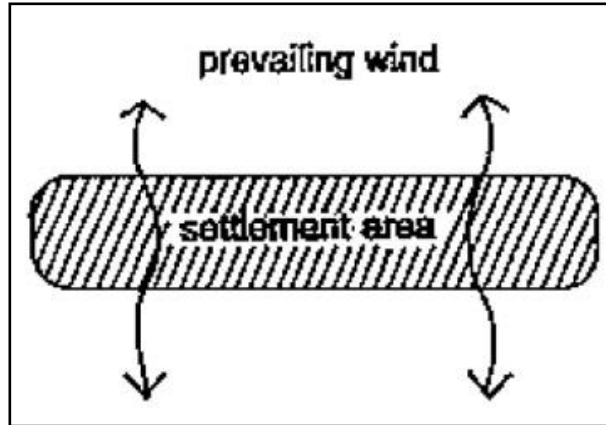
Figure 2.8 Elongated settlement configuration (Gut and Ackerknecht, 1993)
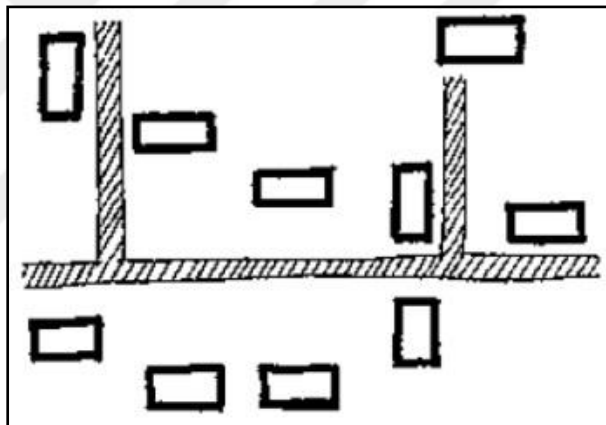
Figure 2.9 Dispersed settlement pattern in tropical climate (Gut and Ackerknecht, 1993)

2.1.3.3 Wind-Adaptation in Temperate Climate

The wind has both positive and negative effects in temperate climates. The cooling effect of the wind is desirable to moderate heat stress in summer; however, it is not desired as it reduces the temperature in winter. The city of Korcula is a vernacular urban settlement that shows the adaptation of the urban fabric to various wind regimes with different characteristics. The city is located in the temperate zone, at latitude 43 °N latitude and longitude 16 °E. It shows the characteristics of a typical Mediterranean climate and experiences mostly hot-dry summers and mild-wet winters.

The wind pattern on this island is multi-directional, with three dominant winds blowing from the East (Jugo), West (Maestral), and North (Bora). In the urban configuration, the streets are arranged along the east and western axes and act as an air channel allowing western and eastern summer breezes to pass through the urban fabric. But the cold North wind (Bora) is blocked by buildings to avoid thermal discomfort in urban open spaces. Figure 2.10 shows the urban configuration of Korcula, exposed to summer breezes and sheltered from the northern winter wind.
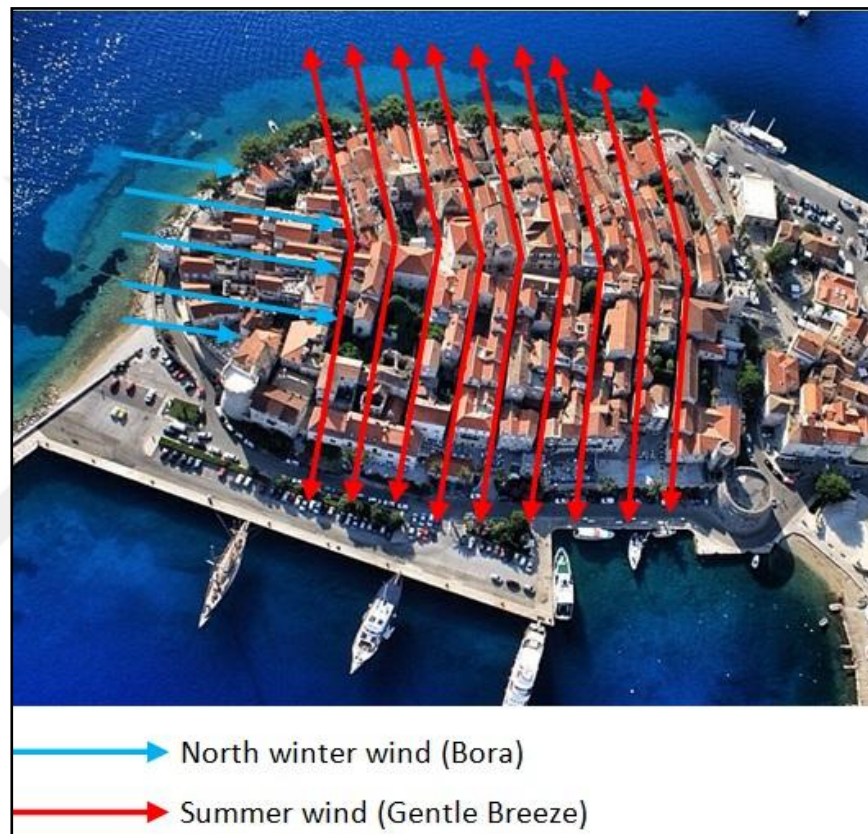
Figure 2.10 Wind flow regimes in Korcula (Baş & Egercioglu, 2016)

2.1.3.4 Wind-Adaptation in Arctic Climate

In Arctic climates, wind protection is essential for the comfort of urban open spaces. Urban blocks have inner courtyards protected by the cold wind, and the streets are often narrow. Wind sheltered effect in urban open spaces is achieved by the high aspect ratio of courtyards and streets. In addition, the dense urban configuration makes public spaces less windy and more sheltered from cold winds.

The town of Ormen Lange is an ecological Arctic city surrounded by an urban wall acting as a windbreak to reduce the influence of cold north winds in urban public spaces. The urban settlement consists of small protected open spaces to promote community life and outdoor activities. Sunny and wind-sheltered areas provide livable open spaces for residents around schools, shops, and bus stops in harsh winter conditions. Figure 2.11 shows the *urban wall* around the town.
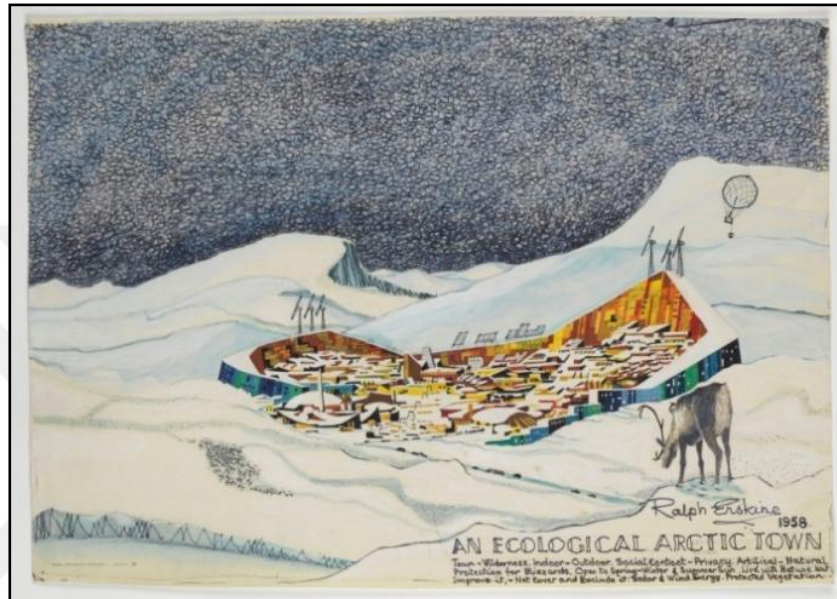
Figure 2.11 Ecological Arctic Town, Ralph Erskine, 1958, (ArkDes collections, ARKM.1986-17-0362)

2.1.4 Wind and Comfort of Urban Open Spaces

Urban open spaces have a central role in urban life. Therefore the comfort of urban open spaces is necessary for viable urban life. However, the loss and little attention to climate-sensitive design with intensive urbanization and the scarcity of knowledge of urban climatology (Eliasson, 2000) make urban open spaces uncomfortable. The comfortable design of urban open space can improve urban quality of life, promote walking and pedestrian activities and thus ensure the sustainability of socio-economic life. However, it is difficult to provide climatic comfort in urban open spaces as they are exposed to various climatic factors such as sun, wind, and rain.

Urban open spaces are the places most affected by the wind effects caused by the buildings. A group of city planners has carried out theoretical and practical studies to

design wind-comfortable cities (Bosselmann et al., 1998; Gehl, 2010; Whyte, 1980). However, urban design experts do not have sufficient technical knowledge and experience in wind flow dynamics and simulation techniques. On the other hand, wind engineers who are competent in this subject do not generate urban planning and design policies. Therefore, these two groups must work together on an interdisciplinary platform to create wind comfortable urban open spaces for pedestrians.

The wind adaptation of urban open spaces can revitalize urban open spaces by increasing health, comfort, and liveability. In providing the comfort of urban open spaces, the wind has a pivotal role. However, the wind is the most complex one within micro-climatic elements. Because the wind is a dynamic phenomenon, the direction and speed are unpredictable. Krautheim et al. (2014) stated that wind has limited scientific predictability; therefore, it is difficult to predict it. These features of the wind make it difficult to provide wind comfort in the design of urban open spaces.

Urban settings are exposed to various wind patterns of different qualities (Skote, Sandberg, Westerberg, Claesson, & Johansson, 2005). However, the urban form has considerable potential to resist, direct and modify the wind flow. It can improve comfort conditions for inhabitants by modifying urban wind patterns (Gut and Ackerknecht, 1993). In addition, the urban form can act as a kind of "selective filter" for wind patterns (Nakamura and Oke, 1988) and manipulate wind behaviour or force the wind to change its direction (Krautheim, 2014).

Depending on the quality of the wind, the urban form can be designed in concentrated form to protect urban public spaces from low-quality wind or in a porous form to improve thermal comfort with the high-quality wind. For example, while the desired wind can be channelled to the urban fabric, the contrary, low-quality wind can be diverted over the site. However, the urban form is limited to controlling the wind flow in the urban environment. The reason for this threefold: first, the wind direction and speed are unpredictable and random. Second, the urban fabric as a static structure has limited potential in response to dynamic and multi-directional wind patterns. Third, it is not straightforward to adapt whole city

structures to the wind. To design a more reactive urban form against wind flow, Gut and Ackerknecht (1993) propose to distinguish prevailing and occasional wind patterns in the urban environment.

2.1.4.1 Pedestrian Wind Comfort of Urban Open Spaces

In the ongoing urbanization process, the size of the buildings, and more specifically their height, tends to increase in urban centres. This trend causes the wind to have strong mechanical effects on the human body in urban open spaces and threatens the comfort and safety of pedestrians (Penwarden, 1973; Stathopoulos and Blocken, 2016; Wise, 1971). When the wind speed and frequency are high, the pedestrian becomes uncomfortable and tries to protect himself. This action is defined as "pedestrian disturbance" by Bottema (2000). Figure 2.12 shows the inhabitants of the city of Izmir struggling with the intense mechanical force of the sea breeze. In Figure 2.12a, the residents are outside the building's influence area, and at this location, only the mechanical force caused by the sea breeze affects the residents. In Figure 2.12b, the residents are under the influence of the building-induced mechanical force at the corner of the building. In this location, the wind causes stronger mechanical forces on the urban inhabitants, and therefore they feel more wind discomfort.
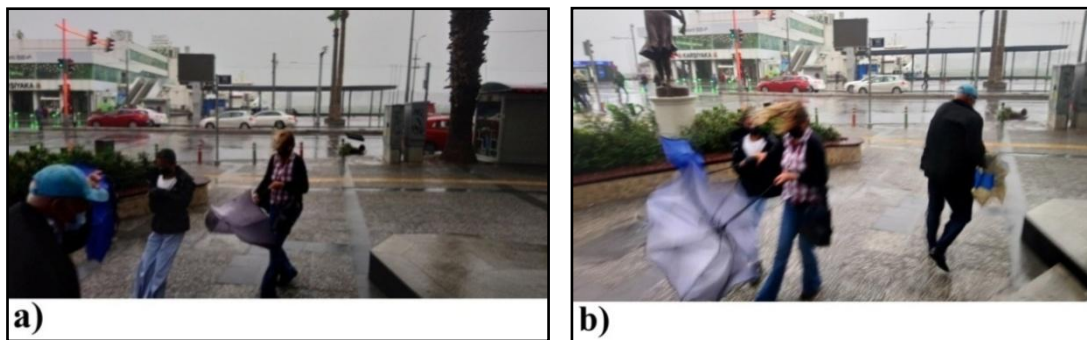
Figure 2.12 Wind discomfort of urban residents in a coastal passage between two parallel buildings, the resident, is outside the building influence area (a); the resident is under the building influence area (b); (the author's own archive, 2021)

Since the early 1970s, many pedestrian wind comfort assessment criteria have been developed (Isyumon and Davenport, 1975; Lawson, 1978; NEN 8100, 2006). These criteria are based on statistics, and therefore, the tolerable and unacceptable wind speed thresholds are different in each comfort criterion. The function of

pedestrian activities is essential in establishing wind comfort criteria, and wind speed limits are determined according to pedestrian activities divided into different categories. Different wind speed limits are defined for each activity, such as walking, strolling, and short and long-term seating. The smaller the wind speed limit is, the higher the comfort criteria.

Isyumon and Davenport (1975) created the pedestrian wind comfort criterion by classifying pedestrian activities such as walking, walking, and sitting. This classification also considers the frequency of exceeding the wind speed limit. Lawson (1978) has created a new comfort criterion based on the Land Beaufort Scale, which classifies the wind speeds on this scale by adding the disturbance effect of wind speed on pedestrians. The NEN 8100 sets the wind speed limit to 5 m/s for wind comfort and 15 m/s for wind safety. However, tolerable and unacceptable threshold wind speed and the frequency of exceeding threshold values are identified differently in each comfort criterion. Melbourne (1978) states that the wind phenomenon and its incidence are very complex, and it is problematic that the threshold values developed for pedestrian comfort are based on statistical data. Therefore, using different wind comfort criteria will have other consequences, and the choice of wind comfort criteria is critical for pedestrian wind comfort assessment.

Many studies have been carried out to understand pedestrian wind comfort in urban open spaces (Beranek and Van Koten, 1982; Blocken, Carmeliet, & Stathopoulos, 2007; Reiter, 2010; Stathopoulos and Blocken, 2016). However, pedestrian wind comfort is a highly complex issue because it includes cross-cutting and multidisciplinary areas such as computational fluid dynamics, aerodynamics, atmospheric boundary layer meteorology, statistics, architecture, and urban planning.

2.1.4.2 Ventilation of Urban Open Spaces

Urban open areas suffer from the urban heat island (UHI) effect and air pollution due to inadequate ventilation. Urban ventilation with wind flow can provide heat dispersion and dilution of pollution in urban open spaces (Chew, Nazarian, & Norford, 2017). In addition, wind flow reduces the intensity of the UHI effect (He et

al., 2020; Jamei et al., 2020; Memon and Leung, 2010) and improves urban air quality (Fenger, 1999).

Air pollution is one of the causes of various health problems such as respiratory diseases (Manisalidis, Stavropoulou, Stavropoulos, & Bezirtzoglou, 2020) and urban air quality strongly depends on wind flows (Fenger, 1999). The wind helps to reduce outdoor air pollution by removing toxic emissions from urban environments. Samson (1988) points out that higher wind speeds dilute pollutants and that the dispersion rate depends on the wind's strength. Therefore, adequate wind speed is necessary to reduce health risks from exposure to high pollutant concentrations in urban environments.

Many studies indicate that the pollutant concentration increases either in calm weather conditions or at very low wind speeds (Dickson, 1961; Lawrence, 1970). Contaminant concentrations are highest, on the ground, behind the building and decrease with height (Oke, 1988). Therefore, stagnant air areas that prevent the spread of pollutants must be minimized. A higher number of COVID-19 cases reported in cities with a low average wind flow velocity during the development of the COVID-19 pandemic (Coccia, M. 2020) shows the importance of ventilation of urban open spaces with the wind flow. In this regard, a higher wind speed is desirable for urban pollutant dilution, and a wind speed of at least 1 m/s is recommended as a standard for urban air pollution diffusion (Q., Xu, & Z., Xu, 2020).

Ventilation with wind flow plays a pivotal role in reducing the thermal discomfort of urban inhabitants in urban open spaces. Ventilation provides relief from the heat, especially in hot and humid coastal areas where humidity causes thermal stress, as it accelerates the body's transpiration. In addition, increasing wind speed near the ground improves thermal comfort in hot climates, as the high wind speed can increase convective heat transfer to the skin (Chew et al., 2017).

The cooling effect increases with the increase in air velocity. 1 m/s wind velocity (equals walking speed) can drop the air temperature from 30,25 °C to 27,25 °C (Krautheim et al., 2014). In tropical regions such as Singapore, a wind velocity of 1-

1,5 m/s results in a 2 °C drop in temperature (Erell, Pearlmutter, & Williamson, 2011). Table 2.2 shows the cooling effect of the wind speed on the sensible air temperature. The striking feature of the table is that the wind speed creates a more cooling effect at low temperatures and for dry skin. For example, when the ambient air temperature is at 15 °C, the wind speed of 2 m/s causes a 10 °C drop in temperature. In comparison, when the ambient air temperature is at 30 °C, the temperature is reduced by only 2.3 °C.

Table 2.2 The cooling effect of the wind at various ambient air temperatures (HABITAT, 1983)

Indoor wind speed	Cooling effect (^{O}C)			
	Dry skin Moist skin			
	Ambient air temperature			
	15 ^{O}C	20 ^{O}C	25 ^{O}C	30 ^{O}C
	Temperature Drops (^{O}C)			
0.1	0	0	0	0
0.25	2	1.3	0.8	0.5
0.5	4	2.7	1.7	1
1.0	6.7	4.5	2.8	1.7
1.5	8.5	5.7	3.5	2
2.0	10	6.7	4	2.3

2.1.5 Section Discussion

In this section of the literature, the characteristics features of the wind were analyzed, the vernacular urban settlements were compared in terms of wind adaptation and finally, the role of wind in the comfort of urban open spaces was examined. The case studies show that wind in vernacular settlements has various characteristics and qualities in hot-arid, tropical, temperate, and Arctic climates. The quality of wind is considered significant in forming the urban form.

In the 21st century, efforts to find the ideal sustainable urban form continue by including the concept of climate adaptation and, more specifically, wind adaptation. In this respect, urban form is defined as the key element for sustainable urban development, and compact urban form is defined as a globally sustainable urban form (Dantzing and Saaty, 1973); Department of the Environment, 1993; The Commission of the European Communities, 1990). The case studies show that the compact urban form is widely preferred in cold and hot-arid climates since it provides a wind-shelter effect. However, it also showed that not suitable for the tropical climatic conditions where more wind flow for ventilation is needed.

While adaptation to climate, or specifically to the wind, is mainly achieved in vernacular urban settlements, it has become challenging to attain climatic adaptation in urban open spaces due to the intensification of cities and the increase in building heights in urban centres. Therefore, it may be difficult to apply knowledge from vernacular settlements to today's urban areas, and lessons from vernacular cases may be ineffective in achieving climatic adaptation in urban areas. This situation may require new innovative research in adapting urban areas to climate.

2.1.5.1 Key Results of the Section

- Climatically, the compact urban form is widely preferred in cold and hot-arid climates since it provides a wind-shelter effect.
- Climatically, the compact urban form is not desired for the tropical climatic conditions where more wind flow for ventilation is needed.
- There is no universal city form that is compatible with every climate zone.

2.2 Wind and Urban Physics

Urban physics is a part of building physics, focuses on the external environment around the buildings, and includes the topics such as UHI, pedestrian wind, and thermal comfort. According to Blocken (2012):

Urban physics is the study of the physical aspects of the outdoor urban environment, including the transfer of heat and mass, acoustics, lighting and energy, and their interaction with the indoor environment and the building envelope. It is aimed at improving outdoor and indoor health, comfort, productivity and sustainability taking into account energetic, ecological and economic constraints.

Building/urban aerodynamics is the specific field of urban physics and investigates the flow behaviour around the buildings, including their surroundings.

2.2.1 The Science of Aerodynamic

Aerodynamics is a branch of physics that investigates various external forces acting on solid objects passing through moving air. It examines how fluids interact with moving solid bodies. The fundamental law of aerodynamics is Bernoulli's Theorem (conservation of energy). According to Bernoulli's Theorem, the sum of atmospheric and dynamic pressures at each point on the same flow path is constant. Bernoulli's Theorem is indicated in Eq. 2.1. This equation shows that an increase in the speed of fluid results in a decrease in the fluid's potential energy or static pressure (Batchelor, 2000; Clancy 1975).

$$P = \frac{pV^2}{2} = H \text{ (constant)} \qquad (2.1)$$

where P is atmospheric pressure (static pressure), p is density, V is velocity, q ($pV^2/2$) is dynamic pressure, and H is total pressure (constant).

Air molecules approaching the front side of a solid object begin to compress, and then air pressure increases in the frontal area. The solid object displaces some air by pushing air out of the way and, therefore, airflow accelerates around the solid

object's corners. The rear vacuum behind the solid object is composed of frontal pressure. When the air is not able to fill the rear vacuum, a drag (air resistance) occurs. This type of drag force is called *pressure* or *form drag*. Form drag depends on the pressure difference between the frontal and rear vacuum areas. The lower the pressure difference is lower the form drag. As the aerodynamic drag force increases, the average kinetic energy of flow decreases. Some kinetic energy is transferred to the secondary flows and the turbulence (Bottema, 1993). The pressure difference can be reduced by decreasing the front pressure or increasing the back pressure. Reducing pressure difference and form drag minimizes airflow acceleration and turbulence generation around a solid object.

Another drag force develops around the solid object based on surface friction, called *friction drag*. Friction drag is the result of friction (shear stress) that slows air movement on the surface (boundary layer). Reducing the side edges of the object minimizes the friction drag. Also, reducing the roughness of the wall (without protruding parts) reduces the friction drag.

Form drag is affected by three parameters:

- drag coefficient (C_d),
- the frontal area of the obstacle,
- the velocity of the air.

The formula of drag is indicated in Eq. 2.

$$\text{Drag (Air resistance)} = C_d \times \text{Area} \times V^2 \tag{2.2}$$

where C_d is the drag coefficient (shape factor), the area represents the frontal area of the obstacle, and V is the relative velocity of the fluid (air).

Eq. 2.2 indicates that drag is a matter of shape and size. However, the size can be different in various objects. A unitless value called drag coefficient Drag (Cd) is used to compare the aerodynamic performance of various shapes of different sizes. C_d is merely a shape factor and determines aerodynamic shape efficiency. It denotes how

much an object resists air movement. The smaller the C_d, is higher the aerodynamic efficiency.

The best C_d is achieved with a *streamlined body*. The streamlined body necessitates a smooth design. Almost all the corners of the body of the object are rounded. The continuous curve allows air molecules to pass smoothly and follow the contours of the solid object. The sharp corners in the bluff body significantly increase the frontal pressure. But the soft contours in the streamlined body reduce the air pressure difference. The rear side is smoothly converged to smoothly fill the air molecules into the vacuum so that the air does not separate. In a streamlined body, the flow is attached to the object's body, and therefore form drag is small. Drag is caused by mostly friction (shear stress). A streamlined body is widely used in the aircraft and airship industry, where aerodynamic flow performance is necessary.

Unlike the streamlined body, the bluff body (sharp-edged) has a higher C_d value and, therefore, creates higher form drag. Sharp corners cause the rear vacuum area and cause flow separation. The fact that air molecules cannot fill the rear vacuum is called flow separation. Flow separation depends on the flow pattern, boundary layer type (laminar or turbulent), and the adverse pressure gradient. When the airflow is separated, the flow becomes turbulent and chaotic. The separation of flow from contours creates flow degradation, such as discontinuity and turbulence. Form drag is mainly due to the pressure difference, and it is greater than the skin friction drag for a bluff body.

Form drag is highly sensitive to building dimensions. In a rectangular building, drag varies with the building's aspect ratio. When the aspect ratio of the building (L: building length / W: building width) increases, the drag decreases where length is the parallel dimension to the wind flow. Figure 2.13 shows the C_d values for various shapes. The C_d value of the rectangular-shaped building with a high length-width ratio is lower than the cube-shaped building. The cylindrical and conical shapes have smaller C_d values and are more aerodynamically efficient than prismatic shapes. However, the ideal shape is the symmetrical shape relative to the horizontal axis, known as the *water drop* shape that causes a minor distortion. Its drag coefficient is just 0.04, while the C_d value of a cube is 1.05.
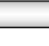
Figure 2.13 Drag coefficients (Cd) values for various shapes (Baker, Cox, Kulesz, Strehlow, & Westine, 2012).
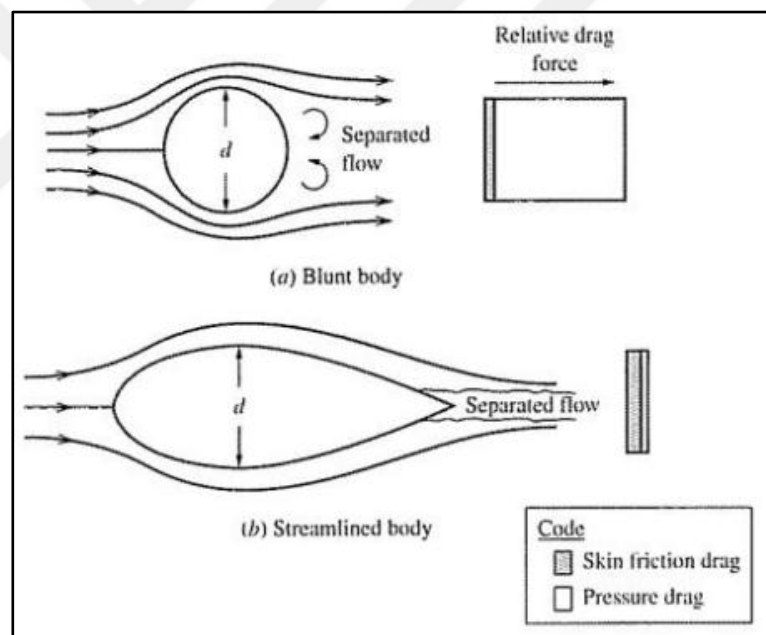
Figure 2.14 Comparison of flow separation and drag on the blunt and streamlined body (Aerospaceweb, 2022)

When the flow moves around an object, flow is separated, and a wake area is created. The higher the wake area means higher the C_d value. Due to the steep pressure gradient, the flow is immediately separated from the bluff body with sharp edges. But, streamlined bodies such as aircraft wings with long trailing sections cause a weak pressure gradient which delays flow separation. Figure 2.14 shows the

flow patterns around the streamlined and cylindrical (bluff-blunt) body. The flow behind the cylinder is separated, and a larger wake area is created, but there is no flow separation around the aerodynamic body, and a smaller wake area develops. Therefore, in a streamlined body, skin friction drag is greater than pressure (form) drag compared to the bluff body. Figure 2.15 shows the form and skin friction drag percentage depending on the shape.
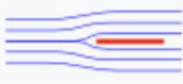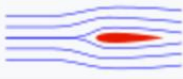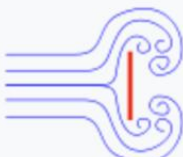
Shape and flow	Form Drag	Skin friction
	0%	100%
	~10%	~90%
	~90%	~10%
	100%	0%

Figure 2.15 Form and skin friction drag depending on the shape (Drag (physics), 2022)

2.2.1.1 Reynolds Number

The Reynolds number (Re) is the key parameter to predict the flow pattern of a fluid and is used to determine whether the flow is laminar, transient, or turbulent. It is the ratio between inertial and viscous forces. The Reynolds number (Re) is calculated according to Eq. 2.3.

$$\text{Re} = \frac{\text{inertial force}}{\text{viscous force}} = \frac{pVL}{\mu} = \frac{VL}{v} \tag{2.3}$$

where p (kg/m^3) is the density of the fluid, V (m/s) is the velocity of the flow, L (m) is the characteristic length, and μ (Pa X s) is the dynamic viscosity of the fluid and v (m^2/s) is the kinematic viscosity.

Flow is turbulent when the inertial forces that are the cause of air motion are dominant. In turbulent flow, wind speed changes, and a chaotic flow field occurs. If viscous forces (flow resistance) are dominant, the flow is defined as laminar. The streamlines are parallel to the ground in laminar flow, and the flow particles move in the same direction. In turbulent flow, the streamlines appear parallel, but flow particles fluctuate along the streamlines. When the flow passes from laminar to turbulent, a transition zone is formed between the laminar and turbulent (Figure 2.16).

The critical Re number determines the transition from laminar to turbulent flow. The flow is laminar up to Re number 2300, transitive when the Re number is between 2300 to 4000, and turbulent when the Re number exceeds 4000. The critical Re number is not precise and differs for internal (confined) and external (open) flow. For example, while the critical Re number for turbulent flow in a pipe (confined flow) is 2×10^3, it ranges from 10^5 to 10^6 in free-stream flow over a flat-plate surface (White, 2002).
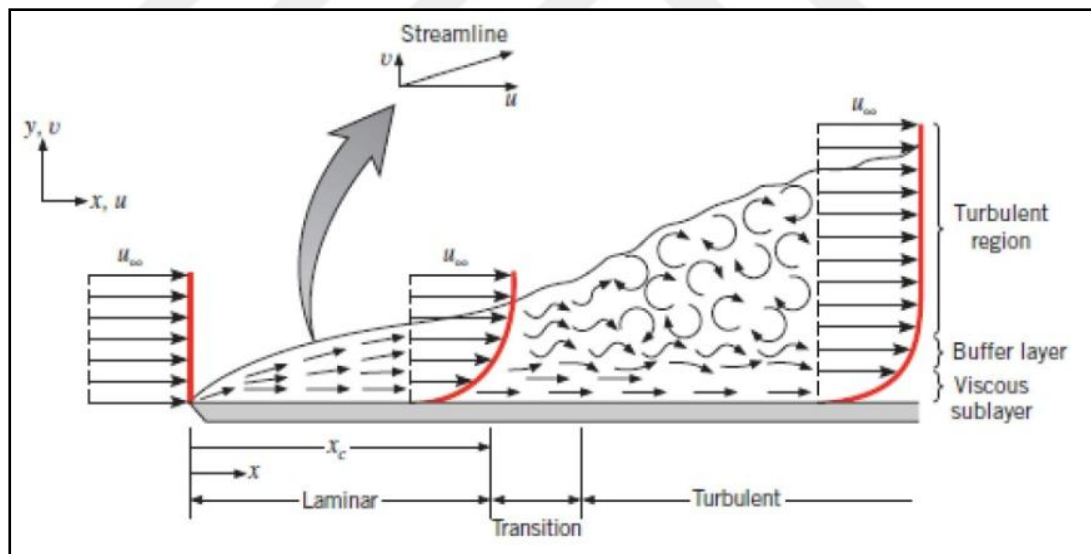
Figure 2.16 Boundary layer development over the flat plate surface (Bergman, Lavine, Incropera, DeWitt, 2011).

Along with the Re number, the transition from laminar to turbulent flow is directly determined by turbulence intensity of approach wind flow and aerodynamic surface roughness of the ground. These terms will be explained in the concept of the *boundary layer.*

2.2.1.2 Boundary Layer

The boundary layer is created by a no-slip wall in viscous fluid and flow conditions. Viscosity is the measure of the resistance of fluid layers to slip against each other. In a viscous flow, the velocity on the wall surface is zero. As the distance from the surface increases, the velocity increases and reaches the maximum level and then remains mostly constant. The boundary layer refers to the distance from the wall where the vertical velocity reaches 99% of the free-stream velocity. Outside the boundary layer, the flow is essentially inviscid. As the Reynolds number increases, the thickness of the boundary layer decreases. Figure 2.17 illustrates the boundary layer concept and boundary layer thickness.
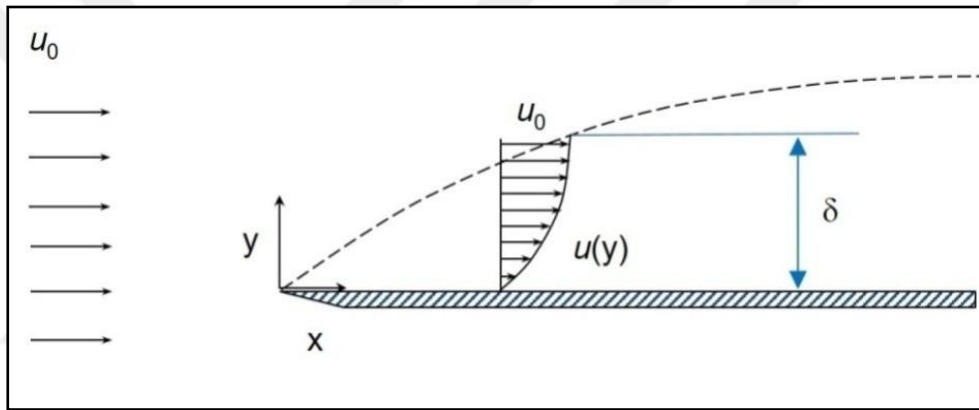
Figure 2.17 Boundary layer concept and boundary layer thickness (Wikipedia Picture Boundary Layer Thickness, 2022)

2.2.1.2 Atmospheric Boundary Layer

Wind flow results from the atmospheric pressure difference created by the temperature difference. When the wind moves from higher pressures to a lower atmosphere, a boundary layer is created on the Earth's surface. The atmospheric boundary layer is the layer influenced by the surface of the Earth. At a lower level of the atmosphere, the wind fluctuates in both direction and magnitude. The Earth's surface roughness significantly affects wind flow at certain heights and acts as a friction force in the opposite direction of the wind's movement. This opposite effect reduces wind speed and tries to change direction. As the height increases, the effect of the Earth's surface on wind flow decreases, and this phenomenon creates an ever-changing wind profile called "wind gradient" or "wind profile. According to the

boundary layer concept of Prandtl, the vertical wind speed, which is zero at the wall surface, increases and reaches its maximum value and finally remains constant. This height between the two velocity positions is defined as ''gradient height''.

Earth surface friction significantly affects wind characteristics and differs in sea, land, and urban environments. The aerodynamic roughness parameter z_0, also known as the aerodynamic roughness length, is used to classify wind characteristics.

Davenport (1961) defined eight different roughness classifications based on the landscape description. Wieringa (1992) later updated this classification and published the new revision of the Davenport roughness classification (Wieringa, Davenport, Grimmond, & Oke, 2001). Table 2.3 shows eight different roughness classifications. The open sea and lake have the lowest roughness parameter according to roughness classification. In contrast, it has the highest value for the large city centers consisting of low-rise and high-rise buildings.

Unlike rural areas, wind velocity in urban environments increases more with height due to many obstructions. Since urban areas have more obstacles than rural areas, the flow also shows high turbulent flow characteristics (Figure 2.18). Along with the wind flow in an urban environment, warm air rises due to the low-pressure zones, and a slow-moving wind effect occurs in the vertical direction.
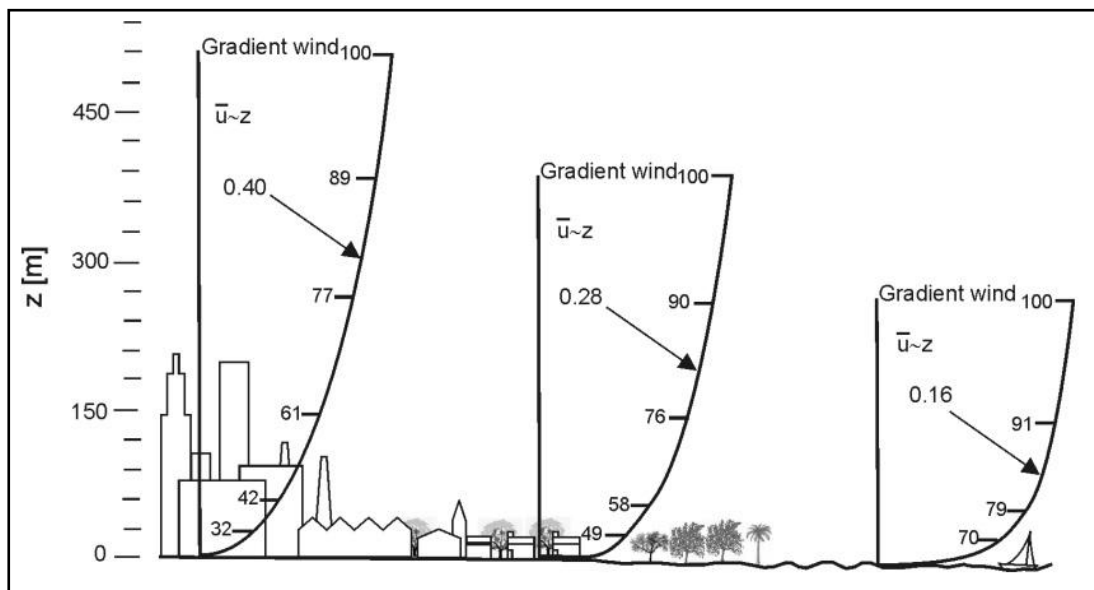
Figure 2.18 Profiles of mean wind speed over different terrain (Plate,1982)

44

Table 2.3 Terrain roughness classification by landscape description - (z_0) is aerodynamic roughness length value. Updated Davenport's classification of effective terrain roughness (Wieringa et al., 2001)

Roughness classification	z0 (m)	Landscape description
1. "Sea"	0.0002	Open sea or lake (irrespective of wave size), tidal flat, snow-covered flat plain, featureless desert, tarmac or concrete, with a free fetch of several kilometres.
2. "Smooth"	0.005	Featureless land surface without any noticeable obstacles and with negligible vegetation, e.g. beaches, pack ice without large ridges, marsh and snow-covered or fallow open country.
3. "Open"	0.03	Level country with low vegetation (e.g. grass) and isolated obstacles with separations of at least 50 obstacle heights; e.g. grazing land without windbreaks, heather, moor or tundra, runway area of airports. Ice with ridges across the wind.
4. "Roughly open"	0.10	Cultivated or natural area with low crops or plants cover, or moderately open country with occasional obstacles (e.g. low hedges, isolated low buildings or trees) at relative horizontal distances of at least 20 obstacle heights.
5. "Rough"	0.25	Cultivated or natural area with high crops or crops of varying height, and scattered obstacles at relative distances of 12 to 15 obstacle heights for porous objects (e.g. shelterbelts) or 8 to 12 obstacle heights for low solid objects (e.g. buildings). Analysis may need zD .
6."Very rough"	0.5	Intensively cultivated landscape with many rather large obstacle groups (large farms, clumps of forest) separated by open space of about 8 obstacle heights. Low densely planted major vegetation like bushland, orchards, young forest. Also, area moderately covered by low buildings with inter-spaces of 3 to 7 building heights and no high trees. Analysis requires zD .
7. "Skimming"	1.0	Landscapes regularly covered with similar size large obstacles, with open spaces of the same order of magnitude as obstacle heights; e.g. mature regular forests, and densely built-up areas without much building height variation. Analysis requires zD .
8. "Chaotic"	≥ 2	City centers with a mixture of low-rise and high-rise buildings or large forests of irregular height with many clearings. Analysis by wind tunnel advised.

2.2.2 Building Aerodynamics

Aerodynamics is a branch of dynamics and focuses on the motion of air. It is widely used in the aircraft, automobile, and airship industries. Aerodynamic science in architecture and urban planning began with the construction of tall buildings. Tall buildings are subject to dynamic wind forces that cause excitations and lateral displacement on buildings. Tall buildings also draw high-speed winds at higher altitudes down. This rapid wind movement creates eddies and turbulences around the building, causing pedestrian wind discomfort. With the introduction of tall buildings in urban areas, aerodynamically efficient building design and pedestrian wind comfort studies in urban open spaces gained importance. Although architectural aerodynamics has developed a lot in modern times, it dates back to ancient times. For example, Vitruvius proposes that the corners of the rows of houses should be turned to the prevailing wind direction so that the wind force breaks, disperses, and loses its strength by hitting the corners of the houses.

Architectural aerodynamics is part of *wind engineering* and focuses on the interactions between buildings and wind flow. In architecture, buildings generally consist of bluff bodies and sharp-edged geometries with high drag force. The bluff body resists the airflow and creates a high-pressure area on the upwind side and a low-pressure area on the downwind side. Pressure differences around the buildings cause various wind effects, such as wind flow acceleration and the risk of pedestrian wind discomfort. Architectural aerodynamics aims to reduce form drag, flow acceleration, and turbulence for wind-comfortable urban areas.

Aerodynamic science generally investigates the motion of the solid body in the air, but in architectural aerodynamics, the buildings are static, and the air is dynamic around the buildings. But, theoretically, there is no difference between the movement of the solid body in the air and the movement of the air around the solid body.

Architectural aerodynamics examines building-wind flow interactions at two scales: single buildings and building groups. Single buildings are not ordinary in dense urban environments, but understanding basic flow patterns around a single building can be helpful.

In modern times, with the development of wind tunnel techniques that simulate the atmospheric boundary layer, the causes of wind problems around buildings have begun to be identified. First, Gandemer (1978) described twelve aerodynamic effects around buildings and groups of buildings with numerical models. Figure 2.19 shows the basic airflow effects around the buildings:
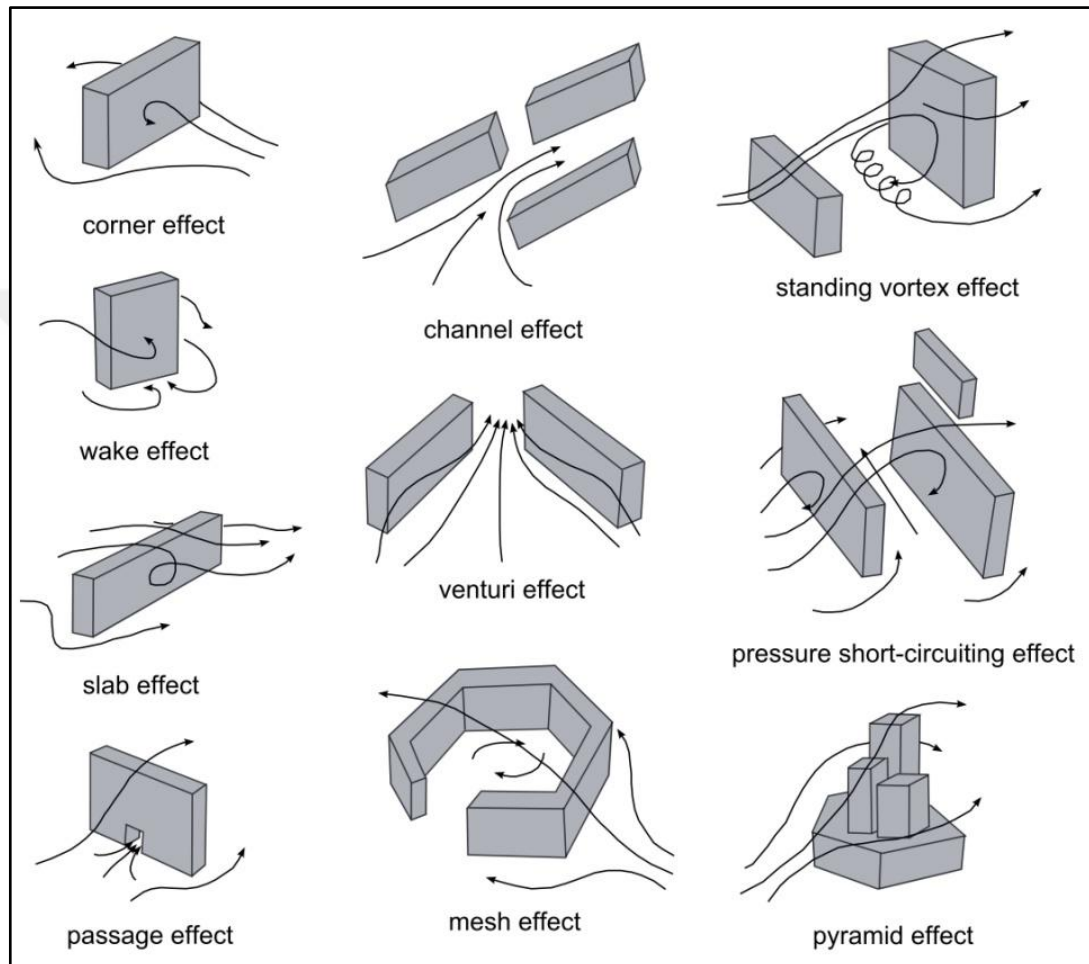
Figure 2.19 Main aerodynamic effects depending on the building and building layouts. (Gandemer, 1975, cited in Merlier, 2015)

The *corner effect* occurs at the corners of the building. Maruta (1984) stated that the corner effect occurs very close to the building corners at the flow separation. The corner effect causes the highest wind speeds near the edges of the upwind face of the buildings due to the increased horizontal pressure difference between the windward and leeward sides of the buildings. To understand the *corner effect*, the intensity and position of maximum wind speed and the dimensions of the corner stream should be known (Bottema, 1993).

The leeward side of the building is the negative pressure area. This area has unstable flow turbulence and creates a disturbing wind environment behind the building. This is called the *wake effect.*

The effect that occurs in front of the building and the opposite direction of the approach flow is called the *standing vortex effect.*

Passages left in the lower parts of buildings accelerate the flow towards the passage and cause a jet stream. This is called the *passage effect.*

The *slab effect* occurs when the building is at a 45-degree angle to the wind incidence. In this effect, a swirled wind flow turns downwards and accelerates excessively.

The *channel effect* occurs when buildings are lined up on both sides of an axis. This configuration can increase the intensity of another wind effect.

The *Venturi effect* occurs when the passage between buildings gradually narrows, and the building configuration is *funnel-shaped*. In this effect, the flow accelerates in the bottleneck. In a confined flow, the average wind speed increases in a passage if the cross-section of the passage becomes smaller due to the principle of mass continuity and conservation of energy. However, in open flow, the upstream weakens the Venturi effect (Bottema, 1993). Therefore, the Venturi effect is considered more effective in a confined flow than in an open flow.

The *pressure short-circuiting effect* occurs when buildings in the shifted configuration are positioned perpendicular to the wind incidence. As a result, strong transverse flow occurs by connecting the two zones of different pressures. Since this effect occurs at the shortest distance, it is called the *pressure short-circuiting* effect.

The *pyramid effect* occurs in a compact building configuration at an ever-increasing height. Although this configuration is aerodynamically efficient, terraces around the buildings can be exposed to high wind speeds.

The upwind buildings are the buildings where the wind first interacted. Therefore they mask the downwind urban areas and create wind-sheltered urban open spaces. This effect is called the *mask effect*.

In addition to the twelve aerodynamic effects around buildings described by Gandemer (1978), the *downwash effect* occurs on the facades of tall buildings. This is because a vertical pressure difference occurs at the front of the building due to the approach wind speed increasing with height. Due to the vertical pressure difference, tall buildings divert relatively high-speed wind flow from higher altitudes to ground level. This rapid wind movement along the facade of the building and towards the ground level creates standing eddies and turbulences around the building. This is called the *downwash effect*.

The aerodynamic effects around a simple, prismatic building are complex. A single rectangular building is generally used to understand the wind flow effects. A single rectangular building is also used as a reference building to be compared to other complex building types and arrangements. Figure 2.20 illustrates the schematic aerodynamic effects and flow behaviour near ground level for a simple rectangular building whose width, length, and height are 80 m, 20 m, and 70 m, respectively (Beranek and Van Koten, (1979), cited in Blocken, Stathopoulos, & Van Beeck, 2016).

As the wind flow approaches the building, millions of air molecules begin to compress, and an over-pressure zone occurs on the windward side of the building. Compressed air molecules try to move away from the high-pressure area and are directed sideways and upwards. Thus a part of the flow is separated over the building (1), and another part flows from the side (2). A stagnation point occurs at approximately 70% of the building height on the windward facade. At this point, the pressure is at the maximum level. From this point, the flow is naturally directed upwards (3), sidewards (4), and downwards (5), where the lower pressure zones of the building. Thus the pressure difference between the front and rear sides of the building are equalized. These regions are the worst affected regions near the building. The flow moving sidewards creates corner streams where high wind speeds and low turbulence intensity (σ_u/U) occur (Bottema 1993).

The flow moving downwards produces a vortex at the ground level called a standing vortex, frontal vortex, or horseshoe vortex (6). The stagnation zone and intensity of the frontal vortex depend on the building width to height ratio (W/H) (Bottema, 1993). The standing vortex is in the opposite direction of the approach wind flow. A stagnation point is formed on the ground and in front of the building, where the approach flow and the standing vortex interact (7). Wind velocity is lower in this region. The standing vortex is also directed sideways and creates high-speed corner streams. A shear layer and flow separation occur at the top and side edges. The shear layer consists of small vortices developed between the corner streams and recirculation zone. At the separation point, the inertial force of the near-wall is equal to the friction force, and the flow begins to separate from the building surface.

An under-pressure zone is created on the leeward side of the building and causes backflow or recirculation flow (10, 13). Similar to the overpressure side, a stagnation zone occurs in the under-pressure area. In the stagnation zone, the flow is reversed at a lower speed and higher turbulence intensity (11) (Peterka, Meroney, & Kothari, 1985).
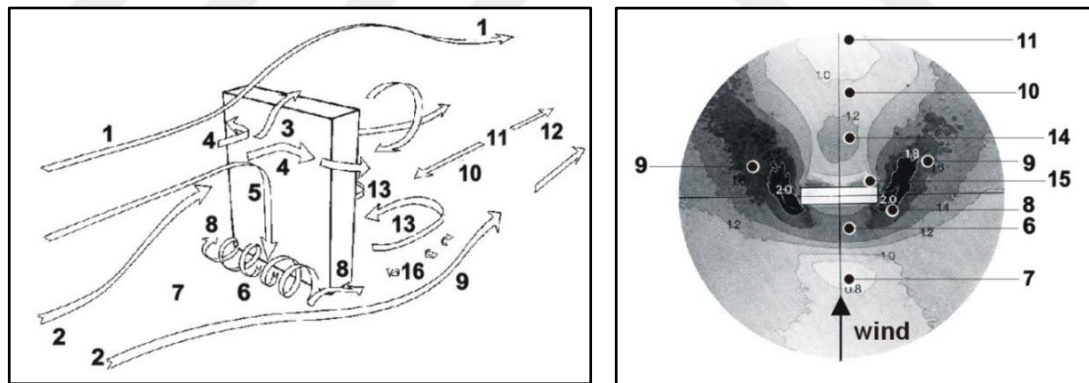
Figure 2.20 Schematic representation of main aerodynamic effects around a simple prismatic building (left),   contour plots of wind velocity ratio visualized with sand-erosion technique (Widht x Lenth x Height = 80x20x100) (right)

The single building dimensions such as width (W), length (L), and height (H) are highly sensitive to wind flow. Along with the single building dimensions, relative dimensionless parameters, such as W/H, W/L, and L/H, are effective on wind flow. Beranek (1980) analyzed the flow patterns around three characteristic building types (Figure 2.21). In the case of a tall building (a), most of the air flows along the edges

of the building, and a frontal vortex is slightly developed, where W/H < 0,5, and L/H (thickness) is the highest. Such a building causes less aerodynamic resistance against the airflow. It also shows that the length of the building supports the reattachment of the flow and the flow turns rapidly towards the wake (Bottema, 1993). In the case of an intermediate-type building (b), a strong frontal vortex occurs. In the case of a wide building (c), most of the air passes over the roof of the building, and the frontal vortex becomes much weaker, but the sheltered area in the wake region becomes larger, where W/H >> 3 (Bottema, 1993).
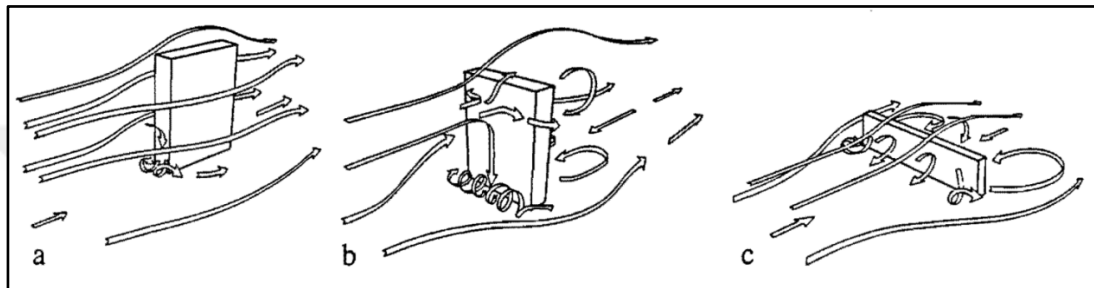
Figure 2.21 Schematic representation of three flow patterns around buildings and characteristic building types (a) tall building (b) intermediate type building (c) wide building (Beranek, 1980)
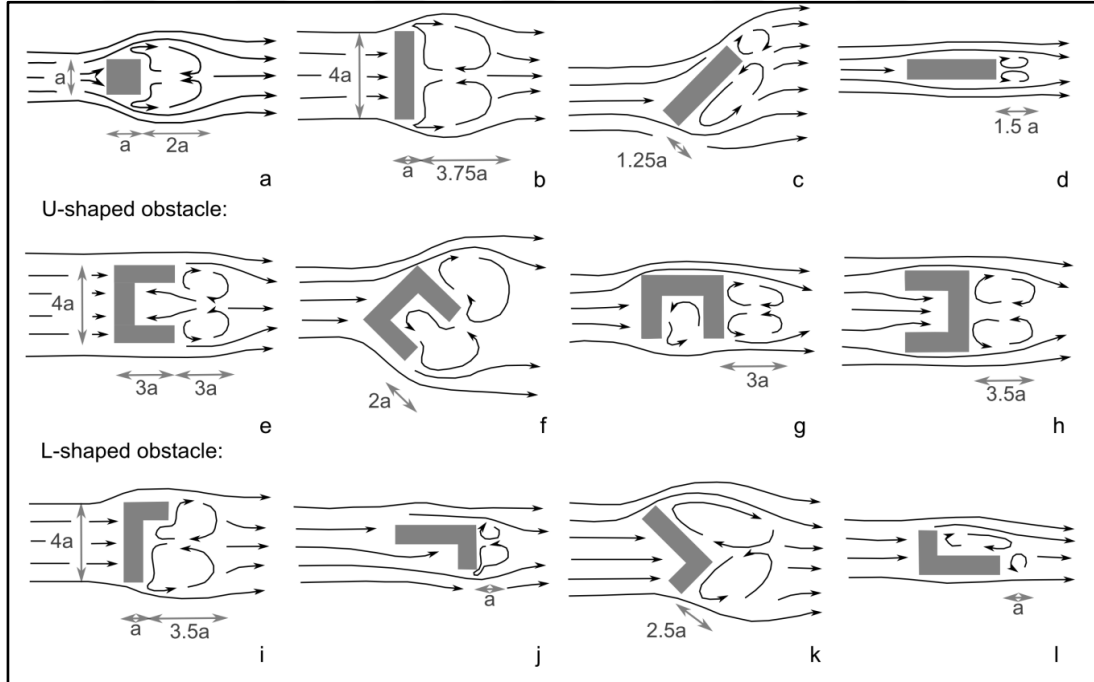
Figure 2.22 Main flow characteristics around obstacles in different shapes and different wind incidences. (Brown and DeKay, (2000) cited in Merlier, (2015))

Today in urban settlements, buildings are not only in a generic and simple form. They can have more protruding parts and semi-enclosed spaces. This makes wind flow more complex. Figure 2.22 compares the main flow characteristics around square, rectangular, U, and L-shaped obstacles for horizontal wind flow. Low-pressure zones behind the obstacles or inside the cavity lead to backflow or recirculation flow formation. The wider the obstacle, the wider the recirculation zone (case b), while the longer the obstacle, the narrow the recirculation zone (case d). Asymmetric shapes (case g-i-j-l) make the flow areas more complex. A larger recirculation zone occurs when obstacles are oblique to the wind incidence (case c-f-k). The relative dimensions of obstacles, the oblique of the obstacles concerning the wind incidence, and the location and size of protrusions initially determine the flow characteristics.

2.2.3 Urban Aerodynamics

Urban aerodynamics is the specific field of urban physics and investigates the flow behaviour around the buildings, including their surroundings. Urban aerodynamics is quite complex due to many reasons. First, urban environments consist of many buildings close to each other and in the form of solid masses with sharp edges. This form and positioning create a site-specific flow pattern. Second, a highly complex flow pattern is observed as the buildings affect each other's flow field and cause flow interaction. Third, wind flow in the urban environment is different from the wind profile of rural areas. In the urban environment, the wind has low speed and high turbulence intensity due to various roughness elements of the buildings. Understanding the turbulence mechanism is difficult as it is random, chaotic, and also complex. This makes the field of urban aerodynamics more challenging.

A single building creates resistance to wind flow and causes drag. Urban drag is equal to the total drag of each building. Urban aerodynamics often focuses on reducing urban drag. Wind flow has energy, and some of the energy is used to overcome urban drag. General flow problems such as flow separation result in the loss of wind flow energy. Therefore, reducing urban drag prevents the acceleration of wind flow and vortex formation.

In urban areas, aerodynamic wind flow with low drag can be achieved with streamlined building mass that prevents the wind flow acceleration around the building and delays flow separation by keeping the flow on the building's contours. However, using a streamlined building body in architecture and urban planning is not common since most buildings consist of sharp-edged geometries. This makes the aerodynamic wind flow in urban areas difficult.

2.2.3.1 Urban Aerodynamics and Urban Geometric Indicators

Wind flow is affected by many factors in urban environments. These are divided into two parts: primary factors, such as distribution of buildings and street network configuration, and secondary factors, such as vegetation and surface characteristics (Memon and Leung, 2010). Regarding primary factors, the wind flow pattern in urban areas depends on four morphological features of the city:

- urban block typology,
- urban block layout,
- the aspect ratio of urban blocks (relative dimensions between building's height, width, and length),
- the aspect ratio of street canyons or courtyards (relative dimensions between streets' height, width, and length).

Many urban wind studies have been conducted on the key components of a city, such as street canyons, courtyards, and block archetypes (Blocken, Carmeliet et al., 2007; Melbourne and Joubert, 1971; Oke, 1988; Steemers et al., 1997; Wise, 1970). For example, Steemers et al. (1997) investigated six urban block archetypes (pavilions, slabs, terraces, terrace-courts, pavilion-courts, and courts). They found that courts were less affected by wind flow (Figure 2.23). Talaghani (2015) examined the wind performance of three main types of urban blocks, such as single, linear, and courtyard, and found that the courtyard received less wind speed than the single and linear urban form and therefore was more wind-sheltered.
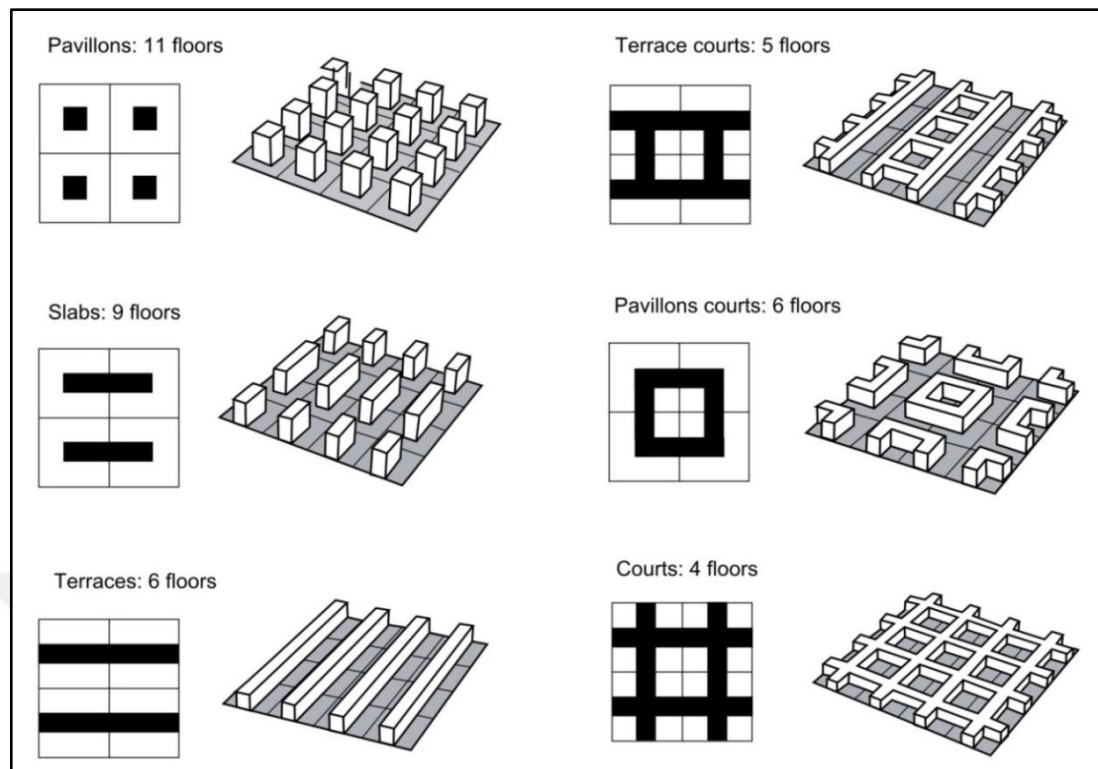
Figure 2.23 Generic urban forms, based on Martin and March (1972); Steemers et al. (1997). From left to right: pavilions, slabs, terraces, terrace-courts, pavilion-courts, and courts

In addition to urban block archetypes, urban design indicators such as density, ground coverage area, the geometry of street canyons, and sky view factor affect the wind flow pattern and significantly change the wind speed in the urban canyon (Priyadarsini and Wong, 2005). Therefore, these indicators are widely used to characterize the urban form aerodynamically. The analyzed urban design indicators related to urban aerodynamics are:

- the aspect ratio of street canyons (Oke, 1988; Steemers et al., 1997),
  - o the length to height ratio (L/H) of canyons (Oke, 1988),
  - o the length to width ratio (L/W) of canyons (Oke, 1988) and (Kastner-Kleinet al., 2004),
- the blockage ratio (BR) (Brown and DeKay, 2000),
- the width to building influence scale ratio (W/S) of passage between two parallel buildings (Blocken, Carmeliet et al., 2007),
- the passage ratio (PR) (Hu and Yoshie, 2013),
- the plan area density (λP) (Grimmond and Oke, 1999),

- the frontal area index (λF) (Grimmond and Oke, 1999),
- the aerodynamic roughness length (z0) (Grimmond and Oke, 1999),
- the mean porosity (Adolphe, 2001)

In urban environments, buildings are continuously aligned, and street canyons are formed. A street canyon refers to a narrow street with buildings aligned on both sides (Nicholson, 1975). The geometry of a street canyon is often characterized by its aspect ratio, which is a dimensionless indicator showing the relative dimensions between building height, width, and length.
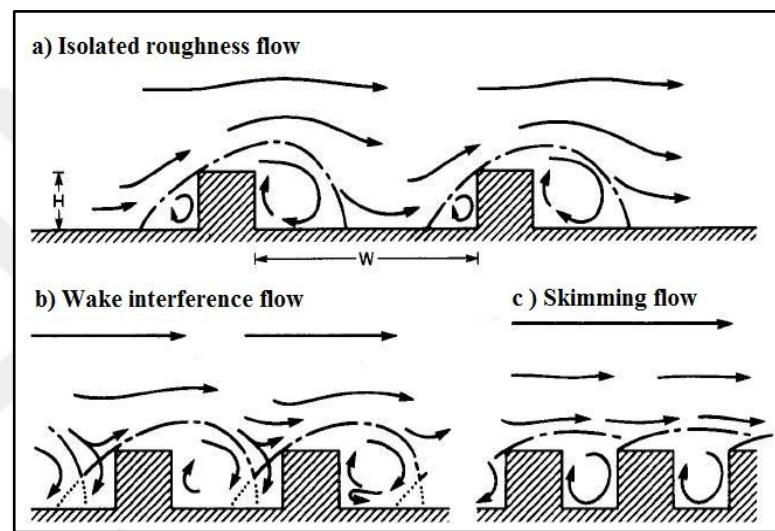
Figure 2.24 The three generic flow regimes as a function of H/W (Oke, 1988)

Hussain and Lee (1980) examined the airflow regimes associated with the aspect ratio of the street canyon. They described three characteristic flow regimes: isolated roughness flow, wake interference flow, and skimming flow. Figure 2.24 shows three airflow regimes according to various aspect ratios of the street canyon. The smaller the aspect ratio (H/W), the more air circulation in the urban canyon. Increasing H/W makes the urban canyon deeper and more isolated from airflow, reducing the air exchange rate while creating a wind-sheltered area. An aspect ratio below 0.5 represents a shallow street canyon, whereas an aspect ratio of 2 is called a deep street canyon. When the aspect ratio equals 1, it represents a uniform street canyon (Ahmad, Khare, & Chaudhry, 2005). In a shallow street canyon, the buildings are well apart (H/W > 0.5), and the flow fields do not interact (Oke, 1988). As a result, the vortices partially interact in a uniform street canyon, and the air mixes. In a deep

street canyon, the airflow cannot enter the street canyon, but the number of vortices increases in the canyon (Kim and Baik, 1999).
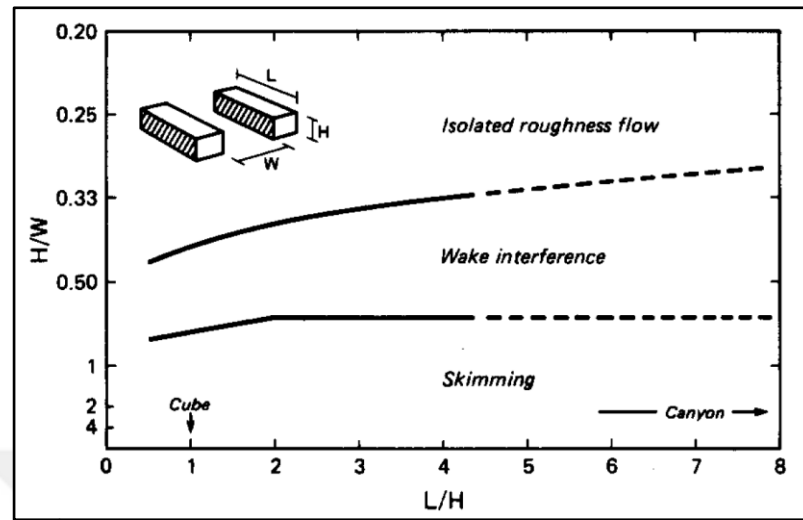
Figure 2.25 Threshold lines dividing the flow into three regimes as functions of the building (L/H) and canyon (H/W) geometry (Oke, 1988)

Oke (1988) and Kim & Baik (1998) investigated the effect of the aspect ratio of L/H of street canyons on flow regimes, where L is the length of the building normal to the flow and H is the height). They found that a wider street canyon delays flow interference and are more wind sheltering than a shorter street canyon (Figure 2.25). In a similar study, Kastner-Kleinet et al. (2004) investigated the effect of the aspect ratio of L/H of street canyons for evaluating local air quality to deal with urban air pollution problems caused by road traffic. They found that shorter street canyons promote ventilation of the canyon and the transport of contaminants. Finally, Walker, Shao, & Woolliscroft (1993) conducted a numerical study focusing on the design of courtyards for natural ventilation to achieve healthy conditions for occupants. The studies showed that the size of street canyons and courtyards in high-density cities are very influential on urban air quality and ventilation.

Passage ratio or passage width is another indicator that affects urban wind flow. This is because the buildings force the wind to direct to the passages and cause high-speed corner streams to form at the passages due to their resistance to the wind flow. Blocken, Carmeliet et al. (2007) investigated wind speed conditions at passages between parallel buildings for a wide range of passage widths using the W/S ratio (W

is the passage width and S is the building's influence scale-relative dimensions of the windward facade). As the W/S ratio increases, three different flow interference regimes: resistance flow (1), interaction flow (2), and isolated flow (3) develop, respectively (Fig. 2.26).

A slight flow interaction occurs, and nearly two separate flow zones and influence areas develop in isolated flow (Figure 2.26d). The flow interaction increases since the passage width decreases (Figures 2.26b and 2.26c). The two flow zones integrate and appear as a single flow zone. The wind speed is higher when the passage width enables the integration of different flow fields.
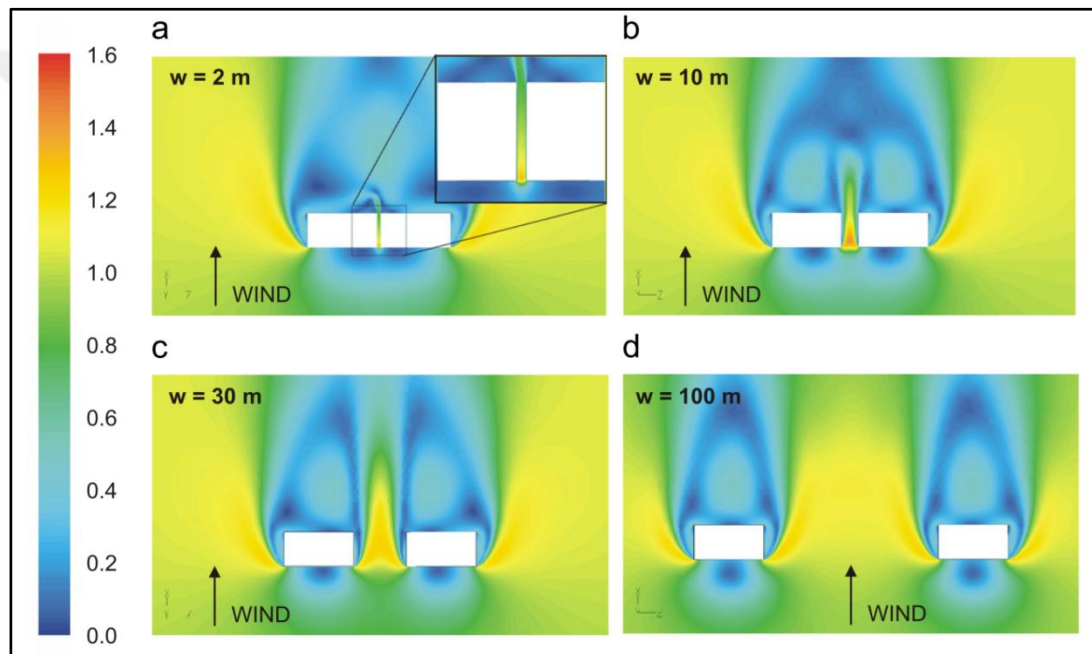
Figure 2.26 Flow regimes at 2m for four passage widths, Blocken, Carmeliet et al. (2007)

Reducing the passage width increases the average wind speed. However, the narrowest passage width (Figure 2.26a) shows high flow resistance to the incidence flow and has the lowest wind speed. In this case, the wind shelter effect develops. Similarly, according to Bottema (1993), narrow streets reduce wind speed and are generally acceptable in terms of wind comfort. However, Figure 2.26a shows that high wind speed does not occur along the passage centreline but at the passage entrance. As the wind passes through the passage between buildings, its speed increases due to the corner effect and decreases. Therefore, the building's corners should be avoided even in a narrow passage. The study shows that the flow around

the buildings does not move separately and that the different flow zones somehow combine, creating new and very high-speed flow characteristics that can sometimes be dangerous.
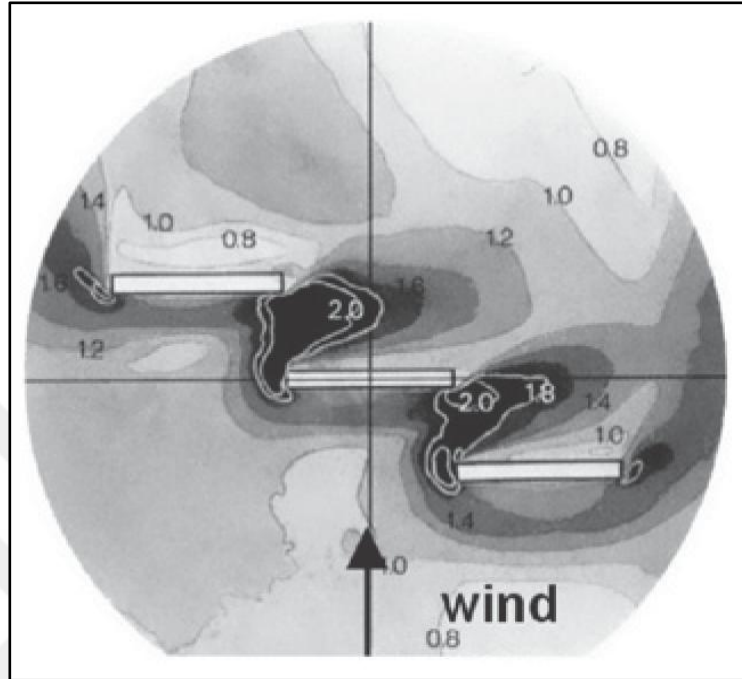
Figure 2.27 Wind speed conditions in the passage between three parallel shifted buildings (Beranek, 1982)

Hu & Yoshie (2013) investigated the passage ratio (PR) to evaluate the urban ventilation efficiency of urban open spaces and found that large passage width improves ventilation efficiency. Beranek (1982) investigated the wind speed conditions at the passages between three parallel shifted buildings and found that due to the strong flow interaction, a *pressure short-circuits effect* occurs, and the wind speed ratio between them can reach 2. Figure 2.27 shows the wind speed conditions in passages between three parallel shifted buildings.

Ramponi & Blocken (2012) investigated the effect of the plan area density (λP) on the urban ventilation efficiency and found that urban ventilation effectiveness depends on the plan area density. The plan area density (λP=AP/AT) is the ratio of the total plan area of the roughness elements to the total surface area (Gal & Sümeghy, 2007). Brown & DeKay (2000) found that as the plan area density increases, ventilation effectiveness decreases (Figure 2.28). Kubota, Miura,

Tominaga, & Mochida (2008) studied the effect of the plan area density, i.e., ground coverage ratio, on wind speed. They found that buildings with a high-ground coverage ratio reduce the wind speed and result in a stepping effect. In contrast, the buildings with a low-ground coverage ratio increase wind velocity and cause the funnelling effect. In general, higher building density (Du & Mak, 2018; Hu, Cheng, & Qian, 2018), higher site coverage (Gu & Zhu, 2017), and compact-type buildings cause lower wind speed (Wai, Yuan, & Peter, 2020).
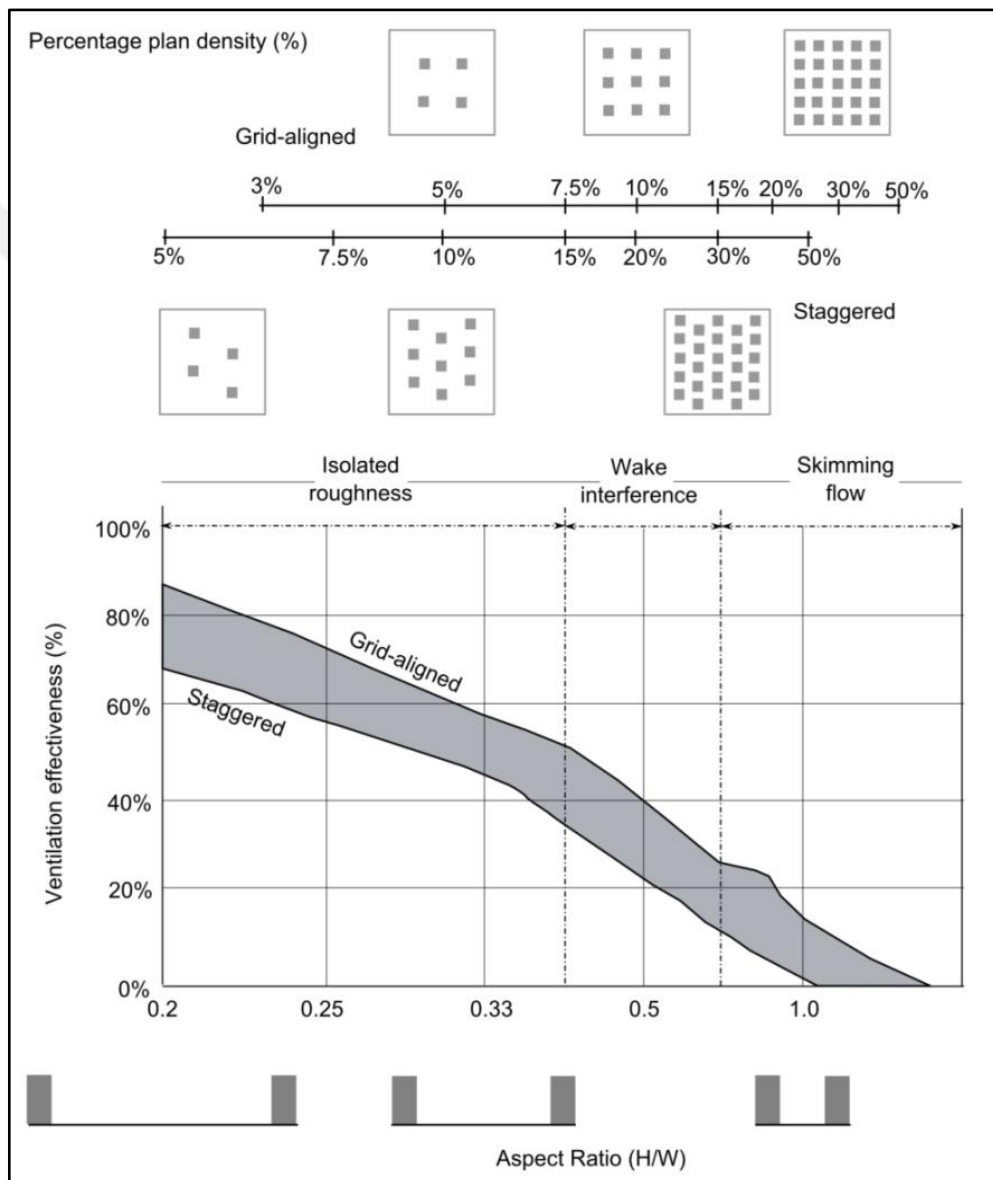
Figure 2.28 Occurrence of urban flow regimes as well as ventilation effectiveness depending on the plan density (adapted from Brown & DeKay, (2000)

2.2.4 Section Discussion

Aerodynamics science refers to the aerodynamic form. But, in architecture, buildings often have a bluff body and sharp-edged geometry that results in high form drag. Reducing the form drag of the buildings and the flow acceleration and turbulence is the main focus of architectural aerodynamics.

Various wind effects occur around buildings depending on the building form or street configuration. Increasing complexity in building form can create more chaotic wind flow behaviour. This situation makes the buildings dangerous in terms of pedestrian wind comfort. Therefore, the design of aerodynamically efficient buildings is necessary to provide pedestrian wind comfort in urban environments and make the urban environment more comfortable and liveable.

The main flow characteristics of general building typologies and flow effects around a simple rectangular building are well documented in the literature on architectural aerodynamics. In addition, many studies have been conducted on the type of flow around asymmetrical and complex structures. The larger the building dimensions, the greater the wind resistance and acceleration around the buildings.

The studies of urban aerodynamics show that the effects of morphology and form-related urban geometric indicators on wind flow have been widely studied. In particular, research on urban open spaces has mainly investigated flow types and characteristics in street canyons. In addition, the aerodynamic flow performance of urban block typologies specifically was studied. However, most studies report the aerodynamic effects of urban geometric indicators without focusing on design. Although the results obtained in numerical studies are comparative, the information provided is limited and does not reveal the codes of the physical environment design adapted to the wind. Along with this, most of the studies either focus on urban ventilation effectiveness or pedestrian wind comfort. However, cities need multi-purpose wind planning approaches that consider all aspects of the wind.

Many studies of urban ventilation analyzed the effect of urban density on urban wind flow. In general, higher building density results in lower wind speed (Brown &

DeKay, 2001; Givoni, 1998) and reduces ventilation efficiency in the urban area. However, larger passage width improves ventilation efficiency (Hu & Yoshie, 2013), and the smaller street aspect ratio (height/width) provides more air circulation (Hussain & Lee, 1980) in the urban canyon. Street configuration is another indicator that affects ventilation efficiency (Golany, 1996; Hu & Yoshie, 2013). Streets with grid-aligned configurations are more exposed to the wind and, therefore, have higher ventilation efficiency (Steemers et al., 1997), but staggered (i.e., shifted) configurations have lower ventilation efficiency than grid-aligned configurations (Brown & DeKay, 2000).

Many studies investigated the effect of urban geometric indicators on pedestrian wind comfort. Gandemer (1975) revealed the flow types around the most common building types and wind discomfort risk. Later, Reiter (2010) investigated the effect of building dimensions on wind speed using a parametric approach and found that wind flow acceleration was highly sensitive to building dimensions (height, width). Blocken, Carmeliet et al. (2007) investigated the effect of various passage widths (2 m, 10 m, 30 m, and 100 m) between parallel buildings on wind speed conditions. They found an *interaction flow (double corner effect)* occurs, and wind speed increases considerably when the passage width is 30 m.

Earlier studies showed that wide passages, sparsely organized urban settlements, and grid-aligned street configurations increase air circulation. However, narrow passages generally reduce air circulation and can cause the risk of pedestrian wind discomfort. In the context of today's sustainable urban developments that require high urban density and compactness, urban density generally contradicts urban ventilation. Earlier studies in the literature clearly show the need for a compromise between the requirements of urban ventilation and pedestrian wind comfort in dense and compact urban developments.

2.2.4.1 Key Results of the Section

- Urban density and compactness conflict with urban ventilation. As the density increases, the ventilation efficiency decreases.

- Streets with staggered (i.e., shifted) configurations have lower ventilation efficiency than grid-aligned configurations

- Wind flow acceleration is inevitable around the buildings with sharp-edged geometries.

- A passage of various sizes placed between parallel buildings causes different wind effects and wind flow acceleration.

CHAPTER 3

EXPERIMENTAL FIELD STUDY: WIND FLOW ASSESSMENT of URBAN BUILDING CONFIGURATIONS

In this chapter of the research, an experimental field study was carried out. Field studies are frequently preferred as they reveal site-specific problems and provide a learning environment from the existing field. In this context, field studies can be carried out for two purposes:

1) Site analysis: In-depth understanding and analysis of the current urban situation and the specific conditions at the site.

2) On-site learning for new designs: Learning initial and basic design knowledge from an actual urban area to create new design variations.

The field study aims to obtain new design codes from the field with the GDfD method rather than analyzing and understanding the current situation in the field. This is because many field studies on wind conditions, air pollution rate, and urban heat island effect have been conducted at the selected site, and current conditions have been extensively reported. These studies will be presented in detail later.

The proposed method will investigate the performance of the different urban building configurations in terms of urban ventilation and pedestrian wind comfort and will choose appropriate ones to create new designs. In this context, a field study with this approach forms the basis of the experimental design study presented in the next section.

3.1 Properties of the Study Area

This research was carried out in the city of Izmir, and there are many reasons for this. Izmir is located around the Izmir Gulf and has a very long coastal line (see Fig. 3.1a). Such urban geography provides regular thermal winds (İmbat) in each district facing the shore throughout the year. Refreshing sea breezes regularly blow from the

Gulf of Izmir. Although the sea breeze can reduce the effects of global temperature increase, urban heat islands (UHI), and air pollution in urban areas, the city cannot use this advantage sufficiently and suffers from the UHI effects and air pollution due to the inability of the existing seafront buildings to adapt to cool sea breezes. In particular, the existing seafront buildings in the city centre (Alsancak neighbourhood) have linear, continuous, and impermeable forms and, therefore, create an *urban wall effect* and prevent the sea breeze from sufficiently entering the city (Figure 3.1b-3.2). For this reason, heat and polluted air accumulate in the low-rise urban areas behind the seafront buildings, causing poor air quality and thermal discomfort.
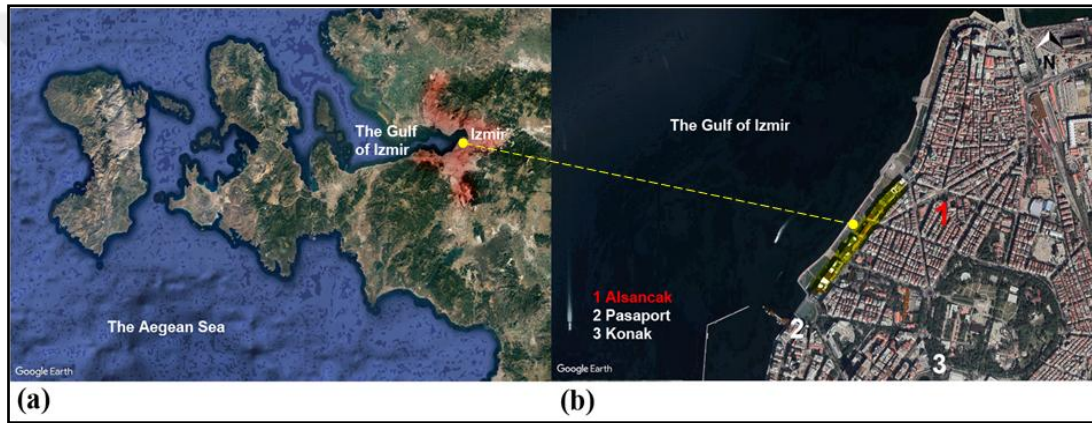
Figure 3.1 (a) Plan view of İzmir (adapted from Google Earth); (b) Plan view of Alsancak Neighbourhood (The yellow line represents the existing, linear seafront buildings)

Figure 3.2 View of the existing seafront buildings on the Alsancak coastline (the author's own archive, 2021)

Until 1950, Alsancak characterized the typical Mediterranean city consisting of 2-3 storey houses with gardens. However, in the 1950s, with the Marshall aids, the acceleration of industrial investments and the increase in mechanization in agriculture started migration from rural areas to big cities and increased the population in İzmir. With this economic transformation and population increase, the building height limit has been increased by the Konak Municipality Council to 12.80 m and 15.80 m on the coastline of Alsancak (Ballice, 2006).

With the enactment into force of the Turkish Condominium Law in 1965 and the Izmir Municipality Zoning Regulation in 1966, urban density increased in İzmir (Ballice, 2006). Apartments replaced low-rise buildings on the same plot layout without considering future planning and climatic conditions. As a result, building heights have increased significantly over time, and the outdoor climatic conditions in the urban environment have deteriorated.

As of today, the planning rule of "maximum eight floors and maximum 24.80 meters building height" is applied in Alsancak with the decision taken by Konak Municipality Council in November 2014. Figure 3.3 shows the transformation process of the seafront buildings over time. This kind of transformation also occurs in many coastal cities for speculative reasons or to make greater use of the seascape.

Figure 3.3 Transformation process of the seafront buildings on the Alsancak coastline over time, (left) the years 1955 and 1980 (Hasan Topal's archive, 2020), (right) the year 2022 (the author's own archive)

Seafront buildings are critical as they are the first place where the wind interacts with the urban fabric. Arkon & Özkol (2013) conducted a field study to examine the existing natural ventilation potential at the pedestrian level in Izmir. Two parallel deep canyons in Alsancak Neighbourhood, whose H/W ratio is 1.6 and 1.68, were selected, and pedestrian-level wind conditions were measured under the influence of sea breeze (see Appendix A). They reported four findings: pedestrian level wind speed is considerably affected by the presence of buildings, and the positioning of the buildings on the seaside in a way that screens the wind flow causes a *canyon effect* and adversely affects the natural ventilation potential of the city (1). The canyon effect causes lower pedestrian-level wind speeds even in streets with lower H/W ratios ($0 < H/W \leq 1$) (2). The uniformity of building heights (equal building height) reduces the potential enhancing pedestrian-level wind speed (3). Finally, the parallel orientation of the urban canyon to the wind flow results in pedestrian-level wind speeds lower than 3 m/s (4).

The city centre of İzmir suffers from thermal discomfort and increased emissions of toxic particles. Elbir (2002) conducted a study to determine the annual average SO_2 concentration in terms of air pollution measurement at different points in İzmir. They found that the city centre had higher values in terms of SO_2 density. Kestane & Ülgen (2013) stated that most of the settlements in city centres, such as Konak and Alsancak, are not suitable for bioclimatic comfort and comfortable urban areas are far from the city centre.

Figure 3.4 The wind gust creates wind discomfort for urban inhabitants in Alsancak city center of Izmir. (Habertürk, 2018)

Due to the temperate climate of the Mediterranean, people tend to use urban open spaces for outdoor activities in Izmir all year round. Sea breezes are desirable to improve ventilation in open spaces, but they cause pedestrian wind discomfort in the coastal part of the city. Wind observations in the field reveal that disturbing surface winds occur, in particular, around large and tall buildings. It has been reported that many streets directly exposed to sea breezes on the Alsancak coastline are very windy, while the parallel passages are calm (Arkon & Özkol, 2014). Figure 3.4 shows the wind discomfort of urban inhabitants at a coastal passage directly exposed to sea breezes in the city centre of Alsancak.

The building corners in Alsancak Neighbourhood are generally used as open areas for restaurants and cafes. In particular, many restaurants are located at the entrances of the coastal passages to benefit from the view of the İzmir Gulf. But these areas are exposed to the wind. Therefore, especially in periods when the wind is fast, seating areas are tried to be protected from the wind with micro-solutions such as wind curtains. In this way, adaptation mechanisms are developed on a micro-scale to protect the open spaces of restaurants from the wind. Figure 3.5 shows restaurants' micro-scale wind adaptation mechanisms in coastal passages of the Alsancak coastline.

Figure 3.5 Micro-scale wind adaptation mechanisms on Ali Çetinkaya Boulevard exposed to the wind flow (the author's own archive, 2021)

While there are many discussions, criticisms, and reports on the climate-insensitive planning of seafront buildings in İzmir, no design study was found in the academic literature that proposes a solution for the wind adaptation of seafront buildings. That was the motivation for this research. The city needs a multi-purpose wind planning approach that considers pedestrian wind comfort, air pollution, and

UHI for more comfortable outdoor spaces. However, it is not easy to provide the ideal outdoor climate due to conflicting requirements (Oke, 1988). For example, too many shelters can cause local air pollution to accumulate, while too few shelters can cause the wind to disturb pedestrians (Bottema, 1993). In this context, there is a need for new planning policies that both benefit from the positive effects of the wind and eliminate its adverse consequences for more comfortable outdoor environments.

Alsancak Neighbourhood was chosen as the study area. Alsancak has a very complex and dynamic urban character. Traditional two and three-storey buildings, eight-storey residential apartments, and commercial high-rise buildings create a diverse and rather heterogeneous urban nature. The reason for conducting this study in Alsancak is that Alsancak is the focal point of urban life and the most walkable and attractive place among the alternative transportation stations frequently used by pedestrians. This area includes many outdoor activities such as recreation, entertainment, shopping, sightseeing, walking, and sitting. Pedestrian activities, especially long-term seating and recreation activities in Alsancak, are wind sensitive. Therefore outdoor use requires the highest wind comfort criterion. For the sustainability of pedestrian activities, this area needs improvements in terms of pedestrian wind comfort.

Most of the streets are pedestrianized. In addition, the streets are used for year-round walking and long-term seating areas by restaurants and cafes regardless of their sizes. This functional division of the activities makes the streets vibrant. Figure 3.6 shows the typical street use in Alsancak Neighbourhood. Although the streets are of different sizes, their function is the same.

Figure 3.6 The typical street use and functional division of the activities in the streets, large street, Kıbrıs Şehitleri Street, (Left); narrow street, 1448. Street (Right) (the author's own archive, 2021)

3.1.1 Morphological Analysis

There are two characteristic building types in Alsancak Neighbourhood: adjacent building type (1); detached building type (2). The existing linear seafront buildings consist of adjacent buildings, while inner buildings consist of detached buildings. Figure 3.7 shows the adjacent and detached buildings in the field.

Figure 3.7 Two characteristic building types in the Alsancak Neighbourhood (yellow colour represents adjacent, grey colour represents detached building type)

Previous studies show that wind flow acceleration is inevitable around large and compact building bodies (Reiter, 2010) and the formation of stagnant flow areas behind them (Oke, 1988). For this reason, the author focused on inner urban areas to find a solution to the pedestrian wind comfort and ventilation problems instead of existing seafront urban areas consisting of large building bodies. An urban area consisting of detached residential building units was selected in this context. In the selected urban area, the buildings are in dispersed layouts of plots and have small open spaces between them. Figure 3.8 shows the plan view of the selected urban area and its detached buildings.

The other reason for choosing this area is related to the urban geometric indicators that affect the urban wind flow. The literature has shown that four urban geometric factors significantly affect wind behaviour in the urban environment: building shape

(1), building size (2), street width (3), and building configuration. The selected urban area consists of buildings having different forms, sizes, configurations, and street widths and in this context, it enables to compare the effect of these urban geometric factors. Therefore, the selected urban area differs from the surrounding urban areas in Alsancak Neighbourhood in providing these features.

Figure 3.8 The selected site in Alsancak Neighbourhood (Left & Top-Right); (adapted from Google Earth) view of slender buildings (Right) (the author's own archive, 2022)

The buildings are in slender form and of medium height (4-8 floors) in the selected urban area. The height of the buildings is between 15 m to 25 m, and the ratio of W/H and L/H is between 0.5 and 0.9; where W is the width; L is the length, and H is the height of the building.

Slender blocks were randomly distributed over the site and formed irregular configurations in some places. Therefore, the relative positioning of the buildings and the spatial arrangements of open spaces are various. The main reason for this is the different configurations created by different passage widths varying between 2 m. up to 6 m. Also, the passage widths are smaller than the width of slender blocks.

Therefore, various block sizes in different patterns create a fractal, irregular, and fine-grain urban character.

Although slender buildings have genotypic similarities in their form, the configuration of the buildings is unique, and the dimensions of the buildings and the spaces between the blocks are different. The combination of these differences constitutes the phenotypic urban texture. Each slender building configuration represents a genetic algorithm (GA) that will generate the phenotypical urban texture. Figure 3.9 shows the descriptive and generative character of the building configurations and code transmission from genotype to phenotype in creating the study area. The selected study area allows the comparative testing of wind flow performance of various GAs.
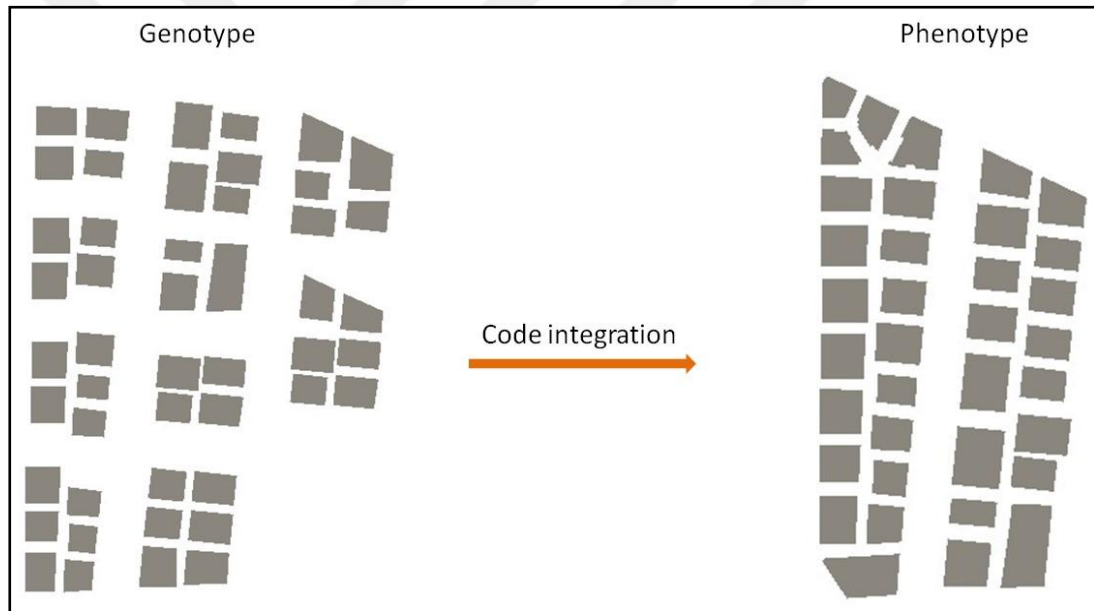
Figure 3.9 Morphological analysis of the site based on genotype and phenotype concept

The buildings on the selected site are in two different configurations: grid-aligned and shifted. In the grid-aligned building configuration, the buildings are straight and parallel to each other, but in the shifted building configuration, they are irregular. The selected urban area is suitable for providing a comparative study to investigate wind flow conditions around grid-aligned and shifted block configurations. Figure 3.10 shows the building configuration types, and Figure 3.11 the view of slender buildings in shifted and grid-aligned building configurations in the existing urban area.
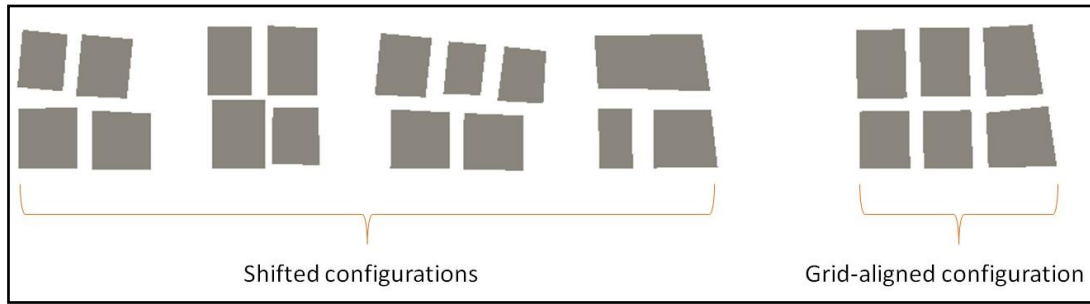
Figure 3.10 The building configuration classification in the study area

Figure 3.11 View of slender buildings in shifted configuration (left); in grid-aligned configuration (right) (the author's own archive, 2022)

3.2 Climatic Considerations

The city of İzmir (Türkiye) is located on the west coast of Türkiye at 38.42°N latitude and 27.14°E longitude. The climate of İzmir is a typical Mediterranean climate, with hot-dry summers and wet-mild winters. According to the Turkish State Meteorological Service [TSMS], the average temperature is 10.7 °C in winter and 27.7 °C in summer.

İmbat primarily influences the city, a local sea breeze blowing from the İzmir Gulf towards the land during the day. Considering the climate and environmental

problems of İzmir, the sea breeze (İmbat) is unique and of high quality compared to other winds in many ways. Depending on the origin of the wind, the wind can be hot or cool, fast or slow, dry or humid, clean or dusty, and regular or irregular (Gut & Ackerknecht, 1993). Since its origin is the sea, the sea breeze carries the clean and cool air mass from the sea to urban environments. Its formation is regular as it depends on the temperature differentiation between the sea and the land. In addition, because the sun's heating energy on the land and water bodies increases in summer, it is faster in summer and weaker in winter. These features are desirable to reduce excessive city temperature in summer, avoid the wind chill effect in winter, and ventilate the city with fresh air. Figure 3.12 shows the relation between wind speed and temperature in İzmir. When the air temperature rises, the wind speed increases and reaches its peak in September.
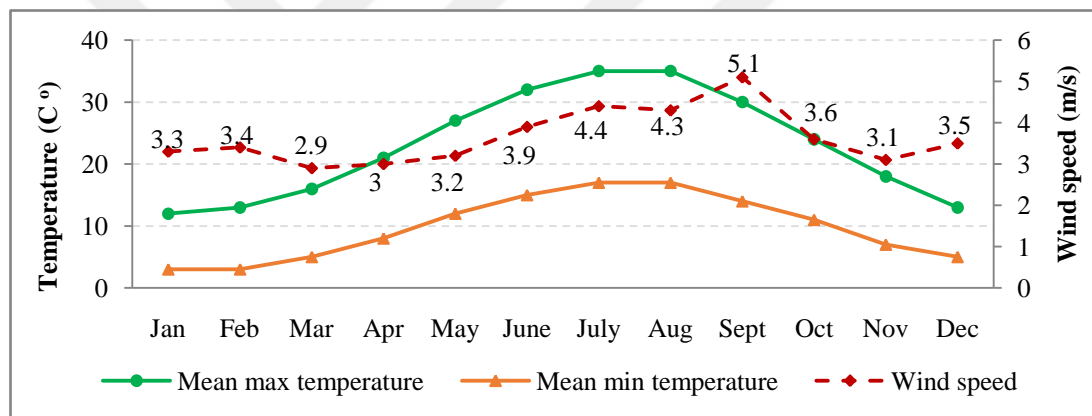
Figure 3.12 Monthly mean temperature and wind speed (z=10 m) in İzmir (TSMS)

According to the Pasaport meteorological station (TSMS) which is the closest station to the Alsancak neighbourhood, the average annual wind speed (z=10 m) is 3.4 m/s in winter and 4.2 m/s in summer. The sea breeze direction is North-Northwest (Figure 3.13) with an average annual wind speed of 3.64 m/s (z=10m), corresponding to a light breeze (3.4-5.4 m/s) and labelled with Force 3 according to the modified Beaufort scale (Penwarden, 1973). Although the wind speed is not as high as in the cities of Wellington (NZ), St. John's (CAN), and Copenhagen (DEN), where the average annual wind speeds are around 6.6 m/s, 6.2 m/s, and 5.6 m/s, respectively (USDOE EnergyPlus Climate Data), the city's coastline, in particular, is at risk of wind discomfort due to the building-induced windy conditions.
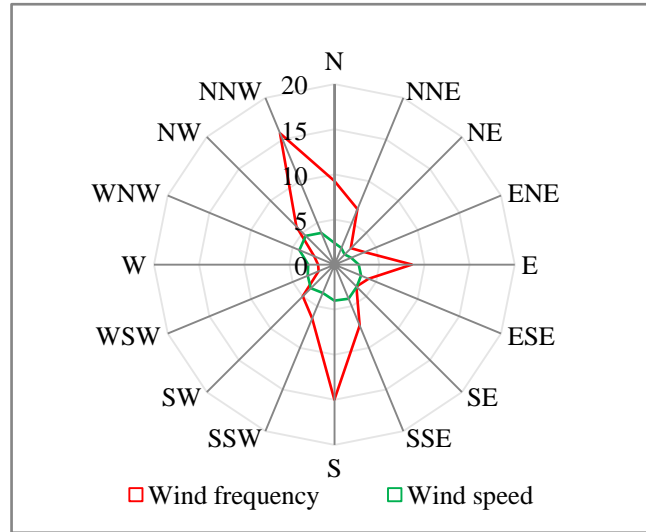
Figure 3.13 Wind-rose diagram of Pasaport/İzmir (TSMS)

Thirty-six wind directions need to be considered when assessing the risk of pedestrian wind discomfort (City of London & RWDI, 2019). Still, we limited the research to local sea breezes (İmbat) due to their many positive effects on urban ventilation, UHI, and global temperature increase. On the other hand, this research is not site-specific wind comfort research. Furthermore, this research is based on a multi-case parametric approach, and therefore, difficult to consider all wind directions in such studies. Therefore, other wind directions were not considered.

3.3 Method of the Field Study

The computational fluid dynamics (CFD) method was used to assist the field study in this research. Four things are needed to produce faster solutions to wind flow problems in urban areas with CFD. The first is to offer CFD codes that can be easily used by architects and urban planners and are suitable for bluff body aerodynamics. The second is to provide easy access to CFD codes and popularize open-source CFD codes. Third, it is necessary to offer reliable and complete wind tunnel data generated for CFD validation to decrease the risk of error or uncertainty. Fourth, to provide detailed explanations of CFD validation processes, including all calculations, to help architects and urban planners to follow the same protocol and increase the CFD solution accuracy. This step is necessary because architects and

urban planners do not have sufficient knowledge of the basics of fluid dynamics and simulation techniques, as required by their field of study.

This section of the research step-by-step describes the validation process of CFD for turbulent atmospheric boundary layer (ABL) on a simple urban building complex. As the choice of the CFD code affects the results, the predictive accuracy of two popular CFD codes, STAR-CCM+ (STAR) and SIMSCALE, were also compared to find the best possible for urban wind environment assessments. Architects and urban planners can create solutions for various urban wind flow problems by following the specified CFD process.

There are three reasons to compare SIMSCALE and STAR: free availability for academic use, user-friendly interface, and similar numerical setup process. SIMSCALE is a cloud-based, online engineering simulation code using the open-source OpenFOAM solver. It has a large amount of online documentation and is widely used for urban wind flow applications. STAR is a general-purpose CFD code but can also be used for urban flow applications. SIMSCALE offers 3000 free core hours per year for academic use, but STAR has no usage limitation. Because the CFD model workflow organization is similarly from top to bottom, both programs run with similar computational efforts. It is possible to create the same CFD model conditions such as boundary conditions, grid structure and entry conditions, and solution methods in both programs. Therefore, they were compared mainly in terms of turbulence models. The turbulent wind flow pattern over the simple urban building complex was obtained by solving the 3-dimensional steady Reynolds-averaged Navier Stokes (RANS) equations with the turbulence models of Standard $k - \varepsilon$ (Jones and Launder, 1972), Realizable $k - \varepsilon$ (Shih, Liou, Shabbir, Yang, & Zhu, 1995), SST $k - \omega$ (Menter, 1994) and Reynolds Stress Model (RSM) by Chou (1945) & Rotta (1951).

3.3.1 Outline of the CFD Validation Process

The CFD validation process begins with the acquisition of reliable experimental data. It may be better to use the data generated for validation purposes to avoid potential errors and uncertainties caused by insufficient information at the beginning

of the process. Calculating inflow parameters based on experimental data and Best Practice Guidelines (BPGs) is critical in obtaining accurate results and keeping initial data uncertainty as low as possible (Franke, Hellsten, Schlünzen, & Carissimo, 2007). At this stage, velocity and turbulence quantities should be as close as possible to the experimental data. Choosing the appropriate turbulence model according to the character of the flow problem and optimum grid resolution based on BPGs is another critical step to achieving an acceptable result rapidly.
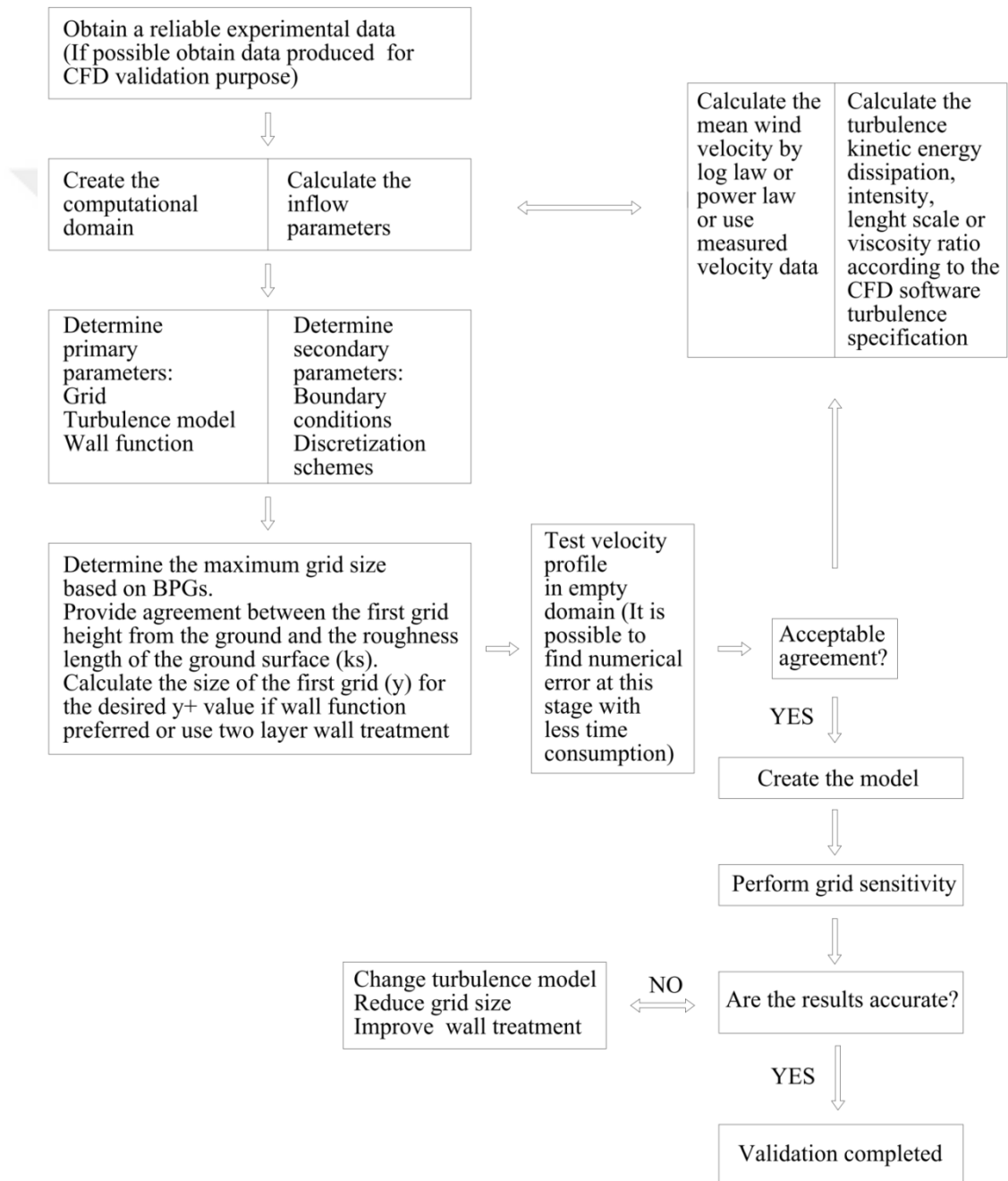
Figure 3.14 Flowchart outlining the CFD validation process for turbulent ABL flow

After determining the CFD setup parameters, it is helpful to perform a simulation in an empty domain to check for "horizontal homogeneity" throughout the computational domain. It is also helpful to check for reverse flow at the outlet. Simulation results may change if acceptable "horizontal homogeneity" is not achieved or if reverse flow exists. It is more time-efficient to check for numerical errors at this stage. If a satisfactory agreement is reached between the inlet and test area flow conditions, the model geometry can be created, and a grid sensitivity test can be started. Choosing the appropriate turbulence model, grid size, and near-wall treatment usually yields accurate results. However, a conflict may occur after the geometric model is created in the computational domain between the model geometry and the turbulence model. For instance, flow separation and recirculation are very relevant to model geometry, and not all turbulence models are good at predicting them (Franke et al., 2004; Thangam & Speziale, 1992). Therefore, if the results are unsatisfactory, other turbulence models should be tested and the grid size reduced. Figure 3.14 shows the flowchart of the step-by-step CFD setup and validation process. The proposed method will also be used in this research to design the best possible urban seafront building configurations.

3.3.2 Validation Test Case and Experimental Data

To validate a CFD model, it is necessary to obtain reliable and detailed experimental data sets generated in ABL. If the experimental data sets are not high quality and not provided for CFD validation purposes, errors and uncertainties may occur due to the lack of required information. The Working Group of the Architectural Institute of Japan (AIJ) (2016) provided many online wind tunnel data-sets files (Excel) for CFD validation purposes and published validation benchmark tests of seven different comparative and parametric studies to assess the pedestrian wind environment around buildings in ABL. The wind tunnel datasets file provides inlet boundary conditions, measurement points for each test scenario, and detailed experimental results. Datasets were generated in the 3 m wide, 1.8 m high, and 22 m long wind tunnel of Fujita Technology Center Co., Ltd. (Nonomura, Kobayashi, Tominaga, & Mochida, 2003).

In this research, standard simple building blocks (Test Case C) proposed by the AIJ (2016) are used to estimate the accuracy of CFD codes for wind environment assessments. The sub-case (Case 1H) of Test Case C (AIJ) consists of a 3 x 3 layout of uniform height (20 m) blocks with 20 m street width. The central building has the same height as the surrounding buildings, and the scale ratio of the buildings is 1:1:1 (height: width: length). The sub-case (Case 1H) represents a standard city plan. Figure 3.15 shows the sub-case (Case 1H) proposed by the AIJ.
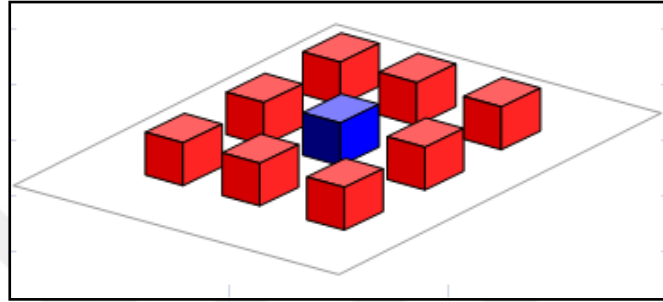
Figure 3.15 3-D view of simple building blocks-Test Case C, Sub-Case 1H (AIJ, 2016)

The experimental study was conducted in an ABL wind tunnel with a 1/100 scale model. Wind speed was measured from the ground of the wind tunnel at 2 mm height, corresponding to 2 m on a real scale. The Test Case C dataset consists of 120 wind speed measurement points around the central building, shown in Figure 3.16. Half of the measurement points (1-63) were assessed since the geometry of the sub-case (Case 1H), and the measurement points are symmetrical. The dataset uses mean wind speed for systematic point-to-point comparison. The potential measurement error due to the location is unknown. It should be noted that any deviation in the location of the probes can cause significant differences in results.

The experimental and CFD results of scalar wind speed were compared only for the normal wind flow direction ($\phi = 0°$) during the validation process. Wind speed values are relatively normalized to the reference wind speed. Expressing the wind speed as a ratio allows for easy cross-comparison of different points. The wind speed ratio formula is defined as: $W.S.R = U/U_{ref}$

where U is the mean wind speed at the measurement point, and U_{ref} is the inlet mean wind speed.
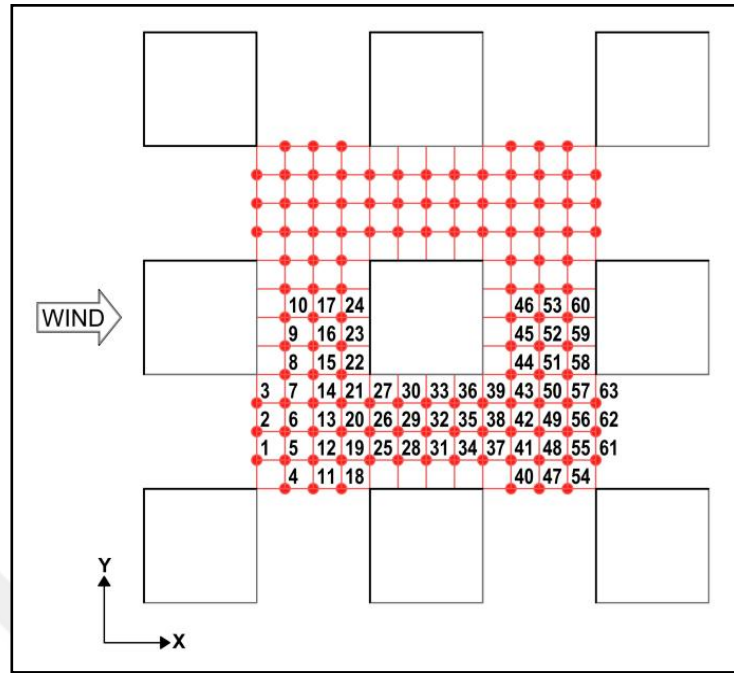
Figure 3.16 Plan view of the measurement points around the central building (AIJ, 2016)

3.3.3 CFD Setup for Validation

CFD tools solve mathematical equations using numerical discretization. As computer power is still limited today, it is necessary to simplify the equations to solve many flow problems. However, simplifying the equations can cause errors and uncertainties that often make CFD results inconsistent and unstable while reducing the computation time. To keep errors and uncertainties as small as possible, BPGs have been created for non-CFD experts that summarize the critical points of calculation parameters (Casey & Wintersgate, 2000; Franke et al., 2007; Tominaga et al., 2008). BPG explains how a set of parameters should be applied systematically to a model for more consistent and stable solutions. In addition, BPG aims to reduce user error due to lack of experience and provides a general recommendation framework for the CFD process.

At all stages of the validation process, the CFD setup was created according to the BPGs. Two key goals, maximum predictive accuracy and minimum computational run-time shaped the CFD process.

3.3.3.1 Size of Computational Domain

The computational domain should have appropriate dimensions to keep the effect of computational boundaries on wind speed at minimum. In CFD validation studies with wind tunnel testing, the computational domain for the CFD model should have the same geometric dimensions and cross-section as the wind tunnel. Therefore, the lateral and upper size of the computational domain is limited by the wind tunnel size -1.8 m (9H) x 3.0 m (15H) (height x width), where H is the height of the building. The inlet boundary edge was located at 10H, and the outflow boundary edge was located 15H from the building (Franke, 2007).

3.3.3.2 Boundary Conditions

For a realistic CFD solution in ABL studies, the inlet wind profile should be created using the logarithmic law corresponding to the terrain exposure category or the profile obtained from the wind tunnel experiment. For the ground surface boundary condition, it is necessary to specify the aerodynamic roughness length (z_0) (Wieringa, 1992) or the equivalent sand-grain roughness height (k_s) (Nikuradse, 1933).

3.3.3.2.1 Inlet Boundary Condition. The inlet wind velocity U (m/s) and the RMS value of velocity fluctuation σ_u (m/s) were obtained from the experimental inlet wind profile for the lower parts of the ABL (0–120 m). However, turbulence kinetic energy k (z) and turbulence dissipation (ε) in the vertical direction is also necessary for CFD simulations in STAR and SIMSCALE.

Using the U and σ_u values, turbulence kinetic energy k (z) was calculated from the relation between k (z) and σ_u (z):

$$k(z) \cong \sigma_u{}^2(z) \tag{3.1}$$

After obtaining the k (z) values for different heights, the values of turbulence dissipation (ε) were calculated from the relation $P_k = (\varepsilon)$, (P_k: production term for k equation):

$$\varepsilon\,(z) = P_k\,(z) = C_\mu{}^{1/2} \cdot k(z) \cdot dU(z)/dz \tag{3.2}$$

where C_μ is the model constant (=0.09).

Inlet wind profile consisting of velocity profile (U), turbulence kinetic energy profile (k), and turbulence kinetic energy dissipation profile (ε) was created with the above calculations (see Appendix B). In STAR and SIMSCALE, the obtained input variables, U, k, and ε, as a function of height (z), were assigned by the XYZ table in CSV file format.

3.3.3.2.2 Ground surface boundary condition. Two methods can be used to model the ground surface boundary condition: aerodynamic roughness length (z_0) using the updated Davenport (1961) roughness classification (Wieringa, 1992) or the equivalent sand-grain roughness height (k_s). The k_s was used for the CFD model since STAR and SIMSCALE use roughness properties based on k_s,

Blocken, Stathopoulos & Carmeliet (2007) recommends using the equation (Eq. 3.3) between z_0 and k_s for horizontal homogeneity in ABL flow and states that this equation can be applied to any CFD code. The equation between k_s and z_0:

$$k_S = \frac{9.793 * z_0}{C_S} \tag{3.3}$$

The value of z_0 was calculated using the inlet experimental data (U_{ref} at z_{ref}) and the logarithmic law:

$$\frac{U_{ref}}{(\tau_w/\rho)^{1/2}} = \frac{1}{\kappa} \ln \left(\frac{z_{ref}}{z_0} \right) \tag{3.4}$$

When the boundary layer near the ground is considered as the constant flux layer, the value of z_0 can be assumed from the logarithmic law using the relation $(\tau_w/\rho)^{1/2} = u^* = C_\mu^{\frac{1}{4}}\sqrt{k}$. The friction velocity (u^*) was estimated by the following equation using the value of turbulence kinetic energy (k) at the closest point from the ground ($z_{ref} = 0.01$ m) in the experiment.

$$u^* \cong C_\mu^{\frac{1}{4}}\sqrt{k} = 0.09^{\frac{1}{4}} \sqrt{0.314} = 0.307 \text{ m/s}, \tag{3.5}$$

Using calculated friction velocity (u^*) and U_{ref} at the height of z_{ref} (=0.01 m) in Eq. 3.4, the value of z_0 was calculated to be 4.386×10^{-4} on the experimental scale. The von Karman constant (κ) is imposed in this study as 0.41.

Using the obtained z_0 value from Eq. 3.3, k_s was found as 4.3×10^{-3} m on the experimental scale where the value of c_s is 1.0. This implies that the equivalent sand-grain roughness height (k_s) is 0.43 m on the real scale.

3.3.3.2.3 Lateral, upper, and building surface boundary conditions. The logarithmic law of no-slip shear stress and smooth wall surface feature was applied to the building surfaces. Slip / Symmetrical wall boundary condition was used for the lateral and upper boundaries to avoid resolving the boundary layer of the wind tunnel wall. However, ignoring the frictional effects of wind tunnel boundaries can affect the simulation results. Therefore, the sensitivity of the no-slip / smooth and slip / symmetric wall boundary conditions on wind flow was compared but found no change in the results. It means that the wind tunnel boundary where the AIJ TEST Case C was conducted does not affect the experiment result. This is reasonable considering the blockage ratio (Area$_{buildings}$ / Area$_{domain}$) of 2.2% in the experiment. Open boundary conditions were used at the outlet boundary, and zero static pressure was applied.

3.3.3.3 Turbulence Models

Providing urban ventilation and pedestrian wind comfort are multi-purposes of this research. Still, the risk of wind gusts and detailed pollutant dispersion research is beyond the scope of this research. Studies to understand wind gust and pollutant dispersion mechanisms in urban canopy layers require transient flow analysis. LES (Large Eddy Simulation) is better at predicting turbulence effect to solve such flow problems but requires much more computation time than RANS (Antoniou et al., 2017; Liu, Leung & Barth, 2005; Salim, Buccolieri, Chan, & Di Sabatino, 2011). LES is also not practical in parametric design studies.

In pedestrian wind comfort studies, it is usually sufficient to obtain only mean speed values; therefore, there is no need to resolve all the details of turbulent

fluctuations. Steady-state RANS can calculate the time-averaged mean speed but do not predict the effect of turbulence on the mean flow. Therefore, there is a need to use an explicit turbulence model that can compute turbulent flows with RANS equations.

In this research, the simulation was performed using the Standard $k - \varepsilon$ (Jones & Launder, 1972), Realizable $k - \varepsilon$ (Shih et al., 1994), SST $k - \omega$ (Menter, 1994), and Reynolds Stress Model (RSM) Chou (1945) and Rotta (1951). These turbulence models are primarily used in urban wind flow applications. The performance of the turbulence models was tested under the same computational conditions (grid, boundary conditions, *etc*.), and the flow was considered turbulent and incompressible.

3.3.3.4 Choice of Computational Grid

Creating a computational grid through discretization is a critical step in CFD modelling. It is also essential to confirm that the CFD result does not change with different grid structures. Therefore, a grid sensitivity study should be performed. Franke et al. (2004) suggest using at least three systematically refined grids to predict the error band of spatial discretization in grid refinement.

Generally, the more grids there are, the higher the accuracy, but the longer the calculation time. CFD requires the highest simulation accuracy but is often performed under time constraints. Therefore, global grid refinement is impractical and time-consuming. Franke et al. (2007) recommend using a local grid refinement in the area of interest instead. The refinement process is of creating a denser grid structure (meshing) in certain parts of the model to achieve more precise results in the refinement area.

In this research, a 3-D finite-volume approach is employed for discretization. Both STAR and SIMSCALE provide not only manual but also automatic meshing. However manual meshing was used to create the same grid and control all meshing processes in both codes.

3.3.3.5 Grid-independence Study

It is necessary to find the optimum grid resolution to ensure the accuracy of the CFD model at an acceptable run time. Therefore, a grid independence study was performed. Three points were taken into account when determining the grid sizes:

1) At least ten grids are required on one side of the building (Franke, 2004; Tominaga, 2008), and at least two or three layers of control volume should be provided at the pedestrian level (0-2 m.) (Franke, 2004).

2) The distance y_P (the centre point (P) of the first cell) should be larger than k_s (Blocken, Stathopoulos et al. 2007). However, it is essential to note that it is impossible to meet the requirement of $y_P > k_s$ for high terrain categories such as category IV where z_0 is 1 m.

3) For high y^+ wall treatment formulation, the dimensionless normal distance (y^+) of the first cell centroids from the wall should be at least 30 ($y^+ = 30$) (Casey, 2000) and should be between 30 and 150 ($30 < y^+ < 150$) (STAR-CCM+ User Guide, 2006).

In this context, the maximum grid size of the building should be 2 m, and the height of the first cell should be ≤ 1 m for pedestrian level wind assessment. Considering the relation between k_s and the first grid height, the height of the first cell should be greater than 0.86 m (> 0.86 m), where k_s is 0.43 m.

For the use of the wall function, the size of the first cell (y) was calculated when the desired y^+ ($30 < y^+ < 150$) equation:

$$y = \frac{y + \mu}{\rho u*} \tag{3.6}$$

where y is the wall distance, ρ is the density of air (kg/m^3), u* is the friction velocity, and μ is the dynamic viscosity of air (kg/m/s). U* was calculated using Eq. 3.6 and found to be 0.307 m/s. For $30 < y^+ < 150$, the wall distance was calculated as 0.14 m < y < 0.71 m. According to this result, the first cell height should be between 0.28 m and 1.42 m.

Based on the requirements and calculations, the height of the first cell should be in the range of 0.86 - 1 m, and only the 1 m grid size provides the required conditions. Therefore, performing a grid sensitivity test with at least three systematically refined grids isn't possible. To solve the problem, Blocken, Stathopoulos et al. (2007) recommends alleviating the requirement of $y_P > k_s$ or using a coarser grid in the upstream and downstream regions and a finer grid in the central region of the domain. However, in the preliminary tests to investigate the sensitivity of the $y_P > k_s$ requirement, it was found that meeting the $y_P > k_s$ requirement gives a more accurate result in such a situation with a low terrain category. In this context, in the grid sensitivity test, four basic strategies were adopted:

1) using a coarser grid in the upstream and downstream regions. This strategy was applied to all grid sizes.

2) fulfilment of the requirement of $y_P > k_s$.

3) alleviation of the rule of providing two or three cells at the pedestrian level recommended by Franke (2004).

4) using high y^+ ($30 < y^+ < 150$) wall treatment method.

Proper creation of vertical velocity profile is essential for high simulation accuracy. At the same time, maintaining the "horizontal homogeneity" throughout the computational domain is another important point. Many studies report the difficulty in creating a horizontally homogeneous ABL flow (Blocken & Carmeliet, 2006; Franke & Frank, 2005; Zhang, 1994). It is recommended to test the velocity profile depending on the ground surface conditions in the empty computational domain (Franke 2007; Blocken, Stathopoulos et al. 2007). The vertical velocity profile where the geometric model would first interact with the wind flow (test area) was measured in the empty computational domain to check the agreement between ks and the first cell size. It was confirmed that no large difference between the vertical velocity profile in the inlet and test area exists when the k_s is 0.43 m, and the cell height is 1 m. However, the deviation in velocity is at the highest level with

5.8% in the first 50 m from the ground, but this difference is acceptable (see Appendix C).

Table 3.1 Grid size and grid number in each region

Grid name	Grid regions	Grid size (% of base size)	Grid number	Absolute grid size
Grid 1	Computational domain (max. size)	100		8
	Upstream/downstream regions	50		4
	Test area	25	10	2
Grid 2	Computational domain (max. size)	100		10
	Upstream/downstream regions	25		2.5
	Test area	12.5	16	1.25
Grid 3	Computational domain (max. size)	100		8
	Upstream/downstream regions	25		2
	Test area	12.5	20	1

A grid independence study was undertaken after checking the vertical velocity profile in the test area. Table 3.1 shows the grid size and grid number for each test case in the grid independence study. It started with ten grids in each direction, and the number of grids gradually increased to 16 and then 20. The computational domain was divided into two different boundary regions with varying grid sizes, such as the upstream and downstream regions and the test area. A set of Cartesian boxes was created for regional refinement. The grid is finer around the test area while it is coarser in the upstream and downstream areas.

For the grid shape, structured hexahedral cells were used as the buildings have a regular and straightforward form. As optional near-wall cell layers, 15 prism layers with gradually increasing size and a stretching ratio of 1.2 were applied. Prism layers are recommended for all wall treatment methods to improve accuracy (STAR-CCM+ User Guide, 2006), and therefore, they were used for wall boundaries. Figure 3.17 shows the grid structure of the computational domain. The grid sensitivity test was carried out with the RSM-Linear Pressure Strain turbulence model of STAR.
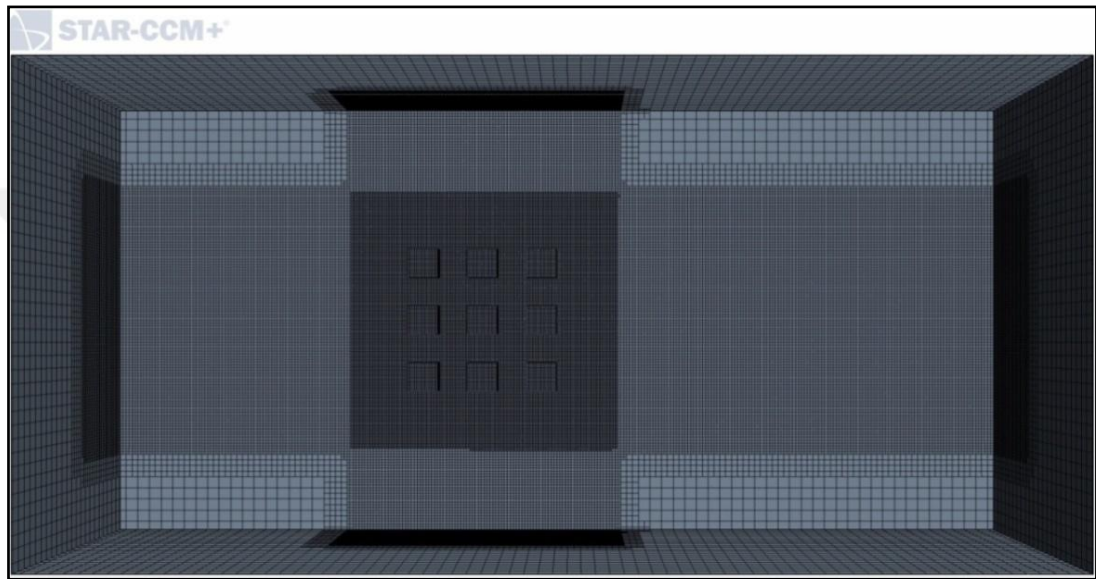
Figure 3.17 View of the global and local grid discretization of the computational domain

Both STAR and SIMSCALE use the finite-volume (FV) method to discrete the Navier-Stokes equation and the SIMPLE (Semi-Implicit Method for Pressure Linked Equations) algorithm to couple the pressure and velocity equations. 2nd - order upwind scheme (Gauss linear Upwind) was used for the advection terms of the governing equations in SIMSCALE. STAR uses both coupled and segregated finite volume flow solvers. In the segregated flow solver, the equations are solved uncoupled. The segregated flow solver based on the SIMPLE algorithm was used because of its computational time efficiency compared with the coupled solver. The fluid in the computational model is the air of constant density.

The results confirm that the solution is grid-independent with 1.25 m or more grid cells in each direction as the wind speed ratio does not change with a further decrease in grid size (see Appendix D). Grid 2 is satisfactory, i.e., one side of the building is

divided into 16 portions or more. However, the 1 m grid provided at least two grids at the pedestrian level (2 m). Thus all the requirements stated in the BPGs have been met.

3.3.4 Results

The performance of the Standard k – ε, Realizable k – ε, SST (Menter) k – ω, and RSM turbulence models by comparing the calculated wind speed magnitudes with the experimental results. Figure 3.18a shows the wind flow field obtained by STAR's RSM model around the urban building complex. The wind-exposed and wind-protected areas are visible. The corner effect develops around the front edge buildings, while the double corner effect, which is more intense than the corner effect, develops around the building in the front centre (PCA). Figure 3.18b shows the wind flow field obtained by SIMSCALE's SST (Menter) k – ω turbulence model around the simple building blocks. Unlike the flow field obtained by STAR, two separate flow regions are formed in the front centre, meaning that the corner effect is more dominant than the double corner effect. This is inconsistent with experimental data. The turbulence models of STAR tested in this study are better than the turbulence models of SIMSCALE at predicting the double corner effect. Accurate prediction of the double corner effect is essential for studies measuring wind speed in passages between two parallel buildings.
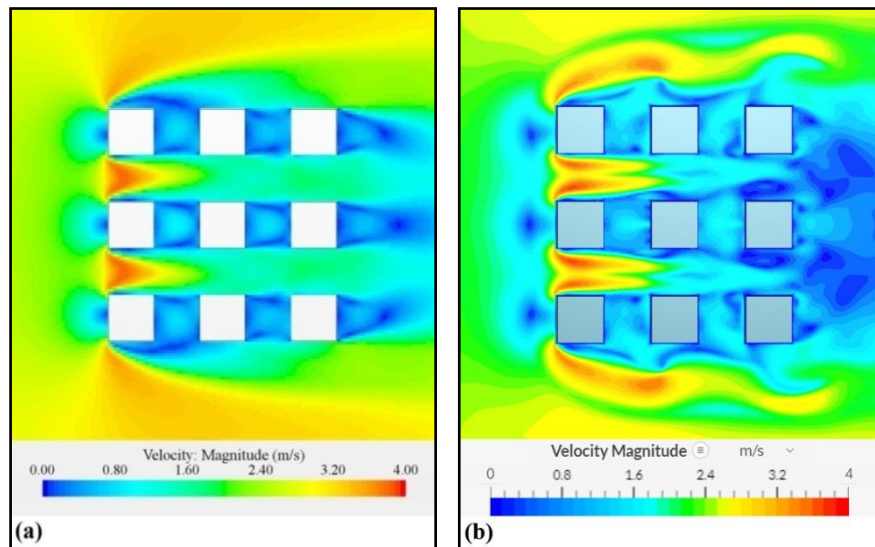
Figure 3.18 Wind speed distribution in horizontal plane (z=2m) (a); STAR's RSM model (b) SIMSCALE SST (Menter) k – ω model

Figure 3.19 compares simulated and experimental W.S.R (U/U_{ref}) at 2 m above the ground obtained with different CFD codes and turbulence models. The results show that none of the CFD results precisely match the experimental data. However, these results are not abnormal for such bluff body aerodynamics in the turbulent atmospheric boundary layer. It is difficult to precisely match the experimental data with CFD based on steady RANS turbulence models. Although there is no complete consistency with the experimental data, the position of the highest speed zone has been simulated very well by STAR and SIMSCALE. The predictive accuracy in the high-speed region of $U/U_{ref} > 1.0$ is satisfactory for all CFD codes. This result is important for accurately predicting pedestrian wind discomfort risk in urban wind flow analysis.
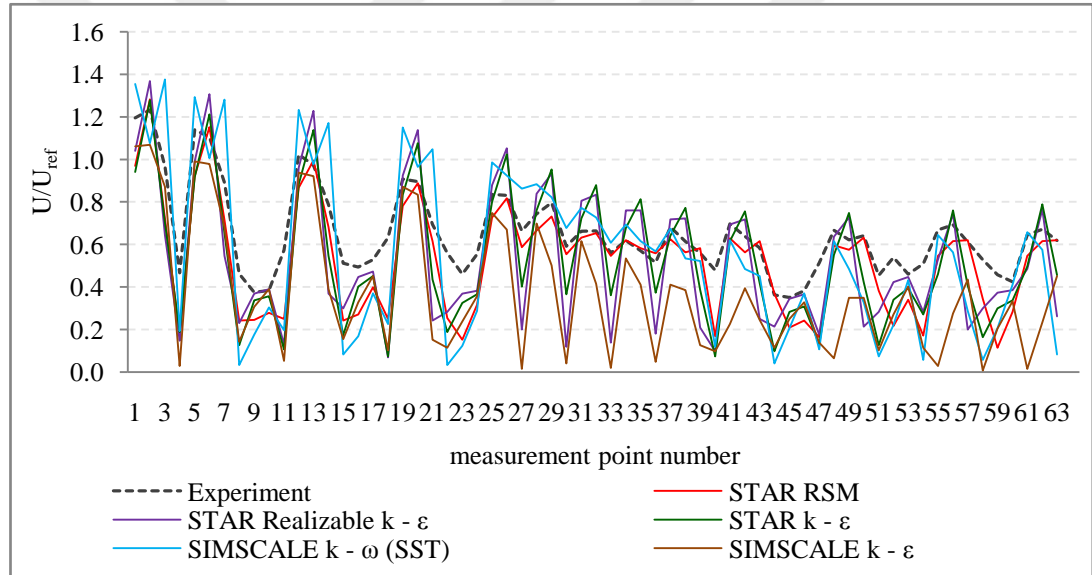
Figure 3.19 Comparison of wind speed ratios between experiment and different CFD turbulence models

The degree of accuracy varies considerably in the high and low-speed regions. The wind speed ratios vary greatly, especially in the Realizable k – ε and the Standard k – ε models. The general trend is that CFD prediction has limited accuracy in wind-sheltered areas behind the buildings. The wind speed ratio was underestimated and lower than the experimental results in these regions. Turbulence models are insufficient to resolve wind-sheltered regions, and CFD codes are not good enough to predict low-speed regions.

Among the CFD codes and turbulence models, the predictive accuracy of STAR's RSM model is remarkable. The trend of wind speed ratio is more similar to the experimental result for the RSM model. The highest speed position has been simulated very well by the RSM. However, RSM underestimates the low-speed region. As a result, there is a high deviation in wind speed ratio, particularly at the measurement points 22-24 and 58-60.

Results showed that STAR performed better than SIMSCALE in validation tests and that STAR's RSM model was more accurate than other turbulence models. Therefore, the predictive accuracy of STAR's RSM model was analysed in detail. The simulated and experimental W.S.R (U/U_{ref}) obtained with STAR's RSM at 2 m above the ground was compared. The location of measurement points in the flow channel was also shown (see Appendix E). The wind flow accelerates in the flow direction, and the speed-up area is formed through the channels. This flow region represents the highest speed region consisting of 39 measurement points. The accuracy of RSM throughout the flow channel was calculated, and the percent error was found to be only 7%, with high predictive accuracy in this region.

To quantitatively evaluate the predictive accuracy of CFD codes and turbulence models, the percent error between the CFD and the experimental result was calculated using the following equation:

$$\text{Percent error} = |(P(v) - M(v))/M(v)| * 100\% \qquad (3.7)$$

where $P(v)$ is the predicted wind velocity calculated by CFD and $M(v)$ is the measured wind velocity obtained from the wind tunnel experiment. Table 3.2 shows the percent error for each code and turbulence model. The table shows a moderate agreement in the low-speed regions and a higher level of agreement in the high-speed regions. The percent error increases for each turbulence model where the wind speed ratio decreases in the regions.

The percent error for the STAR's RSM, which is the best possible model in all tested turbulence models, was around 22.3%. This high percent error is mainly due to the low predictive accuracy in the side-street flow region. However, the most

important point in wind comfort assessment is to find the highest speed region and position with acceptable accuracy. The percent error of STAR's RSM is around 12% in the high-speed region where $U/U_{ref} > 1.0$. In addition, it is 10.8, 17.3 and 21.3% where $U/U_{ref} > 0.6$, 0.5 and 0.4, respectively. STAR's RSM provides higher predictive accuracy in the flow region where $U/U_{ref} > 0.6$. In the evaluation of the high-speed regions with steady RANS, the percent error of up to 10% is considered "very good," while 20% is considered "good" (Blocken et al., 2016). In addition, the percent error of up to 25% can be accepted in urban aerodynamic studies with steady RANS models.

Table 3.2 The percent error for each CFD code and turbulence model

CFD Code	Turbulence model	Percent error (%) ($U/U_{ref} > 1.0$)	Percent error (%) ($U/U_{ref} > 0.6$)	Percent error (%) ($U/U_{ref} > 0$)
STAR-CCM+	RSM	12	10.8	22.3
	Realizable $k - \varepsilon$	12.2	26.5	30.7
	Standard $k - \varepsilon$	13.2	21.4	30.8
SIMSCALE	$k - \omega$ (SST)	13.4	22.5	34
	Standard $k - \varepsilon$	11.2	36	46

STAR's Standard $k - \varepsilon$ and SIMSCALE's SST (Menter) $k - \omega$ model show medium predictive accuracy. The percent errors are 21.4% and 22.5%, respectively. These turbulence models could also predict wind speed ratios above 0.6 with acceptable accuracy in wind comfort studies.

A scatter plot was created for each CFD code and turbulence model to show the correlation between experimental and CFD wind speed ratios (see Appendix F). Results are displayed as a collection of points to illustrate the degree of correlation between CFD and the experiment. STAR's RSM shows better agreement with the experimental results than other turbulence models.

3.3.4.1 Assessment of CFD Codes

The CFD codes were assessed regarding the accuracy, run-time, and ease of use with the user's experience.

3.3.4.1.1 Degree of accuracy. CFD validation results showed that STAR, in general, provided higher simulation accuracy than SIMSCALE as it has more turbulence models choice. Specifically, the predictive accuracy of STAR's RSM is better than other turbulence models. But, in this research, only SIMSCALE's free standard community license was used. SIMSCALE also offers the Lattice Boltzmann method (LBM) under professional license for pedestrian wind comfort studies. As the accuracy of the LBM solver has not been tested, the assessment is limited to the use of the free standard community license.

3.3.4.1.2 Run-time. The run-time of the CFD simulations is similar (6-7 hours) for CFD codes, except for STAR's RSM, which takes about 14 hours when the simulation runs on a workstation with an 8-Core, 3.59 GHz Processor and 32 GB RAM. The meshing time is longer in SIMSCALE, at 25 minutes, while only 4 minutes in STAR. However, since SIMSCALE is a cloud-based CFD code and allows 96 cores, it is possible to reduce simulation run-time considerably with professional SIMSCALE licenses.

3.3.4.1.3 Ease of Use. Both STAR and SIMSCALE are run with similar computing efforts because of the identical CFD model setup process. However, SIMSCALE guides the user in setting the parameters with a drop-down menu explaining the meaning of the parameters in detail. This option helps avoid user errors. However, it is difficult to process data from measurement points in SIMSCALE when there are too many measurement points. This makes the post-processing stage challenging to compare different cases. On the other hand, in SIMSCALE, it is possible to visualize the state of the flow field after each iteration, even after the simulation is complete. This helps to understand how the flow changes during simulation.

3.3.5 CFD Setup

The field study was carried out with the CFD method. The study area was isolated and abstracted from its surroundings and simulated with STAR CCM+. The wind speed was measured at 2 m in height from the ground.

3.3.5.1 Domain size

The size of the calculation area must be calculated correctly to avoid possible artificial accelerations due to the blocking effect. Since the lateral dimensions of the proposed seafront building configurations are larger than their height (H), the blockage ratio for such building configurations should be less than 3% (Baetke, Werner, & Wengle, 1990). Also, the top of the calculation area must be at least 5H away from the tallest building. Initially, the top size was determined as 8H. Thus, keeping the blockage rate below 3%, the lateral dimension was determined as 12H. In addition, the inlet and outflow boundaries from the central area of interest were defined as 10H and 15H, respectively (Franke et al., 2004).

3.3.5.2 Boundary Conditions

While establishing the inflow boundary conditions, the terrain category and the mean wind speed value at any reference altitude should be determined first. The specified study area is close to the sea, and there is a large and low-grass covered area between the seafront buildings and the sea. The aerodynamic roughness length (z_0) of low-grass is 0.01, and the power-law exponent (α) for such a terrain category is 0.13 (Burton, Sharpe, Jenkins, & Bossanyi, 2012). Eq. 3.8 shows the power law to describe the vertical wind profile.

$$\frac{U_h}{U_{ref}} = \left(\frac{h}{h_{ref}}\right)^\alpha \tag{3.8}$$

where U_h is wind speed at any height (m), U_{ref} is the wind speed at the reference height, h is the height corresponding to U_h, h_{ref} is the height corresponding to U_{ref} and α is the power-law exponent related to the terrain category.

Statistical mean wind speed (U_{ref}) and wind direction (z=10 m) obtained from Pasaport/İzmir meteorological station (TSMS) were used to generate the wind speed profile. Using the mean wind speed (U_{ref}) and power-law exponent (α) in Eq. 3.8, the vertical wind velocity profile was generated for the study area.

The formula proposed by Richards and Hoxey (1993) was used to generate the turbulence parameters in the type of k (turbulence kinetic energy) + ϵ (turbulence kinetic energy dissipation):

$$U(z) = \frac{u^*}{\kappa} \ln + (\frac{z+z_0}{z_0}) \tag{3.9}$$

$$k(z) = \frac{u^{*2}}{\sqrt{C_\mu}} \tag{3.10}$$

$$\epsilon(z) = \frac{u^{*3}}{\kappa(z+z_0)} \tag{3.11}$$

where U_z is the mean wind speed, u^* is the ABL friction velocity, z is the height from the ground, z_0 is the aerodynamic roughness length, κ is the von Karman constant, k is the turbulence kinetic energy, C_μ (=0.09) is a model constant, and ϵ is the turbulence dissipation rate.

There are two methods for determining ground surface boundary conditions: aerodynamic roughness length (z_0) (Wieringa, 1992) or equivalent sand-grain roughness height (k_s) (Nikuradse, 1933). Eq. 3.12 shows the relation between k_s and z_0 that could be used in every CFD code (Blocken, Stathopoulos et al. 2007):

$$k_S = \frac{9.793*z_0}{C_S} \tag{3.12}$$

where the value 9.793 is the empirical wall constant E (-), and the value of c_s (roughness constant) is 1.0.

The aerodynamic roughness length (z_0) of low-grass was previously determined as 0.01 (Burton et al., 2012). Using the z_0 value in Eq. 3.12, the equivalent sand-grain roughness height (k_s) was found as 9.8×10^{-2} m, where the value c_s is 1.0.

No-slip and smooth wall boundary conditions on building surfaces and slip / symmetrical wall boundary conditions on the lateral and upper boundaries were applied. In addition, zero static pressure was used at the outlet boundary.

3.3.5.3 Other Parameters

The grid independence test in Chapter 3 showed that a grid size of 1 or 1.25 m is satisfactory. Therefore, a grid size of 1.25 m was applied, and the grid was constructed with tetrahedral cells. Figure 3.20 shows the computational domain and grid arrangement, and Figure 3.21 shows the grid arrangement of the test area.
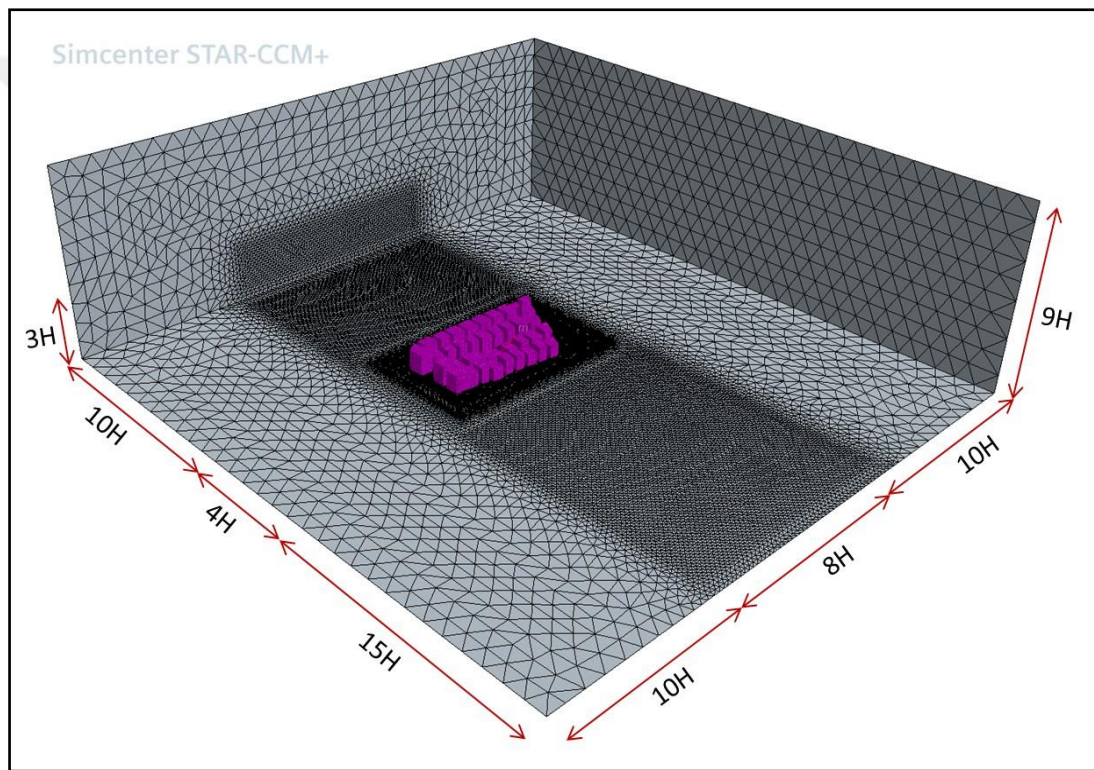

Figure 3.20 Computational domain and grid arrangement

Since the prediction accuracy was better than other turbulence models, STAR's RSM turbulence model was used, and the high y^+ ($30 < y^+ < 150$) wall treatment was applied to solve the near boundary layer. In addition, a separated flow model based on the SIMPLE algorithm was used.
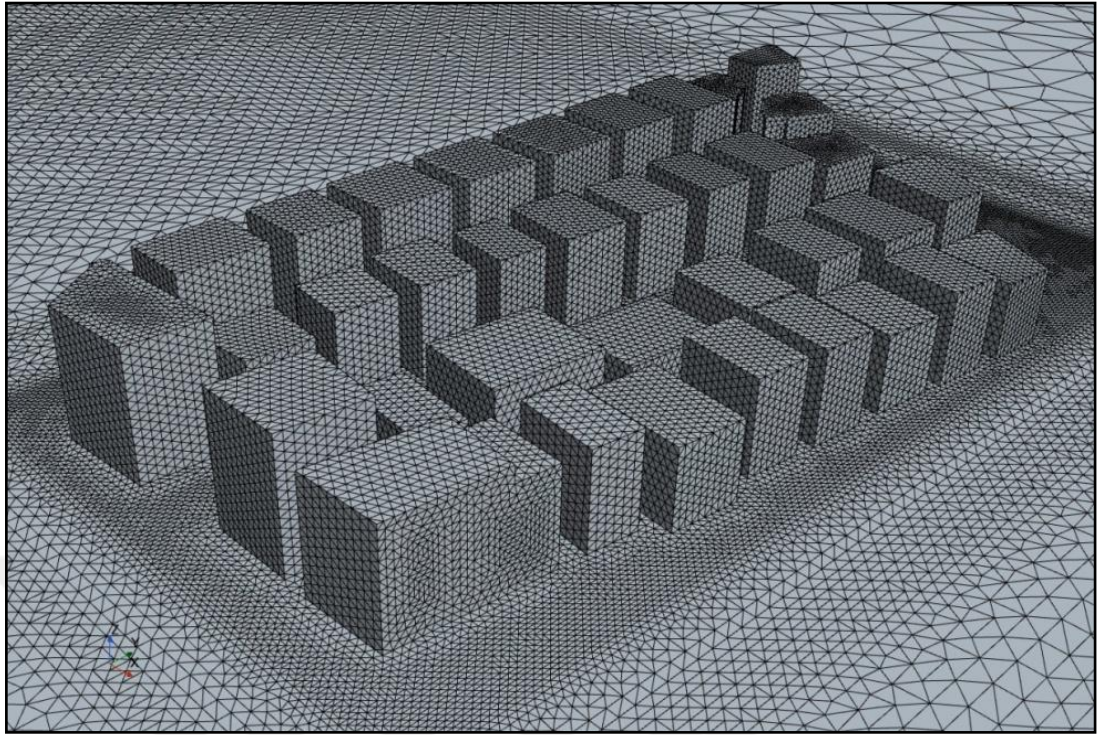
Figure 3.21 Grid arrangement of the test area

3.4 Results

The wind conditions in the selected urban area were investigated, and CFD calculated the wind speed in the passages. Figure 3.22 shows the contour map of the wind speed in the horizontal plane (z=2 m). The wind flow in the study area is quite fluent and continuous. In addition, slender blocks do not impede wind flow due to their detached and permeable plot layout maximizing street network density. Thus, most of the passages reach the wind and are ventilated.

In the selected urban area, the wind speed varies at different passages. When the wind enters large passages, the wind speed increases significantly. In particular, speed-up areas occur between the passages of the grid-aligned blocks. This is due to the corner and channel effect that develops in the passages between grid-aligned blocks. At some points of the passages, the peak speed reaches 4.95 m/s with 67% acceleration. The results show that the grid-aligned configuration causes the channel effect and yields little wind shelter. In this configuration, passages are the windiest

places, but the area behind the buildings is wind-sheltered and has calm wind conditions.
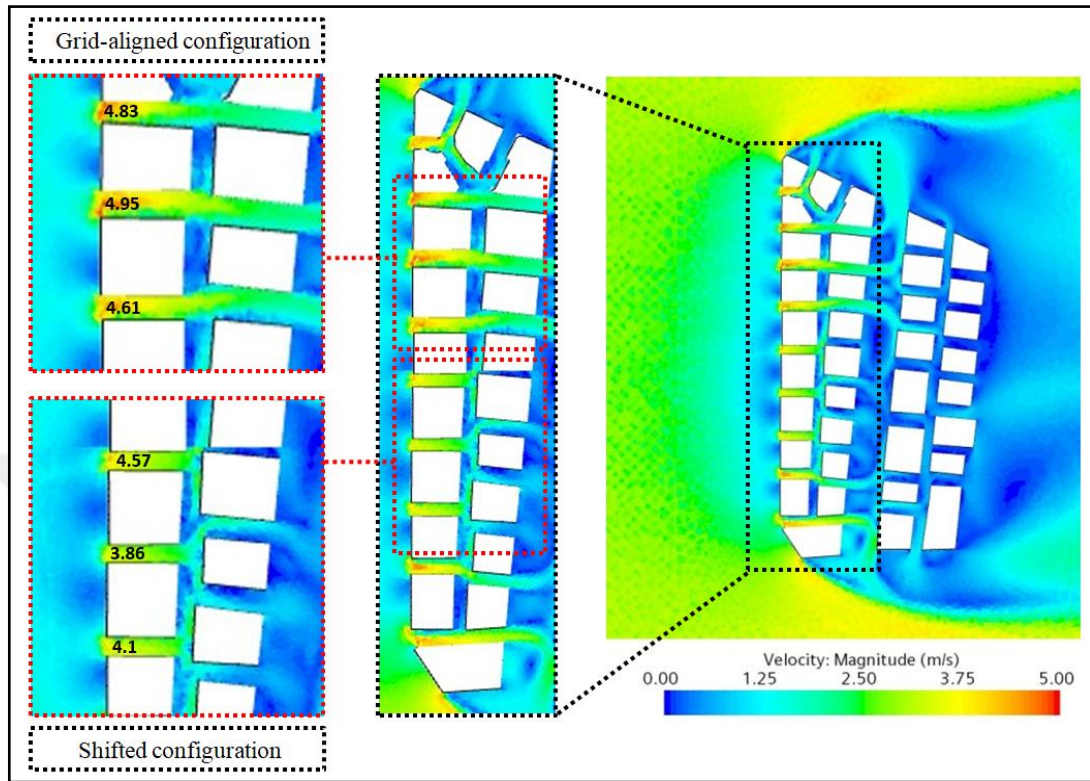
Figure 3.22 Wind velocity magnitude in the horizontal plane (z=2 m)

Unlike the grid-aligned configuration, the wind speed is lower and reaches 3.86 m/s with 30% acceleration at the passages of shifted building configurations. In this configuration, the wind flow is directed sideways but not blocked by downwind blocks located on the passage axis. It is noteworthy that slender blocks of almost similar dimensions but different configurations show different wind speed conditions. The result shows the importance of building configuration for wind comfort and ventilation.

3.5 Chapter Discussion

The field study assessed different urban building configurations in terms of urban ventilation and pedestrian wind discomfort risk. As stated in the study's theoretical basis, insufficient ventilation and pedestrian wind discomfort risk are the most critical problems identified in terms of wind. The results showed that urban

ventilation and pedestrian wind comfort are highly related to the urban block configuration.

Detached and slender type buildings distribute the wind to the field without blocking it and support the ventilation of passages thanks to their permeable structure created by high street network density. The shifted building configuration reduces the influx of wind into the urban fabric and the ventilation rate of the urban environment compared to grid-aligned building configurations.

In terms of pedestrian wind comfort, an acceleration area was observed around all simulated urban building configurations. However, the wind velocity ratio is lower around shifted building configurations than around grid-aligned building configurations. It is noteworthy that shifted building configuration causes a decrease in wind speed. Around the grid-aligned building configuration, the wind is channelled to the passages and increases its speed.

In terms of ventilation and pedestrian wind comfort aspects, shifted building configurations outperformed grid-aligned configurations. In addition, shifted building configurations generally do not impede wind flow and do not cause wind flow acceleration.

The field study highlights that building configuration is an influential factor in ventilation and the risk of wind discomfort. But along with the building configuration, other morphological features such as building size and passage widths can affect the wind flow. The field study cannot explain the extent to which these factors affect wind flow performance. For this reason, the presence of other urban geometric factors makes the produced results site-specific. The shifted slender buildings' genetic and generative principles help to decode the geometry of the best possible shifted building configuration. But, the findings from the field study need to be validated with a systematic investigation based on a multi-case parametric design study. The design study in the next chapter was created for this purpose.

The core and focus of the experimental design study, which will be presented in the next chapter, were determined by the field study results in an actual urban fabric

in the Alsancak Neighbourhood. The field study reveals the importance of the building configuration and limits the experimental design study to the building configuration. But the findings related to the building configuration are not a pre-determined point at the beginning of the research. These findings emerge as a result of field study and shape the experimental design study.

3.5.1 Key Results of the Chapter

- Building configuration is an influential factor in urban ventilation and the risk of wind discomfort.
- Slender blocks of nearly similar sizes but different configurations show different wind speed conditions in passages.
- The shifted building configuration can reduce wind speed more than the grid-aligned building configuration.
- Detached and small building units do not prevent wind flow thanks to the permeable structure created by high street network density.
- Field study provides a learning environment from the existing built environment.
- Two popular CFD codes (STAR and SIMSCALE) can predict the highest wind speed regions where the U/U_{ref} is greater than 1.0.
- Reynolds Stress Model of STAR shows the best compatibility with the experimental result and gives acceptable results in many critical regions such as acceleration, flow separation, corner, and channelling.

CHAPTER 4

EXPERIMENTAL DESIGN STUDY: AERODYNAMIC DESIGN OF URBAN SEAFRONT BUILDINGS

This chapter presents the experimental design of urban seafront buildings based on CFD simulations. Multi-objective optimization of urban seafront buildings was conducted to find the best possible solution to the identified urban ventilation and pedestrian wind discomfort problems.

4.1 Design Inputs

The design study aims to find the best possible seafront buildings and develop generalizable design solutions that can be applied to other cases and cities. For this reason, a multi-case parametric optimization approach was used as it provides flexibility in the optimization process and enables the designer to produce alternative solutions. If the coordinates of the vectors that make up the form are variable, it is parametric (Mitchell, 1986). In the parametric optimization approach, all dimensions of the buildings can be changed, and the coordinates are variable in X, Y, and Z directions.

The design process begins with the determination of climate-based target design wind speed thresholds and then continues with the formulation and creation of the seafront building configurations and is finally completed with the description of numerical models and performing numerical simulations.

4.1.1 Determination of Climate-Based Target Design Wind Speed Thresholds

This study has multi-objective and needs a multi-criteria evaluation. For this reason, the upper and lower target wind speed thresholds for each objective should be determined and then optimized. Different climates have different wind patterns and require different wind adaptation strategies in urban environments, such as (1) reducing wind speed, (2) increasing wind speed, or (3) keeping wind speed constant. Therefore, target design wind speed thresholds should be climate-based. Besides

climatic conditions, specific wind-related problems such as pollutant dilution, heat reduction, and pedestrian wind comfort require the determination of different target design wind speed thresholds. The higher the wind speed, the higher the pollutant dilution and heat reduction, but the lower the pedestrian wind comfort. To resolve this contradiction, firstly, the lower and upper target wind speed thresholds were determined separately for each objective, such as thermal comfort, pedestrian wind comfort, and pollution dilution. Then optimal target design wind speed thresholds were determined with optimization.

While high wind speed is undesirable in winter due to its chilling effect, it is preferred in summer because of its cooling requirement. When the temperature is 28 °C in Hong Kong, a light breeze of 1.0 to 1.5 m/s can provide thermal comfort for the person standing under shade (Ng, 2009). Murakami (1985) recommends that the wind speed should not fall below 0.7 m/s when the temperature exceeds 25 °C at an altitude of 1.5 m to avoid thermal discomfort caused by low wind speed. The average temperature in İzmir in summer is 27.7 °C, and in this condition, a wind speed of 1.0 m/s is necessary to avoid thermal discomfort in summer.

Many pedestrian wind comfort assessment criteria have been developed in different countries (Isyumon and Davenport, 1975; Lawson, 1978; NEN 8100, 2006), and wind speed thresholds are different for each comfort criterion. Alsancak Neighbourhood is the city's central pedestrian zone and is generally used for walking and strolling. In addition, restaurants and cafes along the street are long-term seating places. Isyumon & Davenport (1975) recommend that the wind speed threshold for long-term seating on restaurant terraces is below 3.6 m/s. On the other hand, when the wind speed is above the light breeze conditions (V>3.3 m/s), the hair is disturbed, clothes are flapped, and the newspaper becomes hard to read according to the Beaufort scale. In this context, the wind speed threshold for the long-term seating area has been determined as 3.3 m/s in terms of pedestrian wind comfort. In the area of walking, gentle breeze conditions (3.4-5.4) m/s are acceptable according to the specified comfort criteria.

At very low wind speeds, the pollutant concentration increases (Dickson, 1961; Lawrence, 1970), so higher wind speeds are desirable for improving urban

ventilation. Q, Xu & Z, Xu (2020) recommend a wind speed of at least 1.0 m/s as the standard for urban air pollution diffusion. In this context, the lowest wind speed for urban ventilation was determined as a minimum of 1.0 m/s at pedestrian level (z=2 m).

After separately evaluating the required wind speed thresholds for pollutant dilution, heat dissipation, and pedestrian wind comfort, the target design wind speed threshold was optimized between 1.0 m/s and 3.3 m/s. 1.0 m/s is the minimum wind speed threshold for pollutant dilution and thermal comfort, and 3.3 m/s is the maximum wind speed threshold for pedestrian wind comfort. Thus, a compromise was provided between conflicting design wind speed requirements. In this context, the seafront building design aims to avoid two wind flow conditions: (1) stagnant wind flow conditions: V< 1.0 m/s; (2) windy conditions: V> 3.3 m/s.

The target upper wind speed threshold at pedestrian level was determined as 3.3 m/s, and the prevailing sea breeze (İmbat) with an average annual wind speed of 3.64 m/s (z=10 m) corresponds to 2.96 m/s at pedestrian level (z=2 m) according to the *power law*. Therefore, there is no need to develop the strategy of reducing wind speed to provide wind comfort. However, wind flow acceleration created by buildings should be limited to satisfy the target upper wind speed threshold (3.3 m/s). If the wind flow acceleration caused by the buildings is limited to 12%, it is possible to provide the desired wind comfort.

The process described in this section can be adapted to other climates and cities. Designers can reconstruct target wind speed thresholds based on wind conditions in different cities and can develop their climate-based wind adaptation strategies.

4.1.2 Description of Seafront Building Configurations

The design study is based on the field study as described in the fourth chapter. In the field study, the shifted building configuration was found better than the grid-aligned building configuration in terms of urban ventilation and pedestrian wind comfort.

Characteristically, the rule of creating a shifted urban building configuration is locating two buildings to the sides as upwind buildings and the other one to the back as a downwind building. Figure 4.1 shows the initial shape of the shifted urban building configuration and how it is formed by applying the rule.
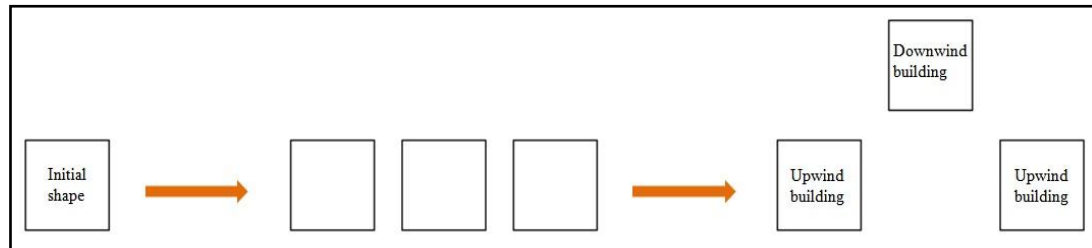

Figure 4.1 Initial shape and formation of shifted urban pattern

The strategy in designing seafront buildings is to maximize urban ventilation efficiency and minimize the risk of wind discomfort. Therefore, the function of the planned seafront buildings is to allow sea breezes to flow and penetrate the inner-city environments without neglecting pedestrian wind comfort.

Before creating the seafront buildings, the existing buildings in the Alsancak Neighbourhood were examined. Apartment blocks are the basic unit forming the current urban form in the Alsancak neighbourhood. They were built either singular or adjacent. Adjacent apartments in linear or courtyard configurations are not wind-adaptive. In particular, the courtyard block causes more stagnant or slower wind movement than a single block (Taleghani, Kleerekoper, Tenpierik, & van den Dobbelsteen, 2015). Since urban ventilation is critical in this climate, using the large linear and courtyard blocks that block the wind flow should be avoided. Singular apartments are more permeable to sea breezes; however, they can significantly reduce urban density.

The planned seafront buildings in this research consist of two rows, and three requirements were taken into account when determining the size of the blocks for the first row:

 (1) Wind discomfort risk and urban ventilation efficiency: large building width can increase the risk of wind discomfort (Reiter, 2010) and cause stagnant wind flow areas behind it. Therefore, large building widths should be avoided.

103

(2) Cross-ventilation of buildings: since the internal ventilation efficiency decreased as the building length increased (Chu and Chiang, 2014), a shallow building form by keeping the building length as short as possible should be used.

(3) Pedestrian movement: placing long linear blocks in a shifted configuration on the coastline can make it difficult for pedestrians to move and find their way in the area.

The three requirements were optimized, and the width and length of the buildings were set at 20 m and 10 m for the first row, respectively. The specified building form is shallow for building ventilation and not kept too wide to avoid corner flow acceleration and stagnant air movement behind it. It is also not too long to not complicate the urban pedestrian movement. The building form is almost a combination of two singular apartments in Alsancak Neighbourhood. It is linear, but dimensions were derived from site-specific climatic conditions, taking into account cross ventilation of buildings, urban ventilation, and wind discomfort risk.

The Alsancak Neighbourhood is the old city centre, and there are many site-specific constraints in urban spatial and building planning. The predetermined height limit by the local planning authority is one of them. The maximum height of the building should not exceed 25 m. Therefore, the height of the buildings was determined as 25 m, representing the mid-rise buildings in Izmir and many dense and compact European cities. The streets in the Alsancak Neighbourhood have mostly pedestrianized streets with widths ranging from 4 m to 12 m. Therefore, the passage width between the buildings in the first row was determined as 10 m to allow walking, strolling, and long-term seating activities.

A parametric design optimization method is adopted for the design of second-row buildings. First of all, urban geometric indicators should be determined. The driving urban geometric indicators determined the optimum width of the downwind buildings and the optimum distance between the upwind (first-row) and downwind (second-row) buildings. In this context, five quantitative geometric indicators consisting of four separate (W, S_{x1}, S_{x2}, S_y) and one interrelated (W/S_{x1}) was created, where W is the width of the downwind buildings, S_{x1} is the passage width between upwind buildings, S_{x2} is the passage width between downwind buildings, and S_y is

the actual passage width between upwind and downwind buildings (Figure 4.2). Using the five specified geometric indicators, two rows of seafront building configurations were created with a parametric approach.
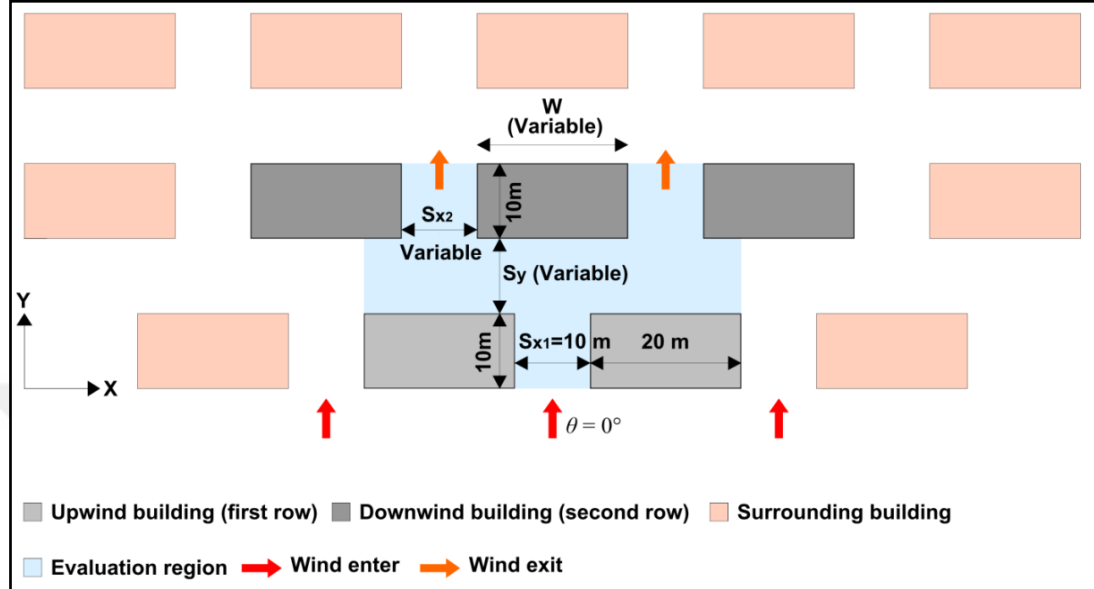

Figure 4.2 Definition of the urban geometric indicators used to design urban seafront building configurations

Figure 4.3 Plan views of twenty-five seafront building configurations

Five different building widths (W) consisting of 8, 12, 16, 20, and 24 m were identified to investigate the effect of the downwind building's width on wind speed. These building widths correspond to aspect ratios (W/S_{x1}) of 0.8, 1.2, 1.6, 2.0, and

2.4, respectively, where S_{x1} is constant and 10 m. Five aspect ratios were matched with five block spacing widths (S_y) of 4, 5, 6, 8, and 10 m. Thus, twenty-five different hypothetical seafront building configurations were created. Depending on the variables, there is a parametric relationship between the configurations. From left to right, the downwind building width (W) increases, so the aspect ratio of W/S_{x1} increases, and from top to bottom, the block spacing width (S_y) between upwind and downwind buildings decreases. Figure 4.3 shows the plan view, and Figure 4.4 shows the 3-D view of the proposed seafront building configurations.
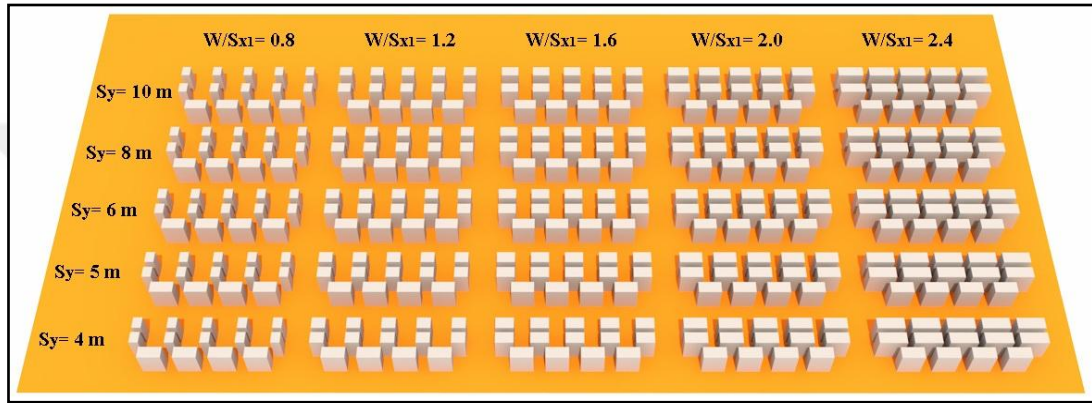
Figure 4.4 3-D view of twenty-five urban seafront building configurations

The level of urban compactness and density of the seafront building configurations were determined using the standardized, climate-based classification of Stewart & Oke (2012). Two indicators are used to physically describe the urban geometry in this classification system: aspect ratio (mean height-to-width ratio of street canyons-H/W) and the building surface fraction (ratio of building plan area to total plan area-%). For the compact-midrise category, the aspect ratio (H/W) should be higher than 1, and the building surface fraction (BSF) should be between 40% and 70% (Stewart & Oke, 2012). As street widths are variable in seafront configurations, aspect ratio and BSF change parametrically. In the first row, the aspect ratio (H/S_{x1}) is constant and equals 2.5, which refers to a highly dense and compact type of urban geometry. The aspect ratio is variable for the x (H/S_{x2}) and y (H/S_y) directions in the second row. The building surface fraction (BSF) of the twenty-five seafront building configurations varies between 31% and 61% (Figure 4.3).

Along with the proposed seafront building configurations, a reference building configuration (Ref. Conf.) representing the typical grid-aligned configuration commonly used in urban environments was created to compare the ventilation efficiency and risk of wind discomfort of designed seafront building configurations (Figure 4.5). In this configuration, the buildings have width, length and height of 20 m, 10 m and 25 m, respectively. In Ref. Conf., the long side of the buildings is perpendicular to the approach wind flow while the aspect ratio equals 2.5 and the BSF is 48%.
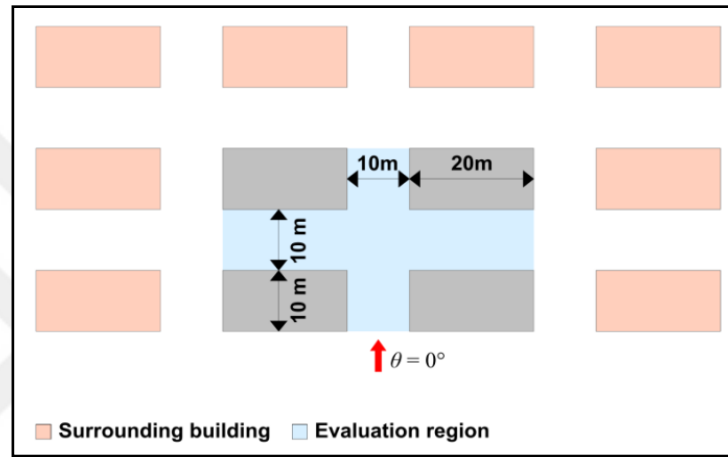
Figure 4.5 Plan view of the reference building configuration (Ref. Conf.)

4.2 Evaluation of Urban Ventilation Efficiency and Pedestrian Wind Comfort

Since this research is mainly aimed at architects and city planners, it is necessary to use a practical quantitative evaluation parameter. Wind velocity and wind direction are effective in the dispersion of exhaust emissions (Ahmad, Khare, & Chaudhry, 2002; Claus et al., 2012; Gu, Zhang, Cheng, & Lee, 2011; Hang, Buccolieri, Sandberg, & Di Sabatino, 2012), outdoor ventilation (Ramponi, Blocken, Laura, & Janssen, 2015; Skote et al., 2005;) and pedestrian wind comfort (Reiter, 2010, Stathopoulos, 2006). Therefore, the widely accepted indicator of wind velocity ratio (VR_w) was used to evaluate urban ventilation efficiency. VR_w is the ratio of wind velocity at the pedestrian level to the free stream velocity of the boundary layer (Ng, 2009; Yim, Fung, Lau, & Kot, 2009).

$VR_w = V/V_{ref}$

where V=mean wind velocity at the measuring point and Vref=free stream mean wind velocity. The higher the VRw value, the higher the urban ventilation efficiency.

VR_w is widely used to consider ventilation efficiency where the free stream velocity is mostly available above the urban canopy layer. At the height of the free stream velocity, it is assumed that the wind velocity is unaffected by the ground surface and surrounding buildings. Therefore, the height (z) of the free stream velocity should be at least 2H (Kastner-Klein, Fedorovich, & Rotach, 2001; Li, Liu, & Leung, 2005) or 2.5H (Bentham & Britter, 2003; Hamlyn & Britter, 2005; Panagiotou, Neophytou, Hamlyn, & Britter, 2013) where H is the maximum building height. However, this research focuses on seafront buildings. In such a case, seafront buildings mainly receive the wind from the front instead of above the canopy. When the reference wind is a sea breeze, horizontal flow displacement acting from the front of the buildings dominates (Britter & Hanna, 2003). Therefore, the free stream velocity (V_{ref}) was evaluated at 2 m height from the ground. We used the following equation to assess the predictive ventilation efficiency quantitatively:

$$\text{Ventilation efficiency } (\%) = \frac{\text{Area of flowing region (VRw)} \geq 0.34)}{\text{Area of the total evaluation region}} \times 100\%$$

The wind velocity ratio (VR_w) was also used to evaluate pedestrian wind comfort. However, higher VR_w values indicate a higher risk of pedestrian wind discomfort.

4.2.1 Distribution of Measuring Points

Correct positioning of measuring points is essential to predict the high velocity and stagnant flow region. Pedestrian street use was taken into account while determining the location of the measuring points. Alsancak neighbourhood is the central pedestrian zone of the city. The street centre axis is used for pedestrian walking, and the 2.5 m wide areas on both sides of the streets are used for long-term seating activities by restaurants and cafes in Alsancak Neighbourhood. This functional division of the activities was decisive in the placement of the measuring points.

The potential locations of the high-speed regions were also considered in determining the location of the measuring points. Critical locations are the building corners and the passage centre axis (PCA). Therefore, the measuring points were located along the passage centre axis representing the pedestrian walking area and the potential location of the *double corner effect*. The measuring points were also located 1.25 meters from the buildings along the central axis of the long-term seating area (SCA), which is the potential location of the corner effect. The measuring points are in the same configuration in all three passages (Figure 4.6).
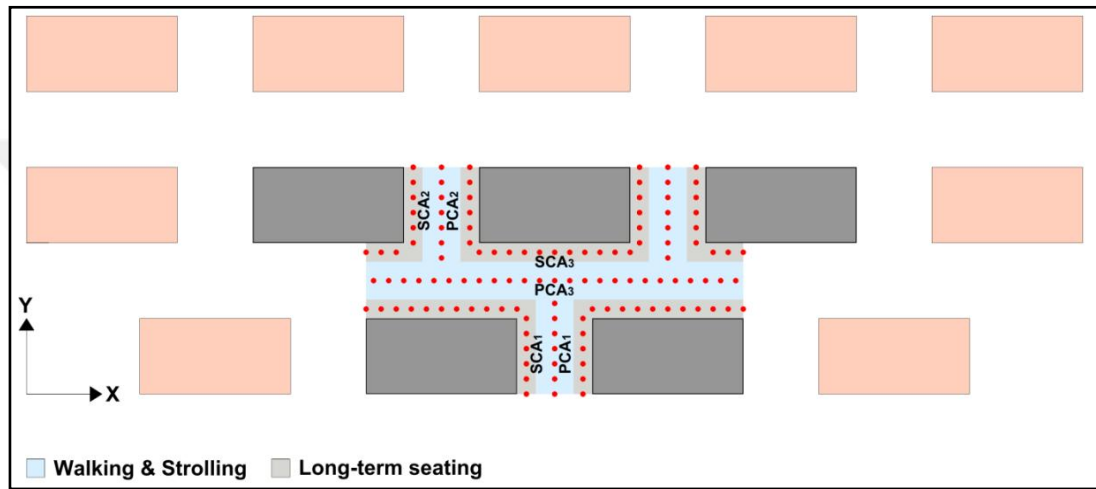
Figure 4.6 Plan view of measuring points

4.3 CFD Setup

4.3.1 Domain size & Boundary Conditions

The domain size was calculated to avoid the blockage effect. We first determined the top size as 8H. Thus, keeping the blockage ratio below 3% (Baetke et al., 1990), we set the lateral dimension as 12H. In addition, we set the inlet and outflow boundaries from the central area of interest as 10H and 15H, respectively (Franke et al., 2004). Figure 4.7 shows the domain size and the distance from the domain's boundaries to the central area of interest, where W, L, and H are the length, width, and height of the central area of interest, respectively.

The parameters related to the boundary conditions detailed in the field study were applied in the same way in the design study. For this reason, it is not described again in this section.
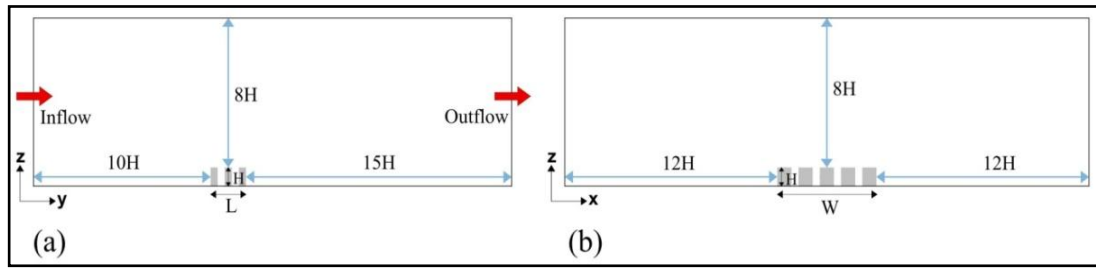
Figure 4.7 The domain size in section views

4.3.2 Other Parameters

The grid independence test showed that a grid size of 1 or 1.25 m is satisfactory. Therefore, a grid size of 1 m was applied, and the grid was constructed with structured hexahedral cells. Figure 4.8 shows the computational domain and structured grid arrangement, and Figure 4.9 shows the grid arrangement of Configuration 5.
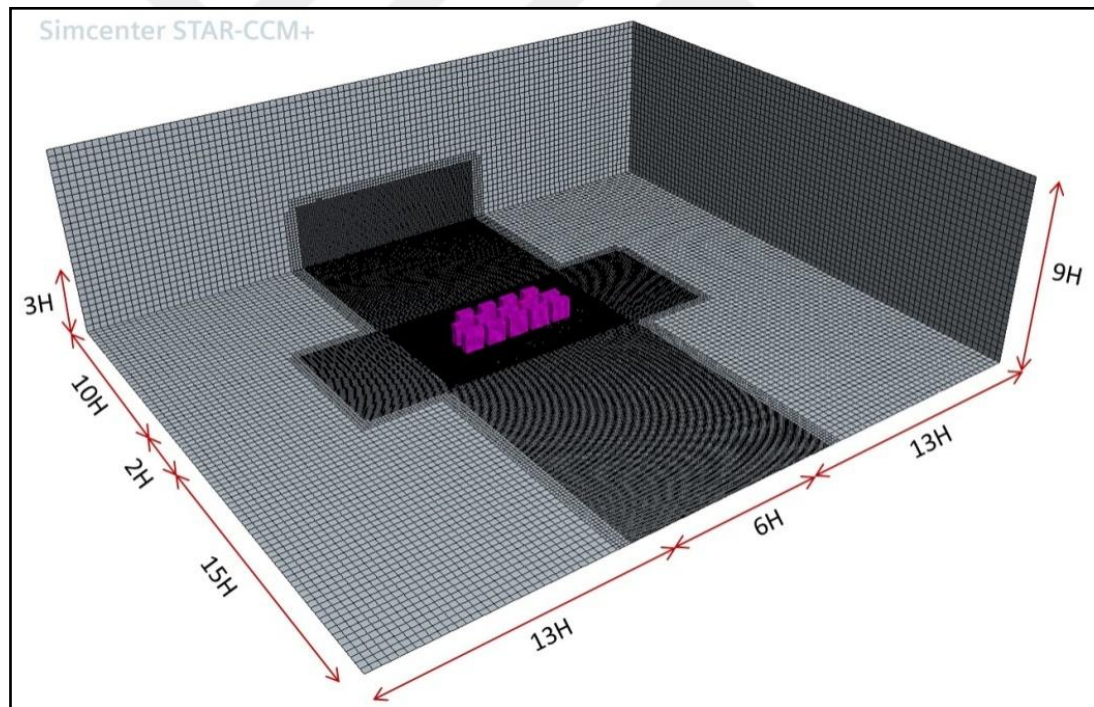
Figure 4.8 Computational domain and structured grid arrangement

Since the prediction accuracy was better than other turbulence models, STAR's RSM turbulence model was used, and the high y^+ ($30 < y^+ < 150$) wall treatment was applied to solve the near boundary layer. In addition, a separated flow model based on the SIMPLE algorithm was used.
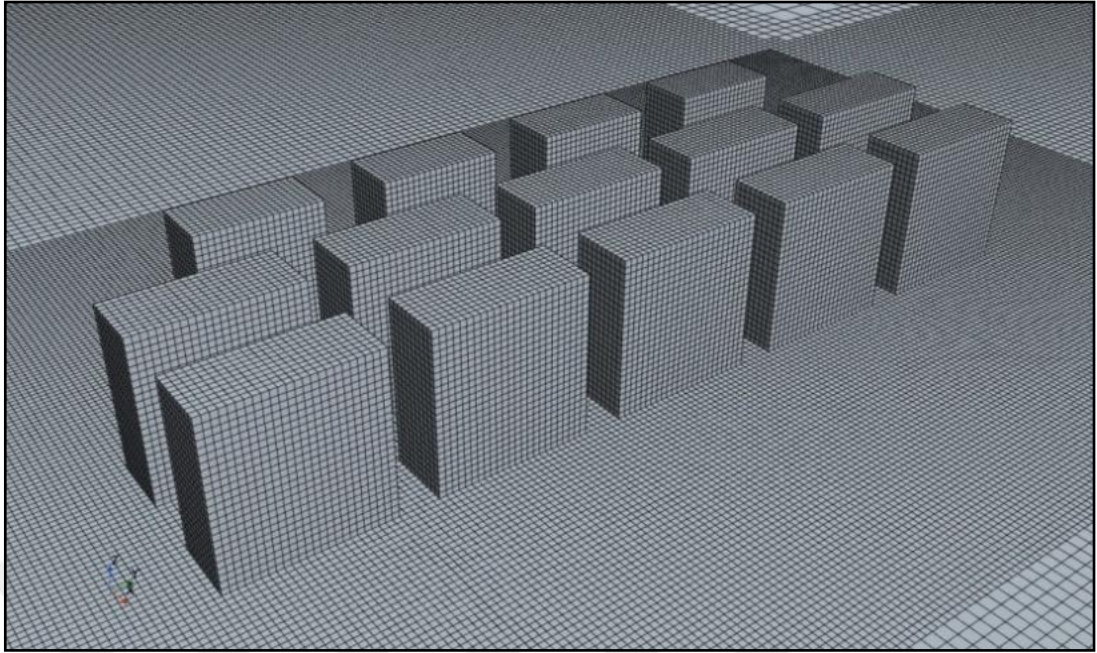
Figure 4.9 Grid arrangement of Configuration 5

4.4 Results

The experimental design study was carried out, and numerical experiments were completed. The CFD simulations of twenty-five seafront building configurations were performed to find the best possible seafront building configuration for urban ventilation and pedestrian wind comfort. Also, the sensitivity of two urban geometric indicators (W/S_{x1} and S_y) on wind velocity was investigated. Wind velocity ratio (VR_w) was measured in three passages (Passage 1, 2, and 3).

4.4.1 Wind Flow Assessment of Reference Building Configurations

First, the velocity distribution and the flow field around the Ref. Conf. were analysed (Figure 4.10). For the reference building configuration, the development of the *double corner effect* at the passage centre axis (PCA) along the approach flow direction is visible. The VR_w is relatively higher (1.55), and the wind discomfort risk is exceptionally high at the row of the first buildings (wind entrance passage). Figure 4.11 visualizes wind discomfort risk and clearly shows the high-speed region's location, size, and magnitude.

In Ref. Conf., a stagnant wind flow region behind the buildings occur (Figure 4.12). These regions are the potential place for air pollution accumulation. The ventilation efficiency for the Ref. Conf. is 36%.

Figure 4.10 Wind velocity distribution in a horizontal plane (z=2 m)

Figure 4.11 Wind velocity distribution for wind discomfort risk ($VR_w > 1.12$)

Figure 4.12 Wind velocity distribution for ventilation efficiency ($VR_w < 0.34$)
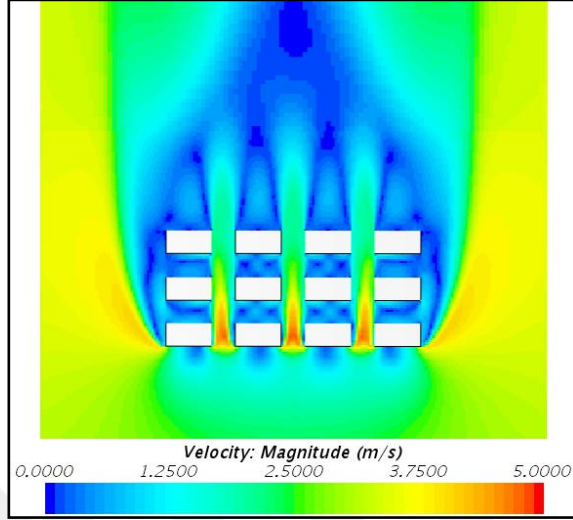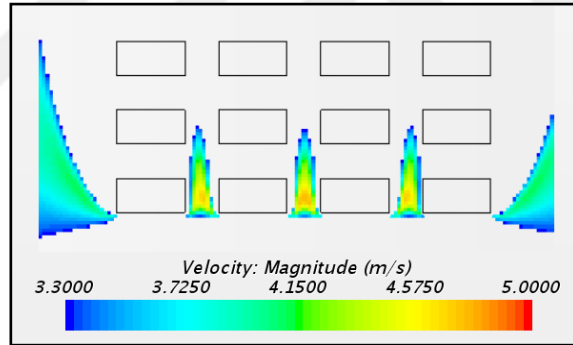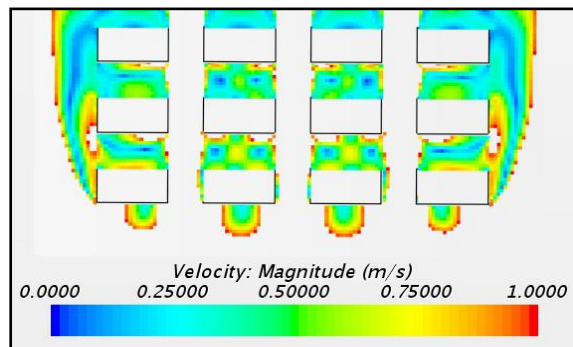
The simulations show that the grid-aligned configuration causes both wind discomfort risk at the wind entrance passage and stagnant flow region at the passages between upwind and downwind buildings. While the parallel passages to the wind flow are very windy, the perpendicular passages are stagnant. Ref. Conf. is the worst in terms of pedestrian wind comfort and urban ventilation, as it causes more flow acceleration and has a larger stagnant flow region.

For the climatic conditions of İzmir, the climate-based target design wind speed thresholds were determined between 1 m / s and 3.3 m / s, corresponding to $0.34 <$ $VR_w <1.12$. However, the Ref. Conf. cannot meet these thresholds. It has been shown that general wind flow problems in urban settings, such as wind discomfort risk and stagnant flow region, are dominant around the Ref. Conf.

4.4.2 Wind Discomfort Assessment of Seafront Building Configurations

4.4.2.1 Wind Discomfort Assessment in Passage 1

Passage 1 is located between parallel upwind buildings and is the wind entrance passage exposed to open wind conditions. Maximum wind velocity ratios (VR_w) range from 0.98 to 1.36 at PCA_1 (Figure 4.13). Six building configurations (Conf. 19, 20, 21, 22, 23, 24, and 25) provide the upper wind speed thresholds ($VR_w \leq 1.12$). However, the best wind climate is provided by Conf. 25, with an aspect ratio (W/S_{x1}) of 2.4 (highest) and S_y of 4 m (lowest). This configuration completely prevents the wind flow from accelerating and slows it down by 2% ($VR_w = 0.98$). Therefore, no wind discomfort risk is present in Passage 1 due to the buildings. On the contrary, the worst wind climate with a 1.36 VR_w is provided by Conf. 1 ($W/S_{x1}=0.8$, $S_y=10m$).

Two strong correlations were found: the first is between W/S_{x1} and VR_w and the second is between S_y and VR_w. Parametrically, as the aspect ratio of $W/Sx1$ increases, VR_w decreases at PCA_1. On the contrary, as S_y increases, VR_w at PCA_1 increases. It should be emphasized that S_y is a more effective geometric indicator for reducing flow acceleration at PCA_1 than W/S_{x1}. When S_y is 4 m, all configurations meet the upper wind design threshold ($VR_w \leq 1.12$) regardless of the W/S_{x1} indicator.
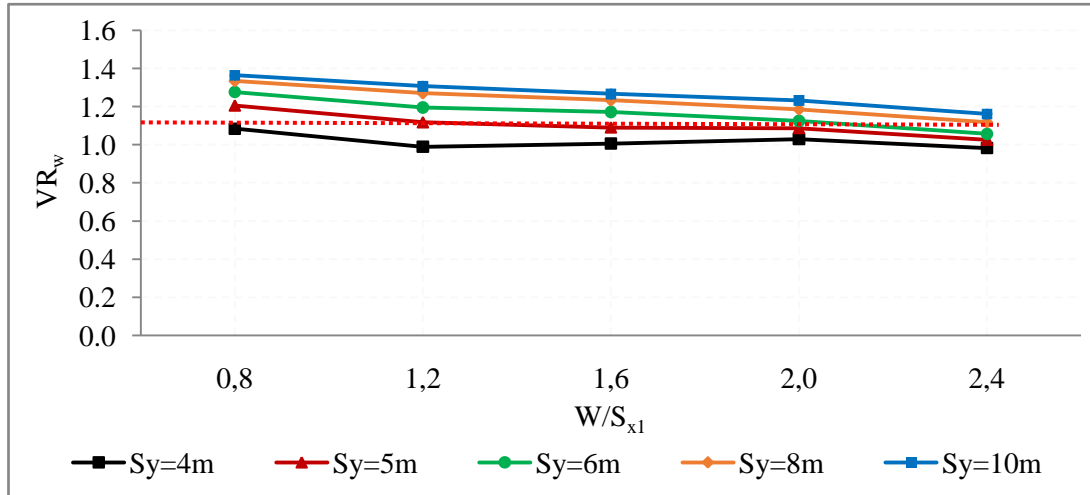
Figure 4.13 Maximum wind velocity ratios (VR_w) in the horizontal plane (z=2m) at PCA_1. *Red dashed line corresponds to upper target wind speed threshold ($VR_w = 1.12$)

Wind discomfort risk was also evaluated at SCA_1. The maximum wind velocity ratio (VR_w) is lower at SCA_1 than at PCA_1. The VR_w at SCA_1 is below 1.12 in all configurations, and therefore, all are comfortable for the long-term seating activity. A higher W/S_{x1} ratio and lower S_y provide lower VR_w at SCA_1. The best wind climate ($VR_w = 0.82$) is achieved by Conf. 25, with an aspect ratio (W/S_{x1}) of 2.4 and S_y of 4 m (Figure 4.14).

Figure 4.14 Maximum wind velocity ratios (VR_w) in the horizontal plane (z=2m) at SCA_1

4.4.2.2 Wind Discomfort Assessment in Passage 2

Passage 2 is the wind exit passage between parallel downwind buildings. Maximum wind velocity ratios (VR_w) range from 0.75 to 1.03 at PCA_2 and do not exceed the upper wind speed threshold ($VR_w \leq 1.12$). There is no wind discomfort risk at PCA_2 for all configurations (Figure 4.15).

Although there is no direct correlation between S_y and VR_w, it does exist between W/S_{x1} and VR_w: as W/S_{x1} increases, so does VR_w. It should be noted that when W/S_{x1} increases, S_{x2} decreases, and Passage 2 becomes narrower. The *Venturi effect* can explain this finding, which means that the wind speed in narrow passages will be higher than in wide passages.
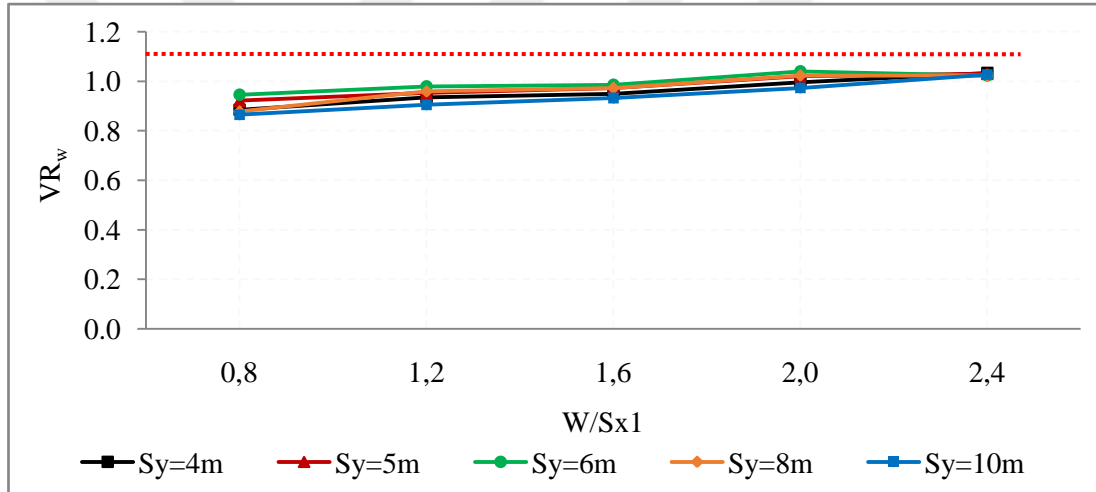
Figure 4.15 Maximum wind velocity ratios (VR_w) in the horizontal plane (z=2m) at PCA_2

The maximum VR_w at SCA_2 is below the upper wind speed threshold ($VR_w \leq 1.12$) in all configurations (Figure 4.16). However, VR_w increases significantly when W/S_{x1} equals 2.4. Unlike other configurations, Conf. 5, 10, 15, 20, and 25 have the highest VR_w value ranging from 0.89 to 0.96. In these configurations, passage width (S_{x2}) decreases to 6 m. The flow interaction developed at PCA_2 interacts with the more stagnant flow region of SCA_2 and thus VR_w at SCA_2, thereby significantly increasing VR_w at SCA_2.
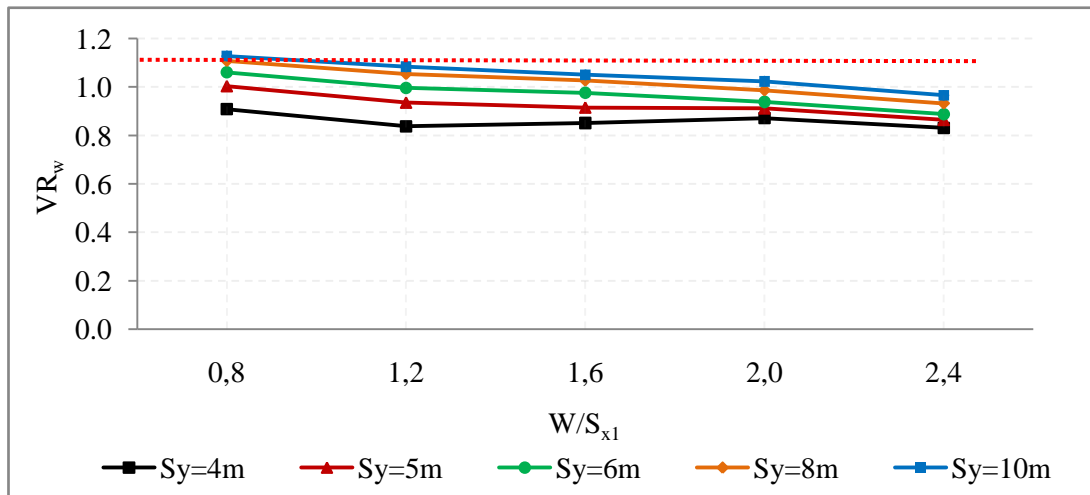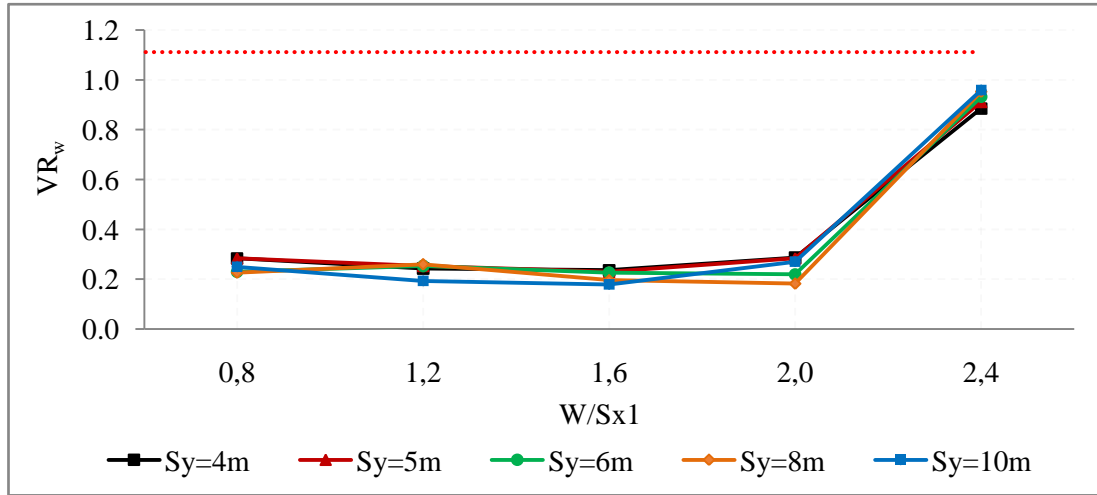
Figure 4.16 Maximum wind velocity ratios (VR_w) in the horizontal plane (z=2m) at SCA_2

4.4.2.3 Wind Discomfort Assessment in Passage 3

Passage 3 is the parallel passage to the wind flow direction and connects Passage 1 and 2. Maximum wind velocity ratios (VR_w) at PCA_3 range from 0.61 to 0.99 (Figure 4.17), and all configurations provide the upper design wind speed threshold ($VR_w \leq 1.12$). No direct correlation was found between S_y and VR_w. However, in very narrow passages where S_y is 4 and 5 m, VR_w is relatively higher but does not pose a risk of wind discomfort. PCA_3 has a comfortable pedestrian-level wind environment, but local flow acceleration occurs at the corner of downwind buildings. At these locations, VR_w can reach 1.26 when S_y is 4 m. Local wind flow acceleration will be explained in detail in the later section.
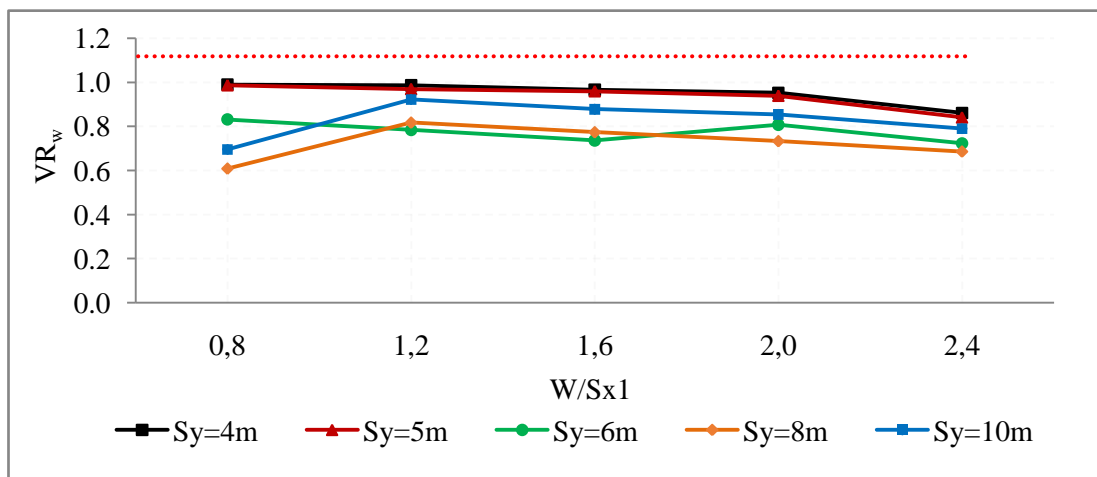
Figure 4.17 Maximum wind velocity ratios (VR_w) in the horizontal plane (z=2m) at PCA_3

In general, PCA$_3$ is wind comfortable, but local flow acceleration occurs at the corner of downwind buildings (SCA$_3$). At these locations, VR$_w$ can reach 1.26 when S$_y$ is 4 m (Figure 4.18). Local wind flow acceleration will be explained in detail in the following sub-section.
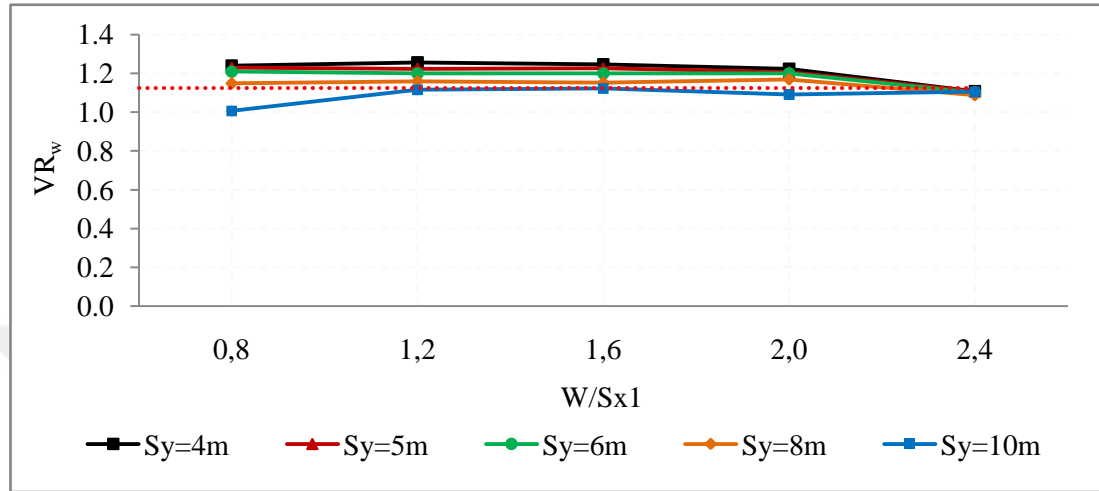
Figure 4.18 Maximum wind velocity ratios (VR$_w$) in the horizontal plane (z=2m) at SCA$_3$

4.4.3 Ventilation Efficiency Assessment of Seafront Building Configurations

In terms of ventilation efficiency, there are strong positive correlations between W/S$_{x1}$, S$_y$, and VR$_w$. In general, the increase of W/S$_{x1}$ and S$_y$ increases ventilation efficiency (Figure 4.19). The ventilation efficiency of different building configurations ranges from 54% to 82% in the evaluation region. The highest ventilation efficiency is achieved by Conf. 25. In this configuration, the lower wind speed threshold (VR$_w$ ≥ 0.34) is exceeded in 82% of the evaluation region.
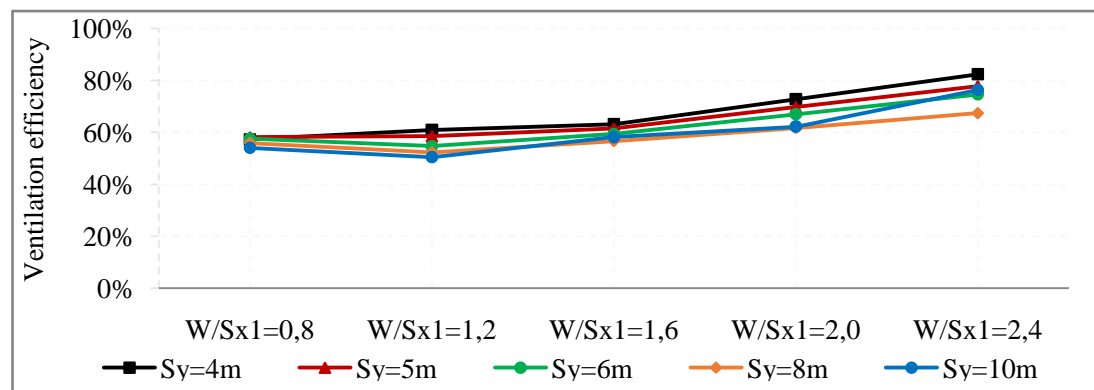
Figure 4.19 Ventilation efficiency (%) in the horizontal plane (z=2m) in the evaluation region

4.4.4 Wind Flow Assessment of Best Possible Seafront Building Configurations

Pedestrian wind discomfort and ventilation efficiency assessments showed that many configurations satisfy the target design wind speed thresholds, and different configurations provide better wind climate at different passages. However, according to the multi-objectives of this study, the best possible seafront building configuration is the configuration that is better in all evaluation regions (Passage 1, 2, and 3) in terms of wind discomfort risk and ventilation efficiency. Unlike other configurations, Conf. 20 and 25 have better wind environments for wind comfort and ventilation efficiency in the evaluation region. For these configurations, W/S_{x1} is 2.4, and S_y is 4 and 5 m for the Conf. 20 and Conf. 25, respectively. Although both satisfy the target design wind speed thresholds in the evaluation region, Conf. 25 has a lower risk of wind discomfort and higher ventilation efficiency than Conf. 20. For this reason, a detailed analysis has been made for Conf. 25 that visualizes the entire flow field.

A detailed analysis was performed for Conf. 25 visualizing the entire evaluation region. Figure 4.20 shows the contour plots of velocity magnitude at pedestrian level (z=2 m), and Figure 4.20 shows the risk of wind discomfort. The blank spaces in Figure 4.21 show VR_w below 1.12, corresponding to wind velocities below 3.3 m/s. In the evaluation region, VR_w never exceeds the upper design wind speed threshold ($VR_w \leq 1.12$). Fig 17c shows the contour plots of velocity magnitude where the wind speed is below 1.0 m/s ($VR_w \leq 0.34$). According to Fig. 17c, Conf. 25 does not completely prevent the stagnant wind flow area in the evaluation region. An area of approximately 1 m wide around the upwind buildings has a stagnant wind environment (Fig. 4.22) due to the *boundary layer effect* of the buildings.

Figure 4.20 Wind velocity distribution in the horizontal plane for Conf. 25 (z=2 m)
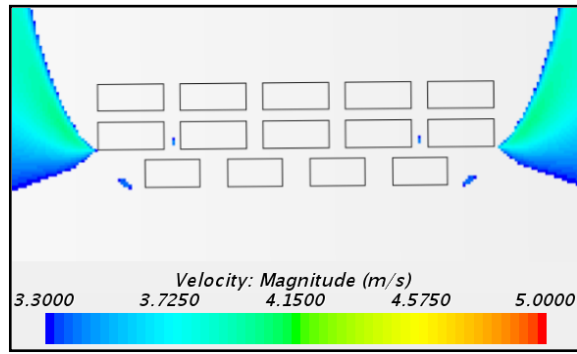
Figure 4.21 Wind discomfort risk in the horizontal plane for Conf. 25 ($VR_w > 1.12$)
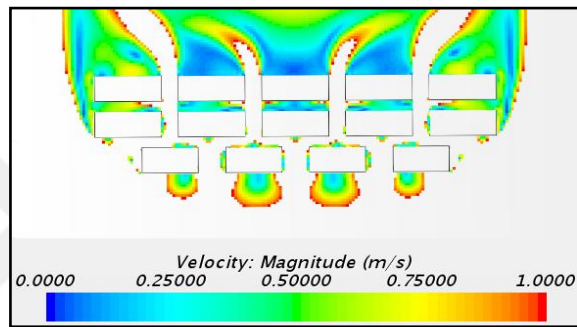
Figure 4.22 Ventilation efficiency in the horizontal plane for Conf. 25 ($VR_w < 0.34$)

Conf. 25 has the highest density/compactness, with the highest aspect ratios ($H/S_{x2}=4.2$; $H/S_y=6.3$) and BSF (61%). It is noteworthy that the more compact and denser seafront building configuration is the best possible one for pedestrian wind comfort and urban ventilation. However, Passage 2 is 6 m wide in this configuration, and Passage 3 is 4 m wide. These passage widths are not functional for both long-term seating and pedestrian walking activities at the same place. Although this configuration performs best for all objectives, it is not functional from urban planning aspects. On the other hand, while the configuration with all passage widths of 10 m (Conf. 4) is more functional, it cannot meet the target wind speed thresholds and does not prevent the risk of wind discomfort in Passage 1. Therefore, a compromise must be provided between the passage function, pedestrian wind comfort, urban ventilation efficiency, and density/compactness. In Conf. 19, Passage 2 is 10 m wide, and Passage 3 is 5 m, providing an acceptable wind environment from wind discomfort risk and ventilation efficiency aspects. Therefore, a detailed analysis was performed for Conf. 19 visualizing the entire evaluation region.
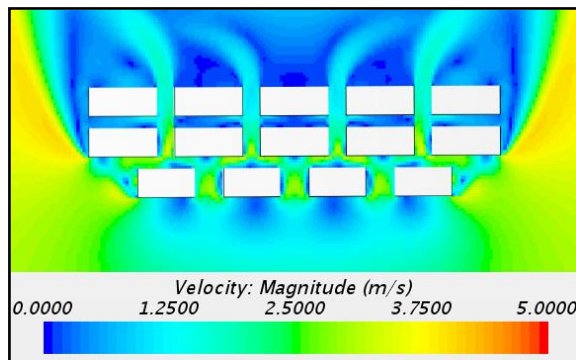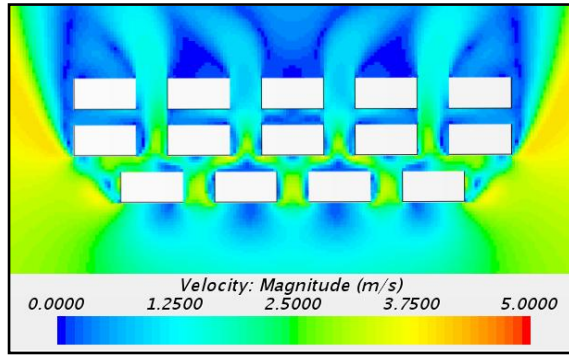
Figure 4.23 Wind velocity distribution in the horizontal plane for Conf. 19 (z=2 m)
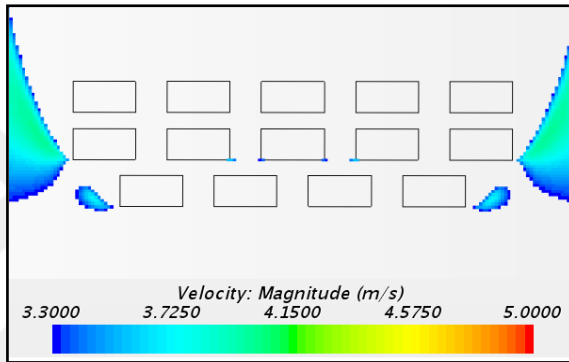
Figure 4.24 Wind discomfort risk in the horizontal plane for Conf. 19 ($VR_w > 1.12$)
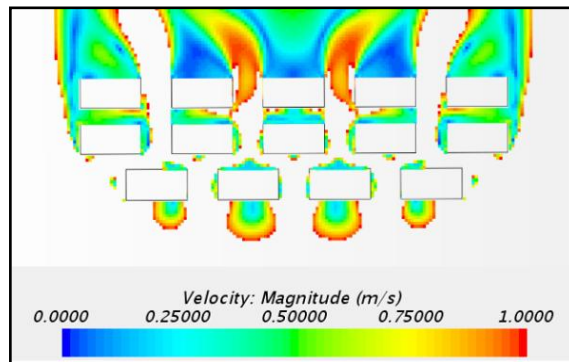
Figure 4.25 Ventilation efficiency in the horizontal plane for Conf. 19 ($VR_w < 0.34$)

Figure 4.23 shows the contour plots of velocity magnitude at pedestrian level (z=2 m) for Conf. 19, and Fig. 4.24 shows the risk of wind discomfort. In general, Conf. 19 meets the upper design wind speed threshold; however, it cannot prevent local flow acceleration (21%) at the corners of downwind buildings (SCA_3). However,

since the local flow acceleration takes place in a limited area, the risk of pedestrian wind discomfort was minimized. Finally, the ventilation efficiency was assessed in Fig. 4.25, which shows the contour plots of velocity magnitude where the wind speed is below 1.0 m/s ($VR_w \leq 0.34$). The ventilation efficiency of Conf. 19 (64%) is 18% less than the ventilation efficiency of Conf. 25 (82%).

Appendix G shows the contour plots of velocity magnitude at pedestrian level (z=2 m) for all seafront building configurations.

4.4.5 Wind Discomfort Assessment Under Oblique (15°, 30°, 45°) Wind Directions

The present study focuses only on the sea breeze, and the simulations were performed based on the site-specific conditions: the direction of the sea breeze is normal to the frontal façade of the buildings on the Alsancak coastline. Although this assumption is present in the selected study area and many coastlines of İzmir, large deviations between the wind direction and the coastline can degrade the designed wind environment and cause a decrease in wind comfort and urban ventilation efficiency. Therefore, it is necessary to test the risk of wind discomfort in oblique wind directions (15°, 30°, 45°) for the best possible configuration.
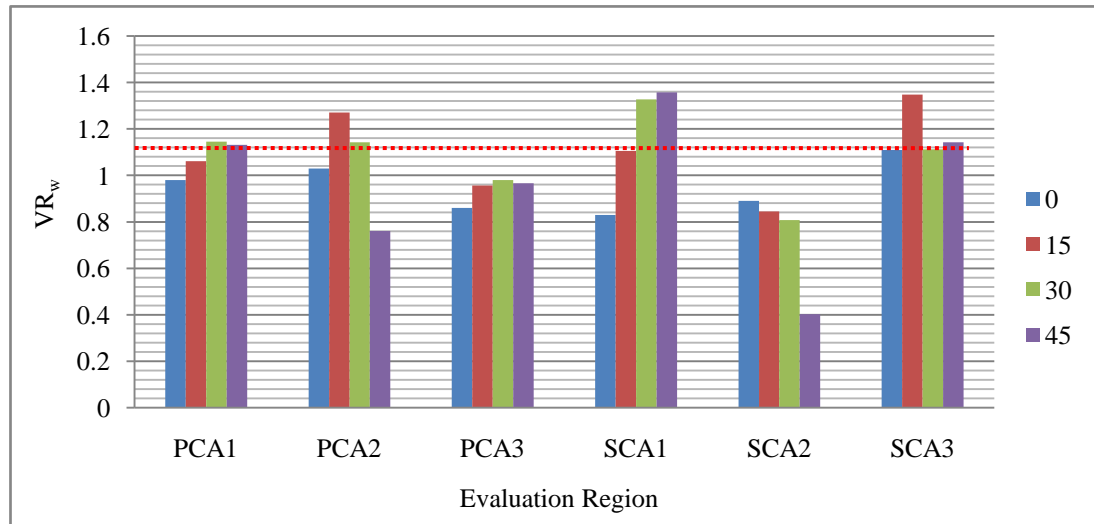
Figure 4.26 Wind velocity under the perpendicular (0°) and oblique (15°, 30°, 45°) wind directions

Figure 4.26 shows the comparison of VR_w under the perpendicular (0°) and oblique (15°, 30°, 45°) wind directions. In general, the upper wind speed threshold is

provided in PCA_1, PCA_3, and SCA_2 under each wind direction. However, the upper wind speed threshold is exceeded for $\phi = 15°$ in PCA_2 and SCA_3, and $\phi = 30°$ and 45° in SCA_1. For $\phi = 45°$, VR_w reaches 1.35 in SCA_3. For $\phi = °$, there is no wind discomfort risk in all SCA because, under this wind direction, the wind in PCA is faster, and the SCA is wind-sheltered due to the boundary layer effect of the buildings. It is noteworthy that when the wind direction increases from 0° to 45°, the wind discomfort risk increases in SCA_1 because this passage is exposed to wind, and oblique winds affect the SCA_1 more than PCA_1. It is noteworthy that when the wind direction increases from 0° to 45°, the risk of wind discomfort increases in SCA_1, as Passage 1 is more exposed to wind, and SCA_1 is more at risk of wind discomfort than PCA as oblique winds flow towards SCA_1. The contour plots of velocity magnitude, wind discomfort risk, and ventilation efficiency at pedestrian level (z=2 m) for Conf. 25 under oblique (15°, 30°, 45°) wind directions are shown in Appendix H.

4.4.6 Cross Comparison of the Results

A complementary field and experimental design study were conducted in this research to obtain the best possible urban seafront building configuration. The field study shows the importance of shifted building configuration but does not show how to prevent the wind discomfort risk and maximize urban ventilation efficiency. Therefore, there is a need to cross-comparison the results obtained from field and design studies. The table shows the maximum wind velocity ratios (VR_w) in wind entrance passages obtained from the field and design study.

Table 4.1 Comparison of the maximum wind velocity ratios (VR_w)

	Grid-aligned building configuration	Shifted building configuration
Field Study	1.67	1.30
Design Study	1.55	0.98

Table 4.1 highlights the two main results:

- Buildings in shifted configurations cause less wind discomfort risk than grid-aligned configurations.
- To achieve the minimum wind discomfort risk, three factors should be provided together:
    - shifted building configuration
    - W/S_{x1} (the width of the downwind buildings / the passage width between upwind buildings)
    - S_y (the actual passage width between upwind and downwind buildings)

The author proposed a functional system consisting of three factors with the experimental design optimization study. These three factors represent *genetic algorithms (GAs)* to achieve urban ventilation and pedestrian wind comfort in the seafront urban areas. Without ignoring these three factors, designers and planners can create new phenotypic urban forms by considering other site-specific environmental conditions in various urban environments.

4.5 Synthesis

The research consists of chapters with relatively independent structures, but all investigate the best possible urban seafront building configuration with cross relations to be established. For this reason, it is essential to ensure the integrity of the research by synthesizing the combination of ideas obtained from each chapter.

Solid mass and void space coexist in urban areas, and there is always a relationship between a solid mass and void space. The size and configuration of void spaces are closely related to the primary solid mass/void space paradigm most discussed in architecture and urban planning. The distribution of solid mass and space in urban areas is the most fundamental debate in architecture and urban planning.

Design decisions are often made at an early design stage to distribute solid mass and void space. For this reason, presenting the empirical knowledge in the form to be used in the early design (sketch) process is necessary so that the knowledge can be easily understood and transferred to the architect and city planner. Therefore, the author created visualized results for architects and urban planners and compared the well-known and characteristic generic building forms in the literature with the best possible seafront building configurations (Conf. 19 and Conf. 25) regarding ventilation and the risk of pedestrian wind discomfort. Such a comparison is necessary to show how a massive linear block located along the seashore should be fragmented and how and in what configuration urban open spaces should be placed between buildings for pedestrian wind comfort and urban ventilation.
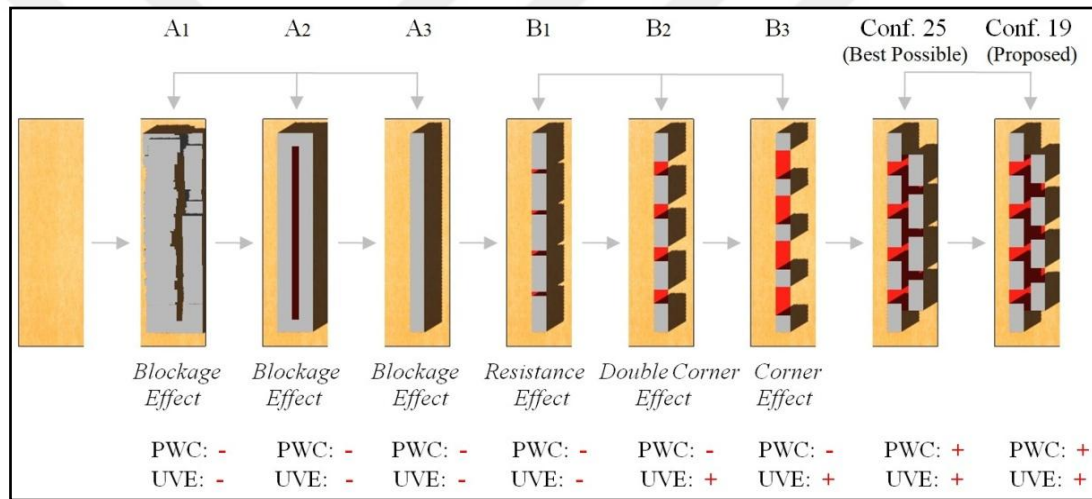
Figure 4.27 Comparison of eight different urban block configurations, (PWC: pedestrian wind comfort; UVE: urban ventilation efficiency)

Eight different urban block types with open space in various sizes and configurations within the same site are visualized in 3-D, as shown in Figure 4.27. Case A1, A2, and A3 represent the massive block in linear form without wind permeability. Case A1 consists of two parallel linear blocks and a small and deep inner courtyard forming an enclosed, single block that fully utilizes the site. It also represents the existing typical seafront buildings on the Alsancak coastline. Case A2 consists of two parallel linear blocks and represents the generic form of the Alsancak urban seafront fabric. Finally, case A3 consists of a single linear block mainly

studied in urban wind studies. Such a block form usually consists of a single urban block or many individual buildings in adjacent order.

These three-block forms have no wind permeability and cause a *flow blockage effect*. Also, the wind impeded by the large building body is channelled to the streets, causing wind acceleration areas. Reiter (2010) studied the wind conditions around a single linear building and found that increasing the width of the building increases the wind speed. In general, larger building increases wind speed at corners. Therefore, Case A1-A3 does not perform well in terms of urban ventilation and pedestrian wind comfort and represents the worst case.

Case B1-B3 represents the linear block that is fragmented and subdivided by adding different-sized passages. Case B1 has the narrowest passage width, and the fragmented buildings are physically located very close to each other. Such an urban block configuration exists in many old settlements and the Alsancak Neighbourhood. The effect of locating narrow passages between parallel buildings on wind conditions has been studied by Blocken, Carmeliet et al. (2007). The narrow passage width has exhibited high flow resistance to incoming flow and low wind speed conditions throughout the passage. In this case, the wind shelter effect develops in the passage. However, as the wind passes through the passage between buildings, its speed increases due to the corner effect and decreases. This configuration results in high flow resistance, poor ventilation along the passage, and a high risk of pedestrian wind discomfort at building corners. Therefore it represents the worst wind conditions.

Case B2 has larger passages than Case B1. According to Blocken, Carmeliet et al. (2007), in such an urban block configuration, *flow interaction* increases in the passages, and the *double corner effect* develops. However, since Case B2 has moderate permeability to wind flow, it does not cause flow resistance and blocks urban ventilation like B1. By this means, it represents moderate wind conditions.

Case B3 has wider passages. Blocken, Carmeliet et al. (2007) found that *a slight flow interaction (isolated flow)* occurs in such an urban block configuration, resulting in a *corner effect* causing less risk of wind discomfort than a double corner effect.

Case B3 with wider streets provides maximum urban ventilation (Golany, 1996) and represents moderate wind conditions.

Case A1-A3 and B1-B3 represent the most used urban block configurations. These have been extensively studied in the literature review. However, these building configurations do not perform well in terms of wind discomfort risk and urban ventilation.

The experimental design chapter designed alternative options for existing seafront buildings on the Alsancak coastline. The author proposed two urban seafront building configurations (Conf. 25 and Conf. 19), consisting of dispersed and small building units located close to each other and containing two rows of parallel buildings. In terms of urban ventilation aspects, small-sized units in dispersed configurations enhance air circulation. In addition, the close proximity of the units minimizes the risk of pedestrian wind discomfort. For this reason, it stands out as the best possible urban seafront building configuration. Conf. 25 and Conf. 19 highlight that the size of open space determined by the proposed urban geometric indicators and the building configuration has a pivotal role in providing urban ventilation and reducing the risk of wind discomfort. The proposed alternative design configurations have a more permeable form to wind flow to mitigate UHI and air pollution and have wind comfortable passages. They also do not neglect to provide density/compactness of the urban form.

The Mediterranean climate requires more permeable buildings. The existing relation between buildings and open spaces in the Alsancak neighbourhood has changed with the proposed seafront building configurations. In terms of architecture and urban planning, this form constructs climatically comfortable semi-public and semi-enclosed spaces without neglecting the density and compactness of urban form. Also, Conf. 25 and 19 refer to a fractal, irregular and fine-grain urban character. This configuration is site-specific but can also be generalized for use in other similar urban environments.

4.6 Discussion

This study provided quantitative findings for providing pedestrian wind comfort and ventilation in urban seafront areas with a multidisciplinary approach combining urban design and urban physics fields. There are numerous studies focused on fulfilling a single criterion, such as providing pedestrian wind comfort or urban ventilation in urban areas. However, this study aims to fulfil both requirements simultaneously with a holistic approach. Therefore, the contradictions encountered in fulfilling both criteria should be discussed.

4.6.1 Role of Urban Density and Compactness on the Risk of Wind Discomfort Risk and Ventilation Efficiency

Today's sustainable urbanization points to a dense and compact urban form as the ideal sustainable urban form. The compact city paradigm provides a wind shelter effect and pedestrian wind comfort however generally contradicts urban ventilation (Brown & DeKay, 2001; Hu et al., 2018). In general, the larger the aspect ratio (H/W) (Hussain and Lee, 1980), the higher the building density (Du & Mak, 2018), the higher site coverage (Gu & Zhu, 2017), and the narrow passage width reduce wind speed and urban ventilation efficiency. The findings of this study support compact and dense urban development as the more compact and denser seafront building configuration (Conf. 25) performs better from pedestrian wind comfort and urban ventilation aspects. However, it should be highlighted that the findings are limited to the seafront urban areas consisting of two parallel row buildings. The findings need to be confirmed by future research that will be conducted in larger urban areas.

4.6.2 Role of Building Configuration on the Risk of Wind Discomfort Risk and Ventilation Efficiency

This research proposes alternative design options for the existing urban seafront buildings in Alsancak Neighbourhood. Given that seafront buildings are exposed to open wind conditions, the risk of wind discomfort at passages is unavoidable, regardless of the size of the passages between single-row buildings along the coast

(Blocken, Carmeliet et al., 2007). On the other hand, although wider passages promote ventilation (Hu & Yoshie, 2013), they are not sufficient to prevent the risk of wind discomfort at passages. This research found that establishing a mutual relationship between the first-row and second-row seafront buildings based on two geometric indicators (higher W/S_{x1} ratio and lower S_y) in shifted configuration has a notable effect on reducing wind flow without neglecting ventilation efficiency.

Numerous studies examined the building configuration on urban ventilation and reported that shifted building configuration has lower ventilation efficiency than the grid-aligned configuration (Lin, Hang, Luo, & Sandberg, 2014; Ma & Chen, 2020). Gülten & Öztop (2020) compared the urban block typologies using the 5×6, 5×5, 5×2, and 4×3 idealized building arrays, while Chen et al. (2021) compared grid-aligned and shifted building configurations using 5×5 idealized building arrays. It should be noted that earlier studies were performed on a larger scale. In these studies, wind flow significantly decreases due to the large frictional drag of shifted building configuration. However, this study is at the mesoscopic block-level consisting of only two rows of buildings in the city's coastal areas. The proposed two-row shifted seafront building configuration provides high ventilation efficiency. Because the wind is strong on the coast and the two rows shifted building configuration does not create much frictional drag compared to those with more rows of buildings. This shows that the location, scale, and number of buildings arranged can considerably affect the results. However, this study needs to be extended to the macroscopic city level in future studies.

Earlier studies on the shifted configuration did not parametrically test the effect of urban geometric indicators on ventilation efficiency. However, in this study, the parametric design method allowed us to find the best possible shifted building configuration by eliminating other building configuration options. This shows the importance of examining the building configuration and urban geometric indicators together and parametrically.

Many studies tested the effect of building configuration on the risk of wind discomfort and reported that shifted building configuration could cause extreme windy conditions due to the pressure short-circuiting effect (Beranek, 1982; Blocken

& Carmeliet, 2008; Bottema, 1993, Janssen, Blocken, & van Hooff, 2013). However, it should be underlined that earlier studies investigated the risk of wind discomfort between two parallel-shifted buildings. Therefore, it should be stated that the number of the buildings in shifted configuration and particularly spacing sizes between buildings (S_{x1}, S_{x2}, and S_y) can cause different results.

Each climate has its unique climate and wind conditions, so typical urban building configurations may not work efficiently in all wind conditions. However, the adaptation of the building configuration to the unique wind conditions can be achieved with the design and modification. For example, the shifted building configuration is recommended in cold northern climates (Blackmore, 2011; Johansson & Yahia, 2020) to block the cold winds and avoid the formation of wind channels. In a similar approach, shifted building configuration is also recommended in hot-arid climates to prevent the free flow of hot and dusty desert wind in urban open spaces (Gut & Ackerknecht, 1993). However, the Mediterranean climate is different. Wind (sea breeze) is cool and thus desirable to regulate urban temperature. On the other hand, the risk of pedestrian wind comfort should be prevented in the coastal passages. Therefore, the free flow of wind should be allowed while blocking the acceleration of the wind flow at the coastal passages. To achieve this, the integrated use of the shifted building configuration and the two proposed urban geometric indicators are critical. Such a strategy block wind flow acceleration, not wind flow. In this way, a balance is achieved between different design requirements. In this context, this study shows how to adapt the shifted building configuration to the Mediterranean climate's unique climatic and wind characteristics, using the parametric design method in coastal urban environments.

4.6.3 Site-Specific Restrictions and Wind Adaptation

Every city has its own specific urban zoning regulations and conditions. The selected urban area (Alsancak Neighbourhood) has a specific local character in this research. It has many site-specific conditions and restrictive planning rules such as predetermined building height limits, plot, and street sizes. In particular, the height limit (max=25m) has limited the design proposals developed for the seafront urban area. Therefore the author created only uniform-height seafront building

configurations. However, the building height is an effective urban geometric indicator on urban wind flow (Rajagopalan et al., 2014) and should be exploited to improve urban ventilation, particularly in warmer climates.

More flexible building and urban zoning regulations are required to create more design proposals and urban geometric indicators for wind adaptation of buildings in existing urban areas. In addition, building zoning regulations may be developed more flexibly for climate and wind adaptation, especially for some urban regions, such as the coastline or newly-developed coastal areas where the wind climate is extreme.

4.6.4 Building and Urban Zoning Regulations and Wind Adaptation

There are different climate types in Türkiye. However, the *Type Zoning Regulation for Planned Areas* is implemented in all provinces without considering different climate types. This regulation is based on the modern automobile-oriented urban planning approach. In this regulation, the heights of the buildings and the passage widths between the buildings are bound to rules, and the climate and wind adaptation of the cities is not taken into account.

Type Zoning Regulation for Planned Areas may consider local climatic conditions, especially in the Mediterranean climate where urban wind flow is beneficial to reducing urban temperature. This can be accomplished by the local planning authorities by creating local Zoning Regulations that complements the Type Zoning Regulation for Planned Areas. The central areas of the cities, and more specifically the coastline in Mediterranean cities, are used by pedestrians for long-term activities. Therefore, these areas are mostly pedestrianized based on today's car-free urban development approach. Therefore, especially in urban areas with pedestrianization, it is possible to arrange building spacing independently of vehicles, thus prioritizing climatic adaptation over car movement. The cities lost the adaptation potential to the climate in the modern automobile-oriented urban planning process, but they can regain it in today's car-free urban planning process.

4.6.5 Adaptation of the Seafront Buildings to the Sun

This study aims to provide wind adaptation of seafront buildings for the comfort and ventilation of urban open spaces. Sun adaptation is beyond the scope of the study; however, it may also be helpful for future studies to discuss the sun adaptation of urban open spaces and buildings in the Mediterranean climate.

The summer term is stressful in the Mediterranean climate due to the hot and humid weather. Urban open spaces, therefore, require both ventilation and sun protection. In this study, the passages provide shaded and windy open areas protected from the sun without neglecting the pedestrian wind comfort due to their dense and compact seaside building configurations. Therefore, the findings support the adaptation of urban open spaces to the sun in summer.

Adaptation of buildings to the sun is different from urban open spaces. First of all, it should be noted that urban density and compactness, due to the buildings' overshadowing effect, contradict the buildings' adaptation to the sun. This is because buildings in dense urban configurations overshadow each other and limit the penetration of the sun into the buildings. In particular, in the winter months, the shadow lengths of the buildings are at the highest level, as the sun is at its lowest level. For this reason, many buildings cannot reach solar radiation in winter.

The buildings should receive sufficient sun in winter in the Mediterranean climate but be shaded by the summer sun. For this reason, the seasonal adaptation of the buildings and their orientation to the sun are essential. Buildings with large south-facing windows and shading on the West and East facade are desirable.

The Alsancak coastline is oriented to North-West. The proposed seafront buildings consist of two apartments, so all apartments have three open facades to the outside environment. This allows benefit more from the sun. In addition, increasing the size between the first row (S_{x1}) and second-row buildings (S_{x2}) improves the sun receiving potential from the south facade. It should be noted that increasing S_{x1} and S_{x2} do not reduce pedestrian wind comfort and ventilation efficiency, as the wider passage width will only result in the corner effect, which is less intense than the

double corner effect. However, S_y is the critical parameter for pedestrian wind comfort and should be as narrow as possible.

Based on this study, future studies can consider both wind and solar adaptation of buildings and urban open spaces in the Mediterranean climate. However, such a study requires a more flexible approach, and site-specific constraints such as height limit, predetermined plot, and street sizes make it difficult to adapt. New urban development areas are more suitable for studies aiming to adapt to both sun and wind than old city settlements.

CHAPTER 5

CONCLUSION

5.1 Summary of the Research

This research has presented the alternative design of urban seafront buildings to mitigate UHI and air pollution through ventilation and minimize the risk of pedestrian wind discomfort in the dense and compact Mediterranean city, İzmir. Site-specific urban seafront building configurations were designed with a complementary, experimental field and design study. In the design of seafront buildings, a multi-objective wind planning strategy and a methodology that integrates the parametric design method with the experimental method based on CFD simulations were adopted.

Each chapter of the research can be listed as follows:

- Understanding the wind phenomena, the quality of the wind, and wind-adaptation strategies in vernacular urban settlements, as well as discussing the fundamentals of building/urban aerodynamics (Chapter 2),
- Morphological analysis of an actual urban fabric (Alsancak Neighbourhood) in terms of urban ventilation and pedestrian wind discomfort risk, including a step-by-step explanation of the CFD validation process, as well as searching for the most appropriate CFD code for the current research by comparing STAR-CCM+ and SIMSCALE (Chapter 3),
- Designing urban seafront building configurations and performing CFD simulations (Chapter 4).

In this research, each chapter, in its context, has contributed to the solution of the stated urban environmental problems and the design of the best possible urban seafront building configuration. However, in the experimental design chapter, urban environmental problems in the seafront urban area have been completely mitigated

by creating new urban geometric indicators with a systematic investigation based on parametric CFD simulations.

5.2 Findings

Findings can be grouped into two main parts. The first group indicates the field study findings based on CFD simulations, including CFD validation (Chapter 3). The second group presents the conclusions of the experimental design study based on parametric CFD simulations (Chapter 4).

First group findings (Chapter 3-Field Study):

- Urban building configuration is an influencing factor on urban ventilation and the risk of wind discomfort.
- In the grid-aligned building configuration, the wind is channelled to the passages and the wind velocity ratio increases.
- Wind velocity ratio (VR_w) is lower in open spaces around the shifted building configurations than in grid-aligned building configurations.
- The shifted building configuration reduces the influx of wind into the urban fabric and the ventilation efficiency compared to the grid-aligned building configurations.
- Both STAR-CCM+ and SIMSCALE can predict the highest wind speed regions where the VR_w is greater than 1.0 with great accuracy.
- The Reynolds Stress Model of STAR-CCM+ is the best compatible with the experimental results and gives acceptable results in many critical flow regions such as acceleration, flow separation, corner, and channelling.

Second group findings (Chapter 4-Design Study):

- Shifted building configuration is not a singular overarching result. To prevent the wind discomfort risk and maximize urban ventilation efficiency in coastal urban open areas, three factors should be applied in conjunction with each other and together: Two-row seafront buildings in shifted configuration (1); higher W/S_{x1} (2); lower S_y (3).

- W/S_{x1} and S_y are the two key and predominant urban geometric indicators to improve pedestrian wind comfort and urban ventilation efficiency. The higher W/S_{x1} and lower S_y provide significant flow slowdown at passages and maximise urban ventilation efficiency.

- There is a strong positive correlation between increasing the compactness and density of the seafront building configurations and improving pedestrian wind comfort and urban ventilation efficiency. Among the configurations, the more compact and denser seafront building configuration (Conf. 25) avoids the double corner effect and maximises urban ventilation efficiency by 82% in the evaluation region.

- A compromise between pedestrian wind comfort and ventilation efficiency requirements was provided without neglecting urban density/compactness in the seafront urban area.

5.3 Concluding Remarks

Urban open spaces have a central role in urban life, and climatic adaptation and comfort in urban open spaces are necessary for liveable urban life. In this regard, this research shows how to reduce the risk of wind discomfort and improve urban ventilation efficiency in coastal urban open spaces to provide wind adaptation and comfort in dense and mid-rise compact Mediterranean cities.

This research assists in creating site-specific wind planning policies in coastal urban areas. However, it is difficult to recommend a universal urban building configuration that can best respond to all specific wind conditions. Nevertheless, the findings and the proposed methodology that integrates design, experiment, and field study, can be used in future urban wind research studies in other coastal cities and similar environments.

The results could be generalized as the research establishes new empirical building spacing rules related to common wind flow problems such as wind flow acceleration and stagnant flow region. Also, the pedestrian wind comfort and ventilation assessments of design projects at the conceptual stage of building mass optimization can be more practical using the findings. This study also supports

today's compact and dense sustainable city approach and promotes the consideration of wind in planning such urban settlements.

Due to its mild climate, the city of Izmir is a place where the open spaces are mainly used, in particular, for long-term seating throughout the year. For this reason, improving pedestrian wind comfort in streets is necessary to make the streets lively. With the application of the findings, the pedestrian-level wind comfort in the coastal part of Izmir can be improved even on the coastal streets exposed to the wind without neglecting urban ventilation. The city also can benefit more from the sea breeze for urban ventilation. The urban open spaces around the best possible seafront buildings are suitable for locating restaurants, cafes, and urban outdoor activities that require the highest pedestrian wind comfort.

Type Zoning Regulation for Planned Areas being implemented in Turkey should take more into account the local climate and wind conditions in the Mediterranean climate. Coastal urban areas are vulnerable to wind effects and therefore the local planning authority in Izmir can create a supplementary local Zoning Regulation for the wind adaptation of the coastline.

The wind is associated with many urban environmental issues such as global warming, UHI, air pollution, and pedestrian wind comfort in the Mediterranean climate; therefore, for more comfortable outdoor spaces, the wind planning approach should be multi-purpose and pedestrian wind comfort, air pollution and UHI should be addressed holistically in urban environments. Architects and planners should consider these issues when making their planning decisions in the Mediterranean climate.

5.4 Perspectives and Future Research

The findings of this research highlight the relevance of implementing an integrated field and experimental study to better understand the site-specific urban wind flow problems and propose solutions. Although this research is handled with a multi-purpose approach including pedestrian wind comfort, air pollution and UHI issues, it could be extended to include building ventilation and building energy use

studies related to urban wind flow. Also as this research establishes new empirical building spacing rules, they could be extended to even building solar orientation and adaptation.

The present research was focused only on the design of the urban seafront building configuration due to the differences in wind conditions and wind adaptation strategies between coastal and inner-city areas. However, considering the importance of ventilating inner urban areas with the sea breeze, a large-scale urban block configuration study that allows the wind effects to penetrate deep into the city will be helpful for future studies.

This research provided genetic algorithms (GAs) and design rules to adapt the urban form to the wind in coastal urban areas. In this context, this research could be extended to phenotypic urban wind flow studies in different contexts and situations, using the generated GAs and existing design rules in the literature.

REFERENCES

Adolphe, L. (2001). A simplified model of urban morphology: application to an analysis of the environmental performance of cities. *Environment and Planning B: Planning and Design*, *28*(2). https://doi.org/10.1068/b2631.

Ahmad, K., Khare, M., & Chaudhry, K. K. (2002). Model vehicle movement system in wind tunnels for exhaust dispersion studies under various urban street configurations. *Journal of Wind Engineering and Industrial Aerodynamics, 90*(9), 1051-1064. https://doi.org/10.1016/S0167-6105(02)00250-7.

Ahmad, K., Khare M., & Chaudhry K. K. (2005). Wind tunnel simulation studies on dispersion at urban street canyons and intersections—a review. *Journal of Wind Engineering and Industrial Aerodynamics*, *93*, 697–717. https://doi.org/10.1016/j.jweia.2005.04.002.

American Society of Civil Engineers Task Committee on Urban Aerodynamics (2011). *Urban Aerodynamics: Wind Engineering for Urban Planners and Designers.* Reston, VA: American Society of Civil Engineers. https://doi.org/10.1061/9780784411797.

Anonymous from the Erskine ArkDes collections (1986). ARKM.1986-17-0362.

Antoniou, N., Montazeri, H., Wigo, H., Neophytou, M. K. A., Blocken, B., & Sandberg, M. (2017). CFD and wind-tunnel analysis of outdoor ventilation in a real compact heterogeneous urban area: Evaluation using "air delay". *Building and Environment, 126*, 355-372. https://doi.org/10.1016/j.buildenv.2017.10.013.

Architectural Institute of Japan (2016). *AIJ Benchmarks for Validation of CFD Simulations Applied to Pedestrian Wind Environment around Buildings*. Tokyo:Architectural Institute of Japan.

Arkon, C. A., & Özkol U. (2013). Effect of urban geometry on pedestrian-level wind velocity. *Architectural Science Review, 57*(1), 4-19. https://doi.org/10.1080/00038628.2013.835709.

Aynsley, R. M., Melbourne, W. H., & Vickery, B. J. (1977). *Architectural Aerodynamics*. London, UK: Applied Science Publishers.

Baetke, F., Werner, H., & Wengle, H. (1990). Numerical simulation of turbulent flow over surface-mounted obstacles with sharp edges and corners. *Journal of Wind Engineering and Industrial Aerodynamics, 35*, 129-147. https://doi.org/10.1016/0167-6105(90)90213-V.

Baker, W. E., Cox, P. A., Kulesz, J. J., Strehlow, R. A., & Westine, P. S. (2012). *Explosion Hazards and Evaluation*. Elsevier.

Ballice, G. (2006). *İzmir'de 20. YY Konut Mimarisindeki Değişim ve Dönüşümlerin Genelde ve İzmir Kordon Alanı Örneğinde Değerlendirilmesi* [Doctoral Dissertation]. Dokuz Eylül University.

Baş, H. & Egercioglu Y. (2016, October 4-6). *Impact of Quality of Wind on Urban Form: Analysis of Vernacular and Contemporary Wind-Adaptive Urban Design Approaches*. Designing Urban Design: Towards a Holistic Perspective, International Symposium, METU, Ankara, TURKEY. DOI:10.14744/megaron.2019.31932.

Batchelor, G. K. (2000). *An Introduction to Fluid Dynamics*. Cambridge: Cambridge University Press. ISBN 978-0-521-66396-0.

Bentham, T., & Britter, R. (2003). Spatially averaged flow within obstacle arrays. *Atmospheric Environment, 37*(15), 2037-2043. https://doi.org/10.1016/S1352-2310(03)00123-7.

Beranek, W. J. (1979). Beperken van windhinder om gebouwen, Deel, 1, Stichting Bouwresearch No. 65, Kluwer Technische Boeken BV, Deventer. (in Dutch).

Beranek, W. J. (1980). General rules for the determination of wind environment. *Wind Engineering*. Pergamon. https://doi.org/10.1016/B978-1-4832-8367-8.50027-9.

Beranek, W. J. (1982). Beperken van windhinder om gebouwen, Deel, 2, Stichting Bouwresearch No. 90, Kluwer Technische Boeken BV, Deventer. (in Dutch).

Beranek, W. J., & Van Koten, H. (1982). Beperken van windhinder om gebouwen. Stichting Bouwresearchg Kluwer Technische Boeken BV, Deventer. (in Dutch).

Bergman, T. L., Lavine, A. S. Incropera, F. P., & DeWitt, D. P. (2011). *Fundamentals of heat and mass transfer*, John Wiley & Sons, (7th ed.), pp. 389-391.

Blackmore, P. (2011) *Wind microclimate around buildings*, IHS BRE Press.

Blocken, B., & Carmeliet, J. (2006). The influence of the wind-blocking effect by a building on its wind-driven rain exposure. *Journal of Wind Engineering and Industrial Aerodynamics*, *94*(2), 101-127. https://doi.org/10.1016/j.jweia.2005.11.001.

Blocken, B., Carmeliet, J., & Stathopoulos, T. (2007). CFD evaluation of wind speed conditions in passages between parallel buildings—effect of wall-function roughness modifications for the atmospheric boundary layer flow. *Journal of Wind Engineering and Industrial Aerodynamics, 95*(9-11), 941-962. https://doi.org/10.1016/j.jweia.2007.01.013

Blocken, B., Stathopoulos, T., & Carmeliet, J. (2007). CFD simulation of the atmospheric boundary layer: wall function problems. *Atmospheric Environment, 41*(2), 238-252. https://doi.org/10.1016/j.atmosenv.2006.08.019.

Blocken, B., & Carmeliet, J. (2008). Pedestrian wind conditions at outdoor platforms in a high-rise apartment building: generic sub-configuration validation, wind comfort assessment and uncertainty issues. *Wind and Structures, (1*), 51-70. https://doi.org/10.12989/was.2008.11.1.051.

Blocken, B. (2012, October 5). Urban Physics [Pdf slides]. http://alexandria.tue.nl/extra2/redes/blocken2012.pdf

Blocken, B., Stathopoulos, T., & Van Beeck, J. P. A. J. (2016). Pedestrian-level wind conditions around buildings: Review of wind-tunnel ad CFD techniques and their accuracy for wind comfort assessment. *Building and Environment, 100*, 50-81. https://doi.org/10.1016/j.buildenv.2016.02.004.

Bosselmann, P., Dake, K., Fountain, M., Kraus, L., Lin, K. T., & Harris, A. (1988). Sun, Wind, and Comfort: A Field Study of Thermal Comfort in San Francisco. (No. CEDR-06-88). Berkeley, CA: Center for Environmental Design Research, University of California, Berkeley.

Bottema, M. (1993). Wind climate and urban geometry. Eindhoven: Technische Universiteit Eindhoven. https://doi.org/10.6100/IR388789/.

Bottema, M. (2000). A Method for Optimisation of Wind Discomfort Criteria. *Building and Environment, 35*, 1–18. https://doi.org/10.1016/S0360-1323(98)00065-1.

Britter, R. E., & Hanna, S. R. (2003). Flow and dispersion in urban areas. *Annual review of fluid mechanics*, *35*(1), 469-496.

Brown, G. Z., & DeKay, M. (2001). Sun, wind & light: *Architectural design strategies* (2nd ed.). New York: Wiley.

Burton, T., Sharpe, D., Jenkins, N., & Bossanyi, E. (2012). *Wind energy handbook 2*, New York: Wiley.

Casey, M., & Wintergerste, T. (2000). *ERCOFTAC Special Interest Group on Quality and Trust in Industrial CFD-Best Practice Guidelines*. European research community on flow, turbulence and combustion, *123*. https://doi.org/10.1115/PVP2002-1530.

Cervero, R. (1998). *The transit metropolis: A global inquiry*. Washington, DC: Island Press.

Chen, G., Rong, L., & Zhang, G. (2021). Impacts of urban geometry on outdoor ventilation within idealized building arrays under unsteady diurnal cycles in

summer, *Building and Environment*. *206*, 108344. https://doi.org/10.1016/j.buildenv.2021.108344.

Chew, L. W., Nazarian, N., & Norford, L. (2017). Pedestrian-level urban wind flow enhancement with wind catchers. *Atmosphere*. *8*(9), 159. https://doi.org/10.3390/atmos8090159.

Chou, P., (1945). On velocity correlations and the solutions of the equations of turbulent fluctuation, *Quarterly of Applied Mathematics, 3*(1), 38-54. https://doi.org/10.1090/qam/11999.

Chu, C. R., & Chiang, B. F. (2014). Wind-driven cross ventilation in long buildings. *Building and Environment, 80*, 150-158. https://doi.org/10.1016/j.buildenv.2014.05.017.

City of London & RWDI, (2019). Wind Microclimate Guidelines for Developments in the City of London.

Clancy, L. J. (1975). *Aerodynamics*. Wiley. ISBN 978-0-470-15837-1.

Claus, J., Coceal, O., Thomas, T.G., Branford, S., Belcher, S.E., & Castro, I.P. (2012). Wind-direction effects on urban-type flows. *Boundary-layer Meteorology, 142*(2), 265-287. DOI 10.1007/s10546-011-9667-4.

Coccia, M. (2020). How (un) sustainable environments are related to the diffusion of COVID-19: the relation between coronavirus disease 2019, air pollution, wind resource and energy, *Sustainability*, *12*(22), 9709. https://doi.org/10.3390/su12229709.

Dantzing, George B., & Saaty, T. (1973). *Compact city: A plan for a livable urban environment.* San Francisco: W.H. Freeman.

Davenport, A. G. (1961). The application of statistical concepts to the wind loading of structures. *Proceedings of the Institution of Civil Engineers*, *19*(4), 449-472. https://doi.org/10.1680/iicep.1961.11304.

Dickson, R. R. (1961). Meteorological factors affecting particulate air pollution of a city. *Bulletin of the American Meteorological Society*, *42*(8), 556-560.

Drag (physics). (2022, February 5). In *Wikipedia*. https://en.wikipedia.org/wiki/Drag_(physics))

Du, Y. & Mak, C. M. (2018). Improving pedestrian level low wind environment in high-density cities: A general framework and case study, *Sustainable Cities and Society, 42*, 314–324. https://doi.org/10.1016/j.scs.2018.08.001.

Duarte, J. P., Rocha, J. M., & Soares, G. D. (2007). Unveiling the structure of the Marrakech Medina: A shape grammar and an interpreter for generating urban form. *Artificial Intelligence for Engineering Design, Analysis and Manufacturing. 21*, 317–349. https://doi.org/10.1017/S0890060407000315.

Elbir, T. (2002). Application of an ISCST3 model for predicting urban air pollution in the İzmir Metropolitan Area. *Environment and Pollution, 18*(05), 498–507. https://doi.org/10.1504/IJEP.2002.002342.

Eliasson I. (2000). The use of climate knowledge in urban planning. *Landscape and Urban* Planning *48*, 31-44. https://doi.org/10.1016/S0169-2046(00)00034-7.

Erell, E., Pearlmutter, D., & Williamson, T. T. J. (2011). *Urban microclimate: designing the spaces between buildings*. Routledge Publications. https://doi.org/10.4324/9781849775397.

Evans, M. (1980) *Housing, Climate and Comfort*. London: The Architectural Press.

Fenger, J. (1999). Urban air quality. *Atmospheric Environment, 33*(29), 4877-4900. https://doi.org/10.1016/S1352-2310(99)00290-3.

Franke, J., Hirsch, C., Jensen, A. G., Krus, H. W., Schatzmann, M., Westbury, P. S., Miles, S. D., Wisse, J. A., & Wright, N. G., (2004). Recommendations on the use of CFD in wind engineering In *Proceedings of the International Conference on Urban Wind Engineering and Building Aerodynamics*. In *van Beeck JPAJ (Ed.),*

COST Action C14, Impact of Wind and Storm on City Life Built Environment. von Karman Institute, Sint-Genesius-Rode, Belgium, 5–7 May 2004.

Franke, J., & Frank, W. (2005). Numerical simulation of the flow across an asymmetric street intersection. In *Proceedings of the Fourth European and African Conference on Wind Engineering* (116-117).

Franke, J., Hellsten, A., Schlünzen, H., & Carissimo, B. (2007). *Best practice guideline for the CFD simulation of flows in the urban environment. COST action 732. Quality Assurance and Improvement of Meteorological Models.* University of Hamburg, Meteorological Institute, Center of Marine and Atmospheric Sciences.

Gal, T. & Sümeghy, Z. (2007). Mapping the roughness parameters in a large urban area for urban climate applications, *Acta Climatologica et Chorologica, Universitatis Szegediensis*, *40*, 27-36.

Gandemer, J. (1975). *Wind environment around buildings: aerodynamic concepts*. Proc., 4th Int. Conf. Wind Effects on Buildings and Structures, Heathrow, Cambridge University Press, 423-432.

Gehl, J. (2010). *Cities for People*. Washington, DC: Island Press.

Georgakis, C., & Santamouris, M. (2008). On the Estimation of Wind Speed in Urban Canyons for Ventilation Purposes– Part 1: Coupling Between the Undisturbed Wind Speed and the Canyon Wind. *Building and Environment, 43*(8), 1404–1410. https://doi.org/10.1016/j.buildenv.2007.01.041.

Givoni B. (1998). *Climate considerations in building and urban design* (1st ed.). New York: Van Nostrand Reinhold.

Golany, G. S. (1996). Urban design morphology and thermal performance. *Atmospheric Environment, 30*(3), 455–465. https://doi.org/10.1016/1352-2310(95)00266-9.

Grimmond, C., & Oke, T. R. (1999). Aerodynamic properties of urban areas derived from analysis of surface form. *Journal of Applied Meteorology*, *38*, 1262–1292. https://doi.org/10.1175/1520-0450(1999)038<1262:APOUAD>2.0.CO;2

Golf Ball Dimples & Drag. (2022, January 13) In *aerospaceweb.*

http://www.aerospaceweb.org/question/aerodynamics/q0215.shtml

Gu, Z. L., Zhang, Y. W., Cheng, Y., & Lee, S. C. (2011). Effect of uneven building layout on air flow and pollutant dispersion in non-uniform street canyons. *Building and Environment,* *46*(12), 2657-2665. https://doi.org/10.1016/j.buildenv.2011.06.028.

Gu, K. K., & Zhu, L. L. (2017). Study on the relationships between development intensity and microclimate in urban residential areas—a case of Hefei. *Ecol. Environ. Sci. 26*(12), 2084–2092. (in Chinese).

Gut, P., & Ackerknecht, D. (1993). *Climate responsive buildings: appropriate building construction in tropical and subtropical regions*. SKAT, Swiss Centre for Development Cooperation in Technology and Management.

Gülten, A., & Öztop, H. F. (2020). Analysis of the natural ventilation performance of residential areas considering different urban configurations in Elazığ, Turkey. *Urban Climate, 34*, 100709. https://doi.org/10.1016/j.uclim.2020.100709.

Habertürk. (2018, January 01) *İzmir'de fırtına ve şiddetli yağışın ardından denizle kara birleşti.* [Press release]. https://www.haberturk.com/izmir-de-siddetli-yagis-ve-firtina-1801683.

HABITAT & CSC (1983). *Passive Solar Architecture Report of the Training Workshop*. London and Nairobi.

Hamlyn, D., & Britter, R. (2005). A numerical study of the flow field and exchange processes within a canopy of urban-type roughness. *Atmospheric Environment, 39*(18), 3243–3254. https://doi.org/10.1016/j.atmosenv.2005.02.020.

Hang, J., Li, Y., Buccolieri, R., Sandberg, M., & Di Sabatino, S. (2012). On the contribution of mean flow and turbulence to city breathability: the case of long streets with tall buildings. *Science of the Total Environment, 416*, (362-373. https://doi.org/10.1016/j.scitotenv.2011.12.016.

Hasan Topal. (2020, October 13) *Çeyrek yüzyılda kentin, mekanın değişimi, (1955-1980) This* [Image attached] [Status update]. Facebook. https://www.facebook.com/photo/?fbid=3850793248266031&set=a.69059467761 9253)

He, B. J., Ding, L., & Prasad, D. (2020). Relationships among local-scale urban morphology, urban ventilation, urban heat island and outdoor thermal comfort under sea breeze influence, *Sustainable Cities and Society*, *60*, 102289. https://doi.org/10.1016/j.scs.2020.102289.

Holden, E. (2004). Ecological Footprints and Sustainable Urban Form, *Journal Of Housing And The Built Environment*, *19*(96). https://doi.org/10.1023/B:JOHO.0000017708.98013.cb.

Holland J. H. (1975). *Adaptation in Natural and Artificial Systems.* Ann Arbor: University of Michigan Press.

Hu, K., Cheng, S., & Qian, Y. (2018). CFD Simulation Analysis of Building Density on Residential Wind Environment, *Journal of Engineering Science and Technology Review*, *11*, 35–43. doi:10.25103/jestr.111.05.

Hu, T., Yoshie, R. (2013). Indices to evaluate ventilation efficiency in newly-built urban area at pedestrian level. *Journal of Wind Engineering and Industrial Aerodynamics, 112*, 39–51. https://doi.org/10.1016/j.jweia.2012.11.002.

Hussain, M., & Lee B.E. (1980). *An investigation of wind forces on three dimensional roughness elements in simulated atmospheric boundary layer flow*. Dept. of Building Science, University of Sheffield Report.

Isyumon, N. & Davenport, A. (1975). The ground level wind environment in built-up areas, In *Proceedings of the 4th International Conference on Wind Effects on Buildings and Structures*, Heathrow, UK, 403–422.

Jamei, E., Ossen, D. R., Seyedmahmoudian, M., Sandanayake, M., Stojcevski, A., & Horan, B. (2020). Urban design parameters for heat mitigation in tropics, *Renewable and Sustainable Energy Reviews, 134*, 110362. https://doi.org/10.1016/j.rser.2020.110362.

Janssen, W. D., Blocken, B., & van Hooff, T. (2013). Pedestrian wind comfort around buildings: Comparison of wind comfort criteria based on whole-flow field data for a complex case study. *Building and Environment, 59*, 547-562. https://doi.org/10.1016/j.buildenv.2012.10.012.

Johanssen, W. (1911). The Genotype conception of heredity. *The American Naturalist. 45*(531).

Johansson, E., & Yahia, M.W. (2020). Wind comfort and solar access in a coastal development in Malmö, Sweden. *Urban Climate. 33*, 100645. https://doi.org/10.1016/j.uclim.2020.100645.

Jones, W. & Launder, B. (1972). The prediction of laminarization with a two-equation model of turbulence. *International Journal of Heat and Mass Transfer, 15*(2), 301–314. https://doi.org/10.1016/0017-9310(72)90076-2.

Kastner-Klein, P., Fedorovich, E., & Rotach, M. W., (2001). A wind tunnel study of organised and turbulent air motions in urban street canyons. *Journal of Wind Engineering and Industrial Aerodynamics*, *89*(9), 849-861. https://doi.org/10.1016/S0167-6105(01)00074-5.

Kestane, Ö., & Ülgen K. (2013). İzmir ili için biyoklimatik konfor bölgelerinin belirlenmesi, *SDÜ Teknik Bilimler Dergisi*, *3*(5), 18-25. (in Turkish).

Kim, J. J., & Baik, J. J. (1999). A numerical study of thermal effects on flow and pollutant dispersion in urban street canyons. *Journal of Applied*

Meteorology, 38(9), 1249-1261. https://doi.org/10.1175/1520-0450(1999)038<1249:ANSOTE>2.0.CO;2.

Knight, T. W. (1981). Languages of designs: from known to new. *Environment and Planning B. 8*, 213–238. https://doi.org/10.1068/b080213.

Krautheim, M., Pasel, R., Pfeiffer, S., & Granberg J. S. (2014). *City and Wind - Climate as an Architectural Instrument.* DOM Publishers.

Kubota, T., Miura, M., Tominaga, Y., & Mochida, A., (2008). Wind tunnel tests on the relationship between building density and pedestrian-level wind velocity: Development of guidelines for realizing acceptable wind environment in residential neighborhoods. *Building and Environment, 43*(10), 1699-1708. https://doi.org/10.1016/j.buildenv.2007.10.015.

Lawrence, N. E. (1970). Forecasting air pollution. *Monthly Weath. Rev*. 88, 3.

Lawson, T. (1978). The wind content of the built environment, *Journal of Wind Engineering and Industrial Aerodynamics, 3,* 93-105. https://doi.org/10.1016/0167-6105(78)90002-8.

Li, X.X., Liu, C.H., & Leung, D.Y. (2005). Development of a k–ε model for the determination of air exchange rates for street canyons. *Atmospheric Environment, 39*(38), 7285-7296. https://doi.org/10.1016/j.atmosenv.2005.09.007.

Lim, J., & Ooka, R. (2021). A CFD-Based Optimization of Building Configuration for Urban Ventilation Potential, *Energies*, *14*(5), 1447. https://doi.org/10.3390/en14051447.

Lin, M., Hang, J., Li, Y., Luo, Z., & Sandberg, M. (2014). Quantitative ventilation assessments of idealized urban canopy layers with various urban layouts and the same building packing density. *Building and Environment, 79*, 152-167. https://doi.org/10.1016/j.buildenv.2014.05.008.

Lin, J. & Yang, A. (2006). Does the compact-city paradigm foster sustainability? An empirical study in Taiwan. *Planning and Design. 33*, 365-380. https://doi.org/10.1068/b31174.

Liu, C. H., Leung, D. Y., & Barth, M. C. (2005). On the prediction of air and pollutant exchange rates in street canyons of different aspect ratios using large-eddy simulation. *Atmospheric Environment, 39*(9), 1567-1574.

Ma, T., & Chen, T. (2020). Classification and pedestrian-level wind environment assessment among Tianjin's residential area based on numerical simulation, *Urban Climate*, *34*, 100702. https://doi.org/10.1016/j.uclim.2020.100702.

Mandić, M., & Tepavčević, B. (2015). *Environment and Planning B: Planning and Design. 42*, 675-687. https://doi.org/10.1068/b130084p.

Manisalidis, I., Stavropoulou, E., Stavropoulos, A., & Bezirtzoglou, E. (2020). Environmental and health impacts of air pollution: a review. *Frontiers in Public Health, 8*. https://doi.org/10.3389/fpubh.2020.00014.

Martin, L. & March L. (1972). *Urban Space and Structures*, Cambridge, University Press, UK.

Maruta, E. (1984). *The study of high wind regions around tall buildings* (in Japanese; translation available at BRE, Watford, UK) [Doctoral Dissertation]. Nihon University, Tokyo.

Merlier, L. (2015). *On the interactions between urban structures and air flows: A numerical study of the effects of urban morphology on the building wind environment and the related building energy loads* [Doctoral Dissertation]. INSA de Lyon.

Melbourne, W. H. (1978). Criteria for Environmental Wind Conditions. *Journal of Wind Engineering and Industrial Aerodynamics*, *3*(2–3), 241–249. https://doi.org/10.1016/0167-6105(78)90013-2.

Memon, R. A., & Leung, D. Y. (2010). Impacts of environmental factors on urban heating. *Journal of Environmental Science, 22*(12), 1903–1909. https://doi.org/10.1016/S1001-0742(09)60337-5.

Menter, F. R. (1994). Two-equation eddy-viscosity turbulence models for engineering applications. *AIAA Journal, 32*(8), 1598–1605. https://doi.org/10.2514/3.12149.

MitchellL, W. J. (1986). Formal represantations: a foundation for computer-aided architectural design, *Environment and Planning B: Planning and Design, 13*, 133-162. https://doi.org/10.1068/b130133

Murakami, S. (1985). Criteria for assessing wind-induced discomfort considering temperature effect. *Journal of Architecture, Planning and Environmental Engineering, AIJ, 358*, 9-17.

Murty, B. P. (1975). Eigenvectors of sulphur dioxide in Metropolitan Toronto and their association with meteorological parameters, *Atmospheric Environment, 9*, 365. https://doi.org/10.1016/0004-6981(75)90147-X.

NEN. (2006). Wind Comfort and Wind Danger in the Built Environment. NEN 8100. Dutch Standard.

Nakamura, Y, & Oke, T. (1998). Wind, temperature, and stability conditions in an East-west oriented urban canyon. *Atmospheric Environment, 22*(12), 2691-2700.

Ng, E. (2009). Policies and technical guidelines for urban planning of high-density cities–air ventilation assessment (AVA) of Hong Kong. *Building and Environment, 44*(7), 1478-1488. doi:10.2495/DNE-V12-N1-16-29.

Nicholson, S. E. (1975). A pollution model for street-level air. *Atmospheric Environment, 9*, 19-31.

Nikuradse, J. (1933). Stormungsgesetze in rauhen Rohren. Forschungsheft auf dem Gebiete des Ingenieurwesens. VDI-Verlag, Berlin. (in German).

Nonomura, Y., Kobayashi, N., Tominaga, Y., & Mochida, A. (2003). The cross comparison of CFD results for flow field around building models (Part 3)-Wind tunnel test for the verification of models for the flow field around building blocks. In Summaries of Technical Papers of Annual Meeting, *Japan Association for Wind Engineering, 95*, 83-84. (in Japanese).

Oke, T. R. (1988). Street design and urban canopy layer climate. *Energy and Buildings, 11*(1-3), 103-113. https://doi.org/10.1016/0378-7788(88)90026-6.

Olgyay, V. (1963). *Design with Climate, bioclimatic approach to architectural regionalism.* Princeton University Press.

O'Reilly, U. M., & Ramachandran, G. (1998). *A preliminary investigation of evolution as a form design strategy*. In Artificial Life VI, Los Angeles, CA, UAS.

Paio, A., & Turkienicz, B. (2011). An urban grammar study: a geometric method for generating planimetric proportional and symmetrical systems. *Nexus Network Journal*, 13, 151-169.

Paio, A., Reis, J., Santos, F., Lopes, P. F., Eloy, S., & Rato, V. (2011). Emerg. cities4all: Towards a shape grammar based computational system tool for generating a sustainable and integrated urban design, In *Proceedings of the 29 th eCAADe Conference,* 152-158.

Panagiotou, I., Neophytou, M. K. A., Hamlyn, D., & Britter, R. E. (2013). City breathability as quantified by the exchange velocity and its spatial variation in real inhomogeneous urban geometries: an example from central London urban area. *Science of the Total Environment, 442*(0), 466–477. https://doi.org/10.1016/j.scitotenv.2012.09.001

Penwarden, A. D. (1973). Acceptable Wind Speeds in Towns. *Building Science, 8*(3), 259–267. doi:10.1016/0007-3628(73)90008-X.

Peterka, J. A., Meroney, R. N., & Kothari, K. M. (1985). Wind flow patterns about buildings, *Journal of Wind Engineering and Industrial Aerodynamics, 21*, 21-38.

Plate, E. J. (1982). *Engineering meteorology*, Elsevier Scientific Publishing Company.

Priyadarsini, R. & Wong N. H. (2005). Parametric Studies on Urban Geometry, Air Flow and Temperature. *International Journal on Architectural Science, 6*, 3.

Rajagopalan, P., Lim, K. C., & Jamei, E. (2014). Urban heat island and wind flow characteristics of a tropical city. *Solar Energy, 107*, 159-170.

Ramponi, R., & Blocken, B. (2012). A computational study on the influence of urban morphology on wind-induced outdoor ventilation. In R. Seppelt, A. A. Voinov, S. Lange, D. Bankamp, *iEMSs International Congress on Environmental Modeling and Software* Germany.

Ramponi, R., Blocken, B., Laura, B., & Janssen, W. D. (2015). CFD simulation of outdoor ventilation of generic urban configurations with different urban densities and equal and unequal street widths. *Building and Environment 92*, 152-166. https://doi.org/10.1016/j.buildenv.2015.04.018.

Reiter, S. (2010). Assessing wind comfort in urban planning. *Environment and Planning B: Planning and Design, 37*(5), 857-873. https://doi.org/10.1068/b35154.

Richards, P., & Hoxey, R. (1993). Appropriate boundary conditions for computational wind engineering models using the k-epsilon turbulence model. *Journal of Wind Engineering and Industrial Aerodynamics, 47*, 145–153. https://doi.org/10.1016/0167-6105(93)90124-7.

Rotta, J. (1951). Statistische theorie nichthomogener turbulenz. *Zeitschrift für Physik A*, *129*(6), 547-572. (in German).

Salim, S. M., Buccolieri, R., Chan, A., & Di Sabatino, S. (2011). Numerical simulation of atmospheric pollutant dispersion in an urban street canyon: Comparison between RANS and LES. *Journal of Wind Engineering and Industrial Aerodynamics, 99*(2-3), 103-113. https://doi.org/10.1016/j.jweia.2010.12.002.

Samson P. J. (1988). Atmospheric transport and dispersion of air pollutants associated with vehicular emissions. In A. Y., Watson, R. R., Bates, & D. Kennedy, *Air Pollution, the Automobile, and Public Health*. US: National Academies Press.

Shih, T. H., Liou, W. W., Shabbir, A., Yang, Z., & Zhu, J. (1995). A new k-ϵ eddy viscosity model for high Reynolds number turbulent flows. *Computers & Fluids, 24*(3), 227-238. https://doi.org/10.1016/0045-7930(94)00032-T.

Skote, M., Sandberg, M., Westerberg, U., Claesson, L., & Johansson, A. V. (2005). Numerical and experimental studies of wind environment in an urban morphology. *Atmospheric Environment, 39*(33), 6147-6158. https://doi.org/10.1016/j.atmosenv.2005.06.052.

Star-CCM+ Version 4.02.011 User Guide, (2006). CD-adapco.

Stathopoulos T. (2006). Pedestrian level winds and outdoor human comfort. *Journal of Wind Engineering and Industrial Aerodynamics, 94*, 769-780. https://doi.org/10.1016/j.jweia.2006.06.011.

Stathopoulos T. & Blocken B. (2016). Pedestrian Wind Environment Around Tall Buildings, In Y. Tamura, & R., Yoshie (Eds.), *Advanced Environmental Wind Engineering.* Springer, Tokyo. https://doi.org/10.1007/978-4-431-55912-2_6/.

Steemers, K., Baker, N., Crowther, D., Dubiel, J., Nikolopoulou, M. H., & Ratti, C. (1997). City texture and microclimate. *Urban Design Studies, 3*(1997), 25-50.

Stewart, I. D. (2011). *Redefining the urban heat island* [Doctoral Dissertation]. Department of Geography, University of British Columbia.

Stewart, I. D., & Oke, T. R. (2012). Local climate zones for urban temperature studies. *Bulletin of the American Meteorological Society. 93*(12), 1879-1900. https://doi.org/10.1175/BAMS-D-11-00019.1.

Stiny, G., & Gips, J. (1972). Shape grammars and the generative specification of painting and sculpture. Information Processing. 71, 1460–1465.

Szűcs, Á. (2013). Wind comfort in a public urban space—case study within Dublin Docklands. *Frontiers of Architectural Research, 2*(1), 50-66. https://doi.org/10.1016/j.foar.2012.12.002.

Tablada De La Torre, A. (2006). *Shape of New Residential Buildings in the Historical Centre of Old Havana to Favour Natural Ventilation and Thermal Comfort* [Doctoral Dissertation]. Catholic University of Leuven, Belgium.

Taleghani, M., Kleerekoper, L., Tenpierik, M. J., & van den Dobbelsteen, A. A. J. F. (2015). Outdoor thermal comfort within five different urban forms in the Netherlands. *Building and Environment, 83*, 65-78. https://doi.org/10.1016/j.buildenv.2014.03.014.

Thangam, S., & Speziale, C. G. (1992). Turbulent flow past a backward-facing step-A critical evaluation of two-equation models. *AIAA journal, 30*(5), 1314-1320. https://doi.org/10.2514/3.11066.

The Commission of the European Communities (1990). Green paper on the urban environment. Office for Official Publications of the European Communities.

The World Commission on Environment and Development, Brundtland Commission [WCED]. (1987). *Our Common future.* United Nations, New York.

Tominaga, Y., Mochida, A., Yoshie, R., Kataoka, H., Nozu, T., Yoshikawa, M., & Shirasawa, T. (2008). AIJ guidelines for practical applications of CFD to pedestrian wind environment around buildings. *Journal of Wind Engineering and Industrial Aerodynamics*, *96*(10-11), 1749-1761. https://doi.org/10.1016/j.jweia.2008.02.058.

Turkish State Meteorological Service [TSMS], Climate Data, Türkiye. [https://www.mgm.gov.tr/veridegerlendirme/il-ve-ilceler-istatistik.aspx?m=IZMIR], Accessed Date (10.10.2018).

UK Department of the Environment (1993). UK Strategy for Sustainable Development. A consultation paper, London: DoE.

USDOE EnergyPlus Climate Data (2021). Available Online: https://energyplus.net/weather.

U.S. Environmental Protection Agency [EPA]. (2001). Our built and natural environments: A technical review of the interactions between land use, transportation, and environmental quality. EPA 231-R-01-002.

Wai, K. M., Yuan, C., Lai, A., & Peter, K. N. (2020). Relationship between pedestrian-level outdoor thermal comfort and building morphology in a high-density city, *Science of the Total Environment*, *708*, 134516. https://doi.org/10.1016/j.scitotenv.2019.134516.

Walker, R. R., Shao, L., & Woolliscroft, M. (1993, September). Natural ventilation via courtyards: theory & measurements. In *Document-Air Infiltration Centre AIC PROC* (pp. 235-235), Oscar Faber Plc.

Van Hooff, T., & Blocken, B. (2010). Coupled urban wind flow and indoor natural ventilation modelling on a high-resolution grid: A case study for the Amsterdam Arena stadium. *Environmental Modelling & Software, 25*(1), 51-65.

White, F. (2002). *Fluid Mechanics* (4th ed.). New York: McGraw-Hill Higher Education. ISBN: 0-07-228192-8.

Whyte, W. H. (1980). *The Social Life of Small Urban Spaces*. New York, NY: Project for Public Spaces.

Wieringa, J. (1992). Updating the Davenport roughness classification. *Journal of Wind Engineering and Industrial Aerodynamics, 41*(1-3), 357-368. https://doi.org/10.1016/0167-6105(92)90434-C.

Wieringa, J., Davenport A. G., Grimmond C. S. B & Oke T. R. (2001). New Revision of Davenport roughness classification. In *Proceedings of the 3rd European & African Conference on Wind Engineering*. Eindhoven, Netherlands.

Wikipedia Picture Boundary Layer Thickness. (2022, February 06). In *Wikipedia.* https://commons.wikimedia.org/wiki/File:Wickipedia_Picture_Boundary_Layer_ Thickness.jpg

Wise, A. F. E. (1970). Wind effects due to groups of buildings (Vol. 23). Garston, Watford, England: *Building Research Station*

Wise, A. F. E. (1971). Effects Due to Groups of Buildings. Philosophical Transactions of the Royal Society of London, Series A. *Mathematical and Physical Sciences, 269*(1199), 469–485. https://doi.org/10.1098/rsta.1971.0045.

World Meteorological Organization. (2022, March, 12). *Sand and Dust Storm Warning Advisory and Assessment System.* https://public.wmo.int/en/our-mandate/focus-areas/environment/SDS/warnings

Xu, Q., Xu, Z. (2020). What can urban design learn from changing winds?. *Journal of Public Space. 5*(2), 7-22. https://doi.org/10.32891/jps.v5i2.1278.

Yang, J., Shi, B., Shi, Y., Marvin, S., Zheng, Y., & Xia, G. (2020). Air pollution dispersal in high density urban areas: Research on the triadic relation of wind, air pollution, and urban form. *Sustainable Cities and Society*, *54*, 101941.

Yeni Vizyon. (2016, June 24). *İzmir'i karıştıran karikatür.* http://www.yenivizyon.net/izmiri-karistiran-karikatur-13007h.htm.

Yim, S. H., Fung, J. C. H., Lau, A. K. H., & Kot, S. C. (2009). Air ventilation impacts of the "wall effect" resulting from the alignment of high-rise buildings. *Atmospheric Environment, 43*(32), 4982-4994. https://doi.org/10.1016/j.atmosenv.2009.07.002.

Zhang, C. X. (1994). Numerical predictions of turbulent recirculating flows with a k-ϵ model. *Journal of Wind Engineering and Industrial Aerodynamics, 51*(2), 177-201. https://doi.org/10.1016/0167-6105(94)90003-5.

APPENDICES

Appendix A; (Chapter 3, 3.1. Choice of Field Study Area)
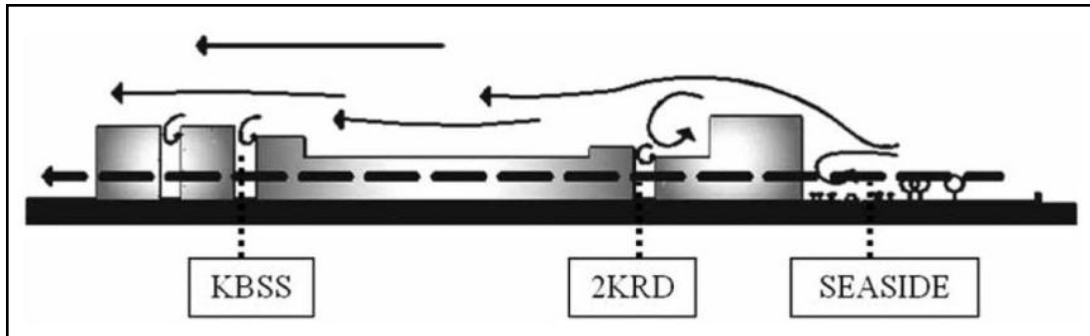
Figure A-1: Cross-section of the site in Alsancak (Arkon and Özkol, 2014)
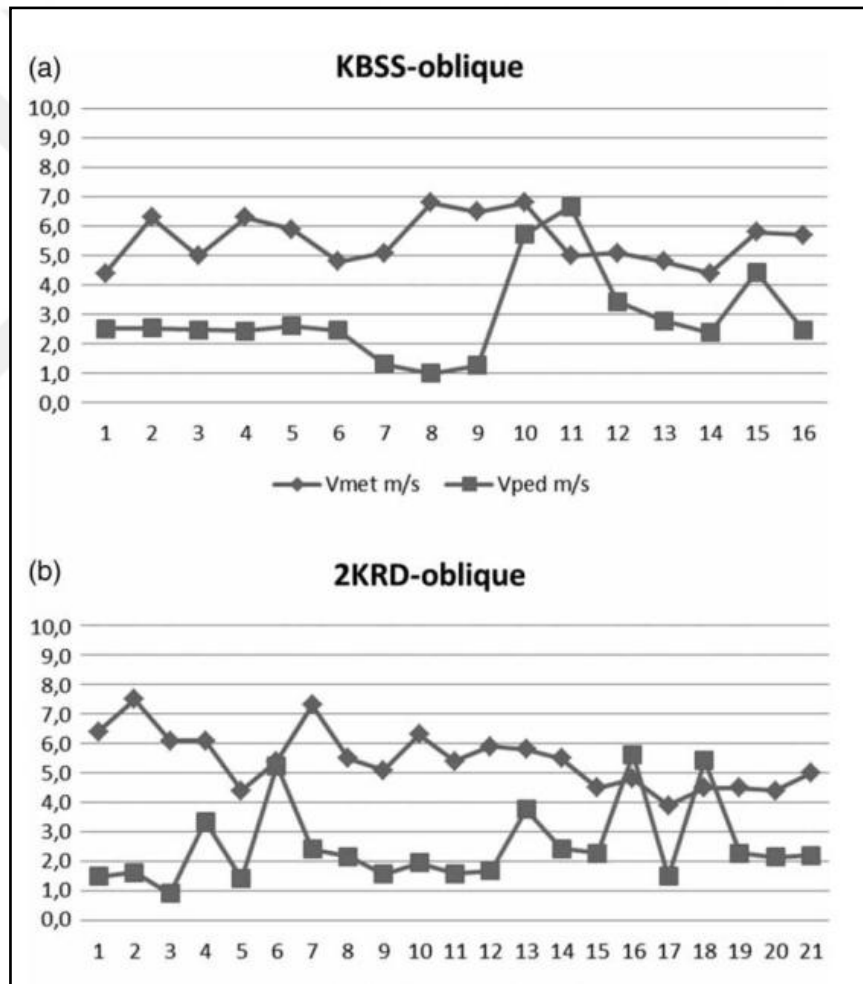
Figure A-2: Measurements (a) KBSS and (b) 2KRD in August: Vmet and Vped (Arkon and Özkol, 2014)

Appendix B; (Chapter 3, 3.3.3.2.1 Inlet boundary condition)
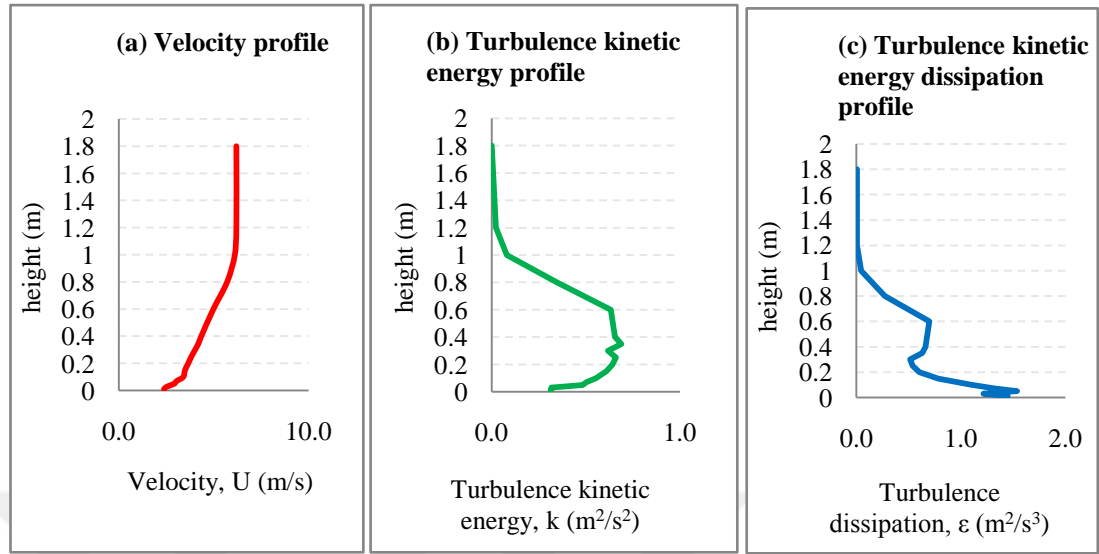
Figure B: Inlet boundary conditions (1) velocity profile (2) turbulence kinetic energy profile (3) turbulence kinetic energy dissipation profile

Appendix C; (Chapter 3, 3.3.3.5 Grid-independence Study)
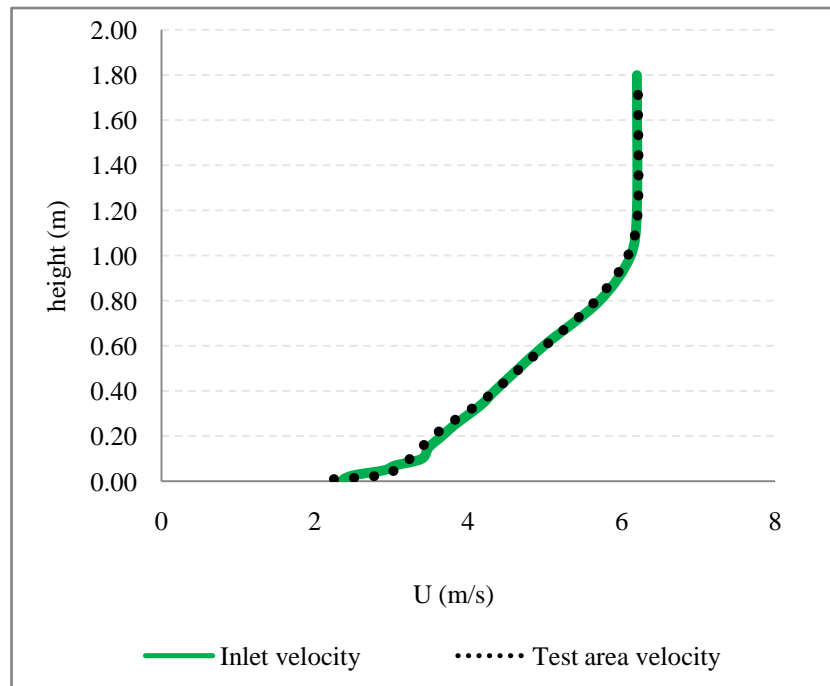
Figure C-1 Vertical velocity profile comparison in empty domain

Appendix D; (Chapter 3, 3.3.3.5 Grid-independence Study)
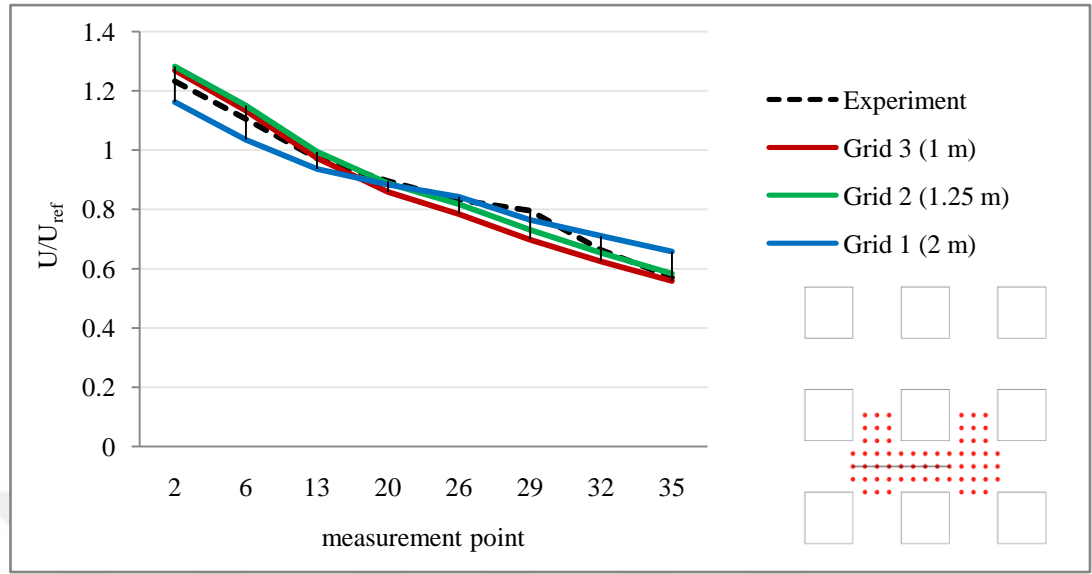
Figure D-1 Comparison of the velocity profiles in high-speed region for the 3 grids tested

Appendix E; (Chapter 3, 3.3.4 Results)
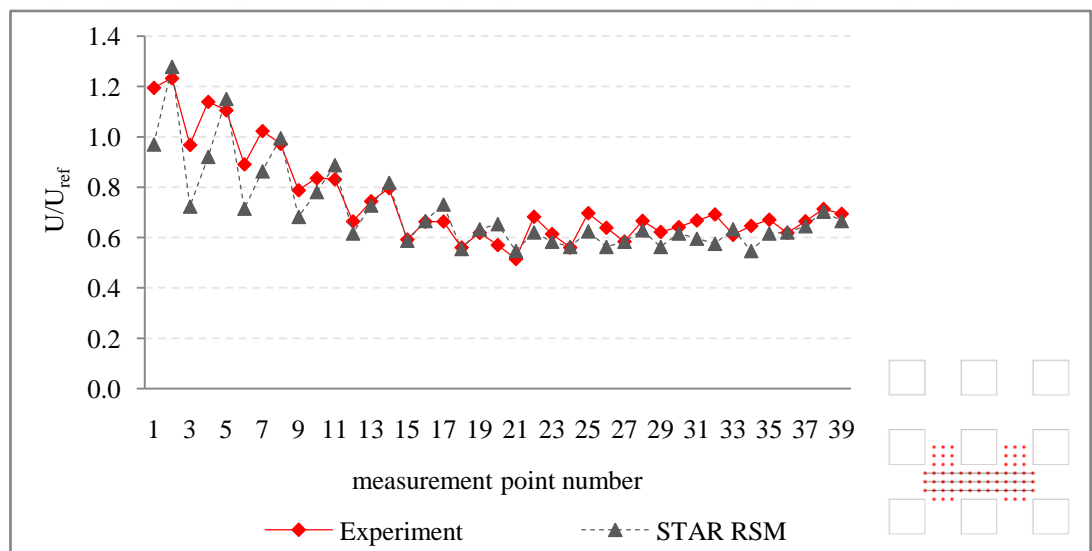
Figure E-1 Comparison between experiment and STAR's RSM model

Appendix F; (Chapter 3, 3.3.4 Results)
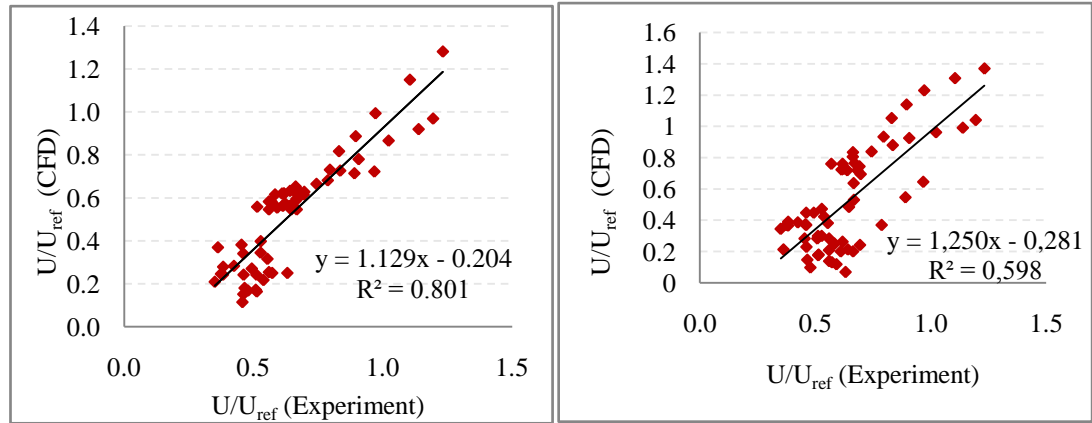
a) STAR RSM model

b) STAR Realizable k – ε model
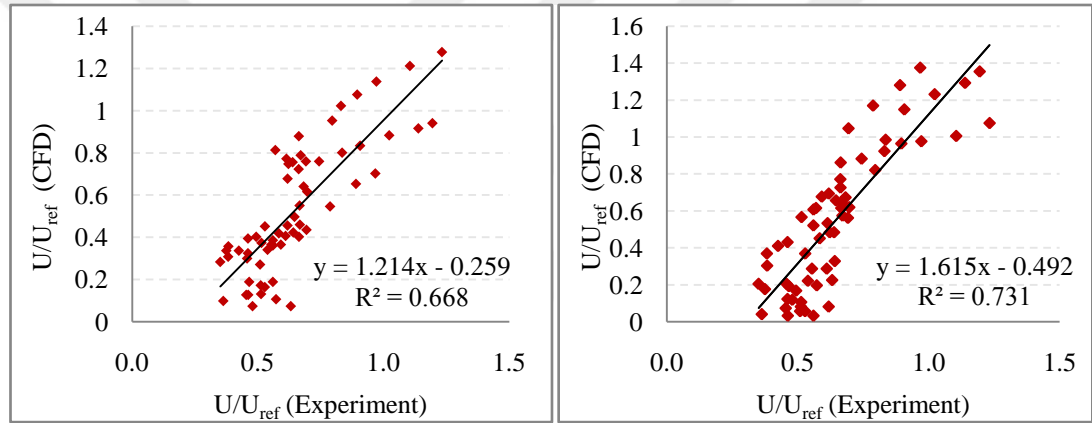
c) STAR Standard k – ε model

d) SIMSCALE k – ω SST (Menter) model
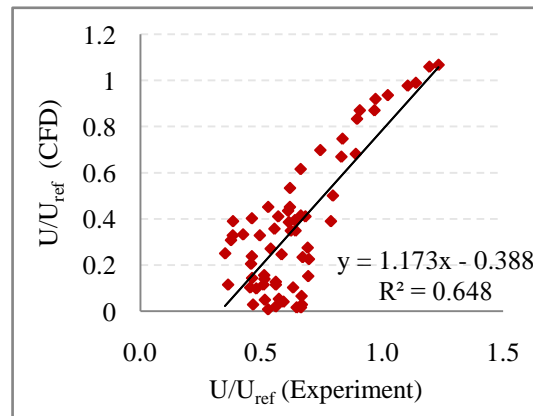
e) SIMSCALE Standard k – ε

Figure F: Correlation between experimental wind speed ratios and CFD (a) STAR RSM model (b) STAR Realizable k – ε model (c) STAR Standard k – ε model (d) SIMSCALE k – ω SST (Menter) model (e) SIMSCALE Standard k – ε

Appendix G; (Chapter 4, 4.4.4 Wind Flow Assessment of Best Possible Seafront Building Configurations)
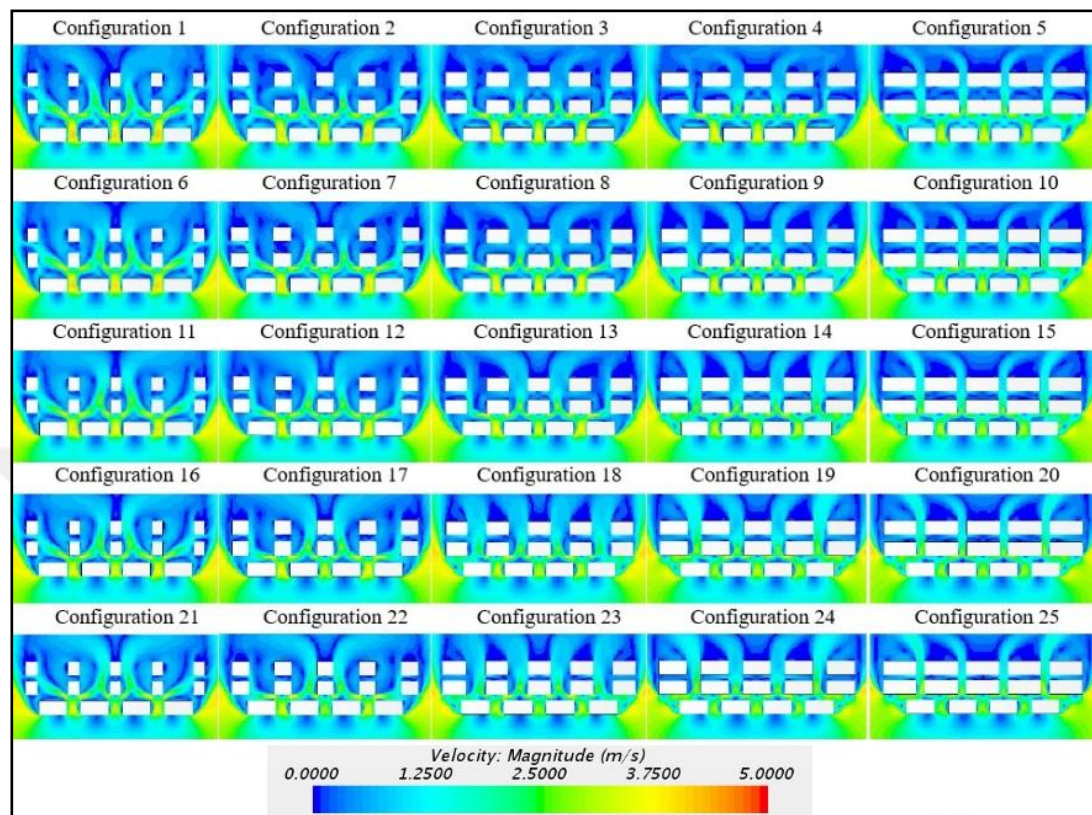
Figure G-1 Contour plots of velocity magnitude for all seafront building configurations

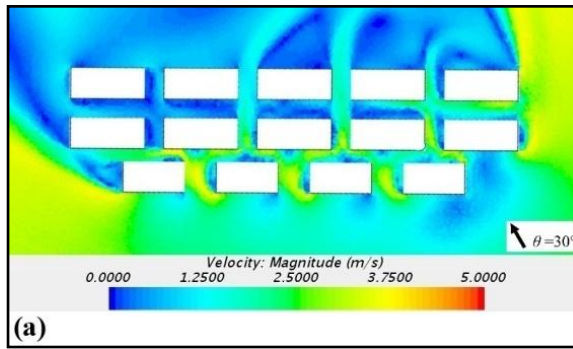Appendix H; (Chapter 4, 4.4.5 Wind Discomfort Assessment Under Oblique (15°, 30°, 45°) Wind Directions
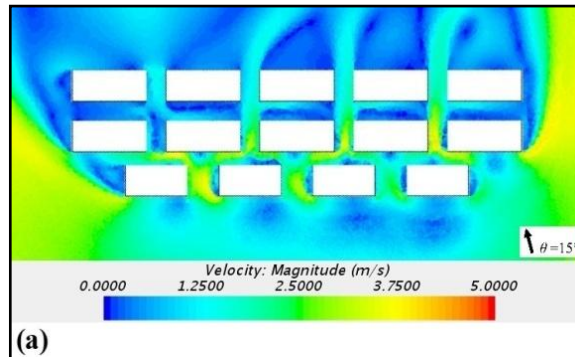
Figure H-1 Wind velocity distribution around Conf. 25 for $\phi = 15°$
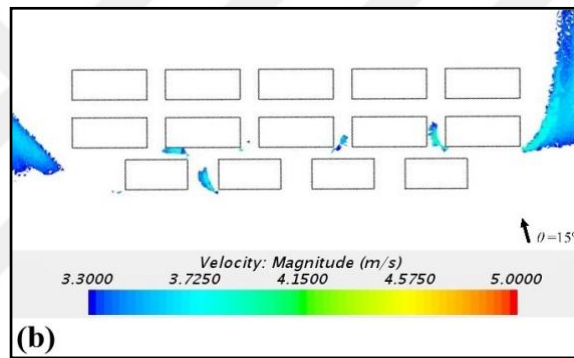
Figure H-2 Wind discomfort risk around Conf. 25 for $\phi = 15°$
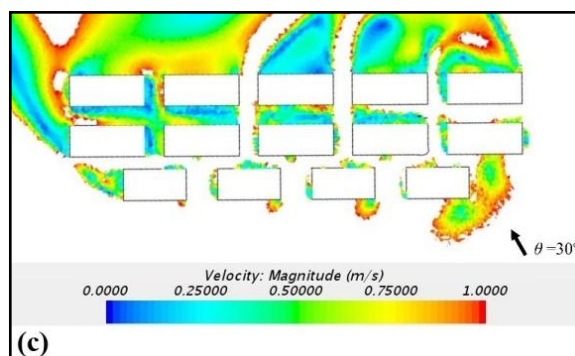
Figure H-3 Ventilation efficiency around Conf. 25 for $\phi = 15°$

Figure H-4 Wind velocity distribution around Conf. 25 for $\phi = 30°$
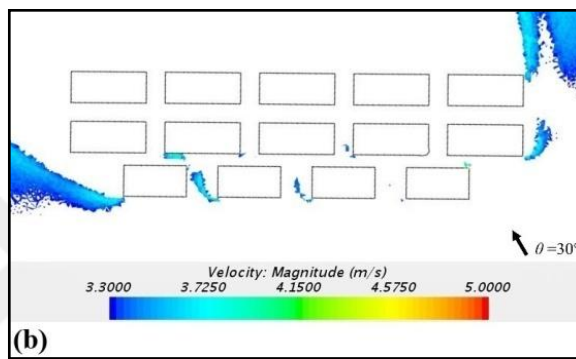
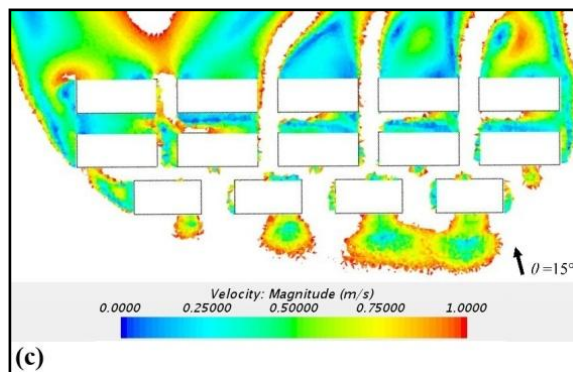Figure H-5 Wind discomfort risk around Conf. 25 for $\phi = 30°$

Figure H-6 Ventilation efficiency around Conf. 25 for $\phi = 30°$

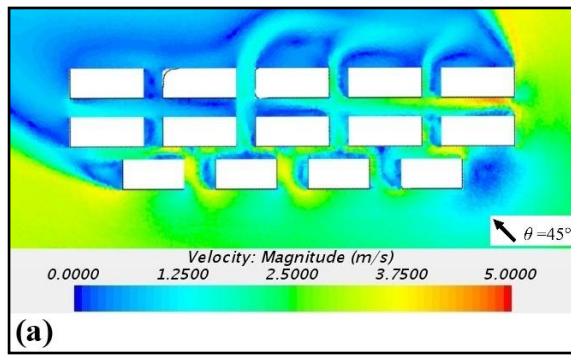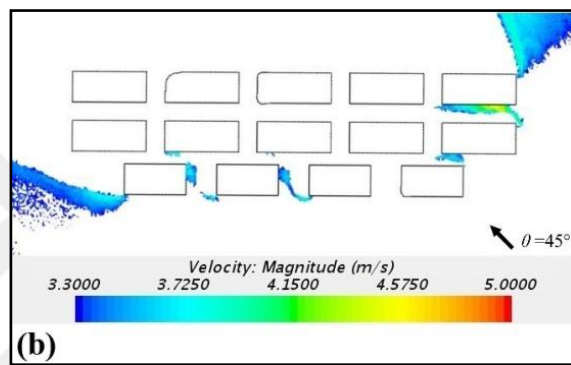Figure H-7 Wind velocity distribution around Conf. 25 for $\phi = 45°$

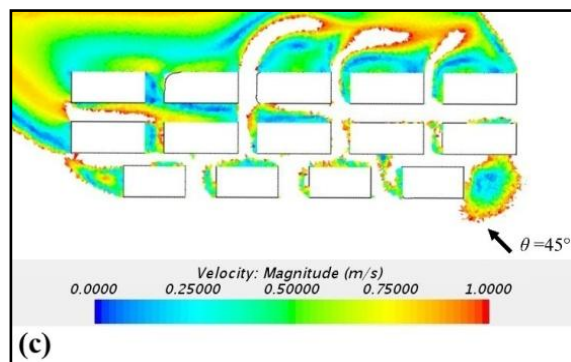Figure H-8 Wind discomfort risk around Conf. 25 for $\phi = 45°$

Figure H-9 Ventilation efficiency around Conf. 25 for $\phi = 45°$